Aus dem Zentrum für Augenheilkunde der Universität zu Köln
Klinik und Poliklinik für Allgemeine Augenheilkunde
Direktor: Universitätsprofessor Dr. med. C. Cursiefen

Targeting NOX2 to combat oxidative stress and neuroinflammation and provide neuroprotection in neurodegeneration

Inaugural-Dissertation zur Erlangung der Doktorwürde
der Medizinischen Fakultät
der Universität zu Köln

vorgelegt von
Xin Shi
aus Yunnan

promoviert am 16. August 2024

Gedruckt mit Genehmigung der Medizinischen Fakultät der Universität zu Köln

2024

Dekan: Universitätsprofessor Dr. med. G. R. Fink

1. Gutachterin: Universitätsprofessorin Dr. med. V. Prokosch
2. Gutachter: Universitätsprofessor Dr. med. O. Utermöhlen

Erklärung

Ich erkläre hiermit, dass ich die vorliegende Dissertationsschrift ohne unzulässige Hilfe Dritter und ohne Benutzung anderer als der angegebenen Hilfsmittel angefertigt habe; die aus fremden Quellen direkt oder indirekt übernommenen Gedanken sind als solche kenntlich gemacht.

Bei der Auswahl und Auswertung des Materials sowie bei der Herstellung des Manuskriptes habe ich Unterstützungsleistungen von folgenden Personen erhalten:

Universitätsprofessor Dr. med. Verena Prokosch, Universitätsprofessor PhD Huige Li, PhD Marc Herb, PhD Maoren Wang, PhD Ning Xia, Dr. med. Hanhan Liu, Frau Panpan Li, Herrn Tim van Beers, Frau Xiaosha Wang und Frau Yuan Feng.

Weitere Personen waren an der Erstellung der vorliegenden Arbeit nicht beteiligt. Insbesondere habe ich nicht die Hilfe einer Promotionsberaterin/eines Promotionsberaters in Anspruch genommen. Dritte haben von mir weder unmittelbar noch mittelbar geldwerte Leistungen für Arbeiten erhalten, die im Zusammenhang mit dem Inhalt der vorgelegten Dissertationsschrift stehen.

Die Dissertationsschrift wurde von mir bisher weder im Inland noch im Ausland in gleicher oder ähnlicher Form einer anderen Prüfungsbehörde vorgelegt.

Die in dieser Arbeit angegebenen Experimente sind nach entsprechender Anleitung durch Universitätsprofessor Dr. med. Verena Prokosch und PhD Marc Herb.

Ich habe eigenständig die folgenden experimentellen Arbeiten durchgeführt: die in vitro Kultivierung von Retina-Explantaten, die Etablierung eines in vivo Mausmodells mit erhöhtem Augeninnendruck, die Probenentnahme von Sehnerven und die Isolierung von Netzhautgewebe, die Kultivierung von Mikrogliazellen, die Immunfluoreszenzfärbung von Netzhaut und Mikroglia, sowie Western Blots von Netzhaut- und Mikroglia-Lysaten.

Die dieser Arbeit zugrunde liegenden Experimente sind von mir mit Unterstützung von Universitätsprofessor PhD Huige Li, PhD Marc Herb, PhD Ning Xia, PhD Maoren Wang, Dr. med. Hanhan Liu, Frau Panpan Li, Herrn Tim van Beers, Frau Xiaosha Wang und Frau Yuan Feng durchgeführt worden.

Erklärung zur guten wissenschaftlichen Praxis:

Ich erkläre hiermit, dass ich die Ordnung zur Sicherung guter wissenschaftlicher Praxis und zum Umgang mit wissenschaftlichem Fehlverhalten (Amtliche Mitteilung der Universität zu Köln AM 132/2020) der Universität zu Köln gelesen habe und verpflichte mich hiermit, die dort genannten Vorgaben bei allen wissenschaftlichen Tätigkeiten zu beachten und umzusetzen.

Köln, 29.04.2024

Unterschrift: Xin Shi

ACKNOWLEDGEMENTS

At this pivotal moment, my heart is filled with profound gratitude. I extend my sincerest thanks to my friends and colleagues who supported me in composing and editing my academic paper.

First and foremost, I am compelled to express my most profound admiration for Professor Verena Prokosch. She afforded me the invaluable opportunity to delve into this field and served as the scientific advisor for this study. Her extensive support throughout the research exceeded what words can convey. For everything, I am deeply thankful.

I would also like to express my sincere gratitude to Univ.-Prof. Dr. med. Olaf Utermöhlen for his thorough review of this thesis and for offering constructive suggestions that significantly enhanced the quality of the work. His insights and recommendations were crucial to the final outcome, and I am truly appreciative of his contribution.

My heartfelt appreciation goes to Dr. Marc Herb for his insightful discussions, constructive feedback, and crucial collaboration in providing experimental animals and laboratory assistance, which played a pivotal role in the success of our project.

I am also grateful to Professor Huige Li, Dr. Ning Xia, Dr. Maoren Wang, Dr. Hanhan Liu, Ms. Panpan Li, Ms. Xiaosha Wang, Ms. Yuan Feng, Mr. Tim van Beers, and our technical assistant, Ms. Rodica-Aurelia Maniu, for their generous support of this project. Their collective efforts ensured the smooth progression of our work.

I want to thank all current and former research team members for their support, the pleasant working environment, and the team spirit they provided. The assistance of Layla Fruehn, Dr. Jennifer Kern, Sylvi El Agha, Dr. Julia Prinz, and Tienan Qi made this work smoother and more enjoyable.

Lastly, I extend my special gratitude to my parents and family, whose relentless encouragement and support in pursuing my dreams have been a continuous source of motivation and confidence. The positive energy I felt stems from their unwavering love and support, instilling a stronger belief and courage in me.

Dedication

To my beloved

TABLE OF CONTENTS

ABBREVIATION

$\bullet O_2^-$	superoxide radical anion
AD	Alzheimer's disease
AH	aqueous humor
BBB	blood-brain barrier
BP	blood pressure
BP	biological processes
BRB	blood-retinal barrier
CC	cellular components
CNS	central nervous system
COX	cyclooxygenases
CTGF	connective tissue growth factor
DCF	2,7-dichlorofluorescein derivative 6-carboxy-2,7-dichlorodihydrofluorescein diacetate
DEPs	differentially expressed proteins
DHE	dihydroethidium
ECs	Endothelial cells
ED	Endothelial dysfunction
EDCF	endothelium-derived cyclic oxygenase-dependent contractile factor
EDH	endothelium-dependent hyperpolarizing
ELISA	enzyme-linked immunosorbent assay
ELM	external limiting membrane
eNOS	endothelial NO synthase
ER	endoplasmic reticulum
ET-1	endothelin-1
GCL	ganglion cell layer
GDNF	glial cell line-derived neurotrophic factor
GO	Gene Ontology
GPx	glutathione peroxidase
H_2O_2	hydrogen peroxide
HHcy	hyperhomocysteinemia
H-IOP	high intraocular pressure
HO	hemoglobin oxygenase
HO•	hydroxyl radicals
HO_2•	hydroperoxyl radicals

HTG	high-pressure glaucoma
iBRB	internal blood-retinal barrier
ICAM-1	intercellular adhesion molecule 1
IL	interleukin
iNOS	inducible nitric oxide synthase
IOP	intraocular pressure
KEGG	Kyoto Encyclopedia of Genes and Genomes
LDL	low-density lipoprotein
LOX	lipoxygenases
MAPK	mitogen-activated protein kinases
MCE	Mixed Cellulose Ester
MDD	major depressive disorder
MF	molecular function
NADPH	nicotinamide adenine dinucleotide phosphate
NF-κB	nuclear factor kappa B
NO	nitric oxide
NOX	NADPH oxidase
NTG	normal-temperature glaucoma
NTN	neurturin
NVU	neurovascular unit
O_2-	superoxide anion
oBRB	Outer blood–retinal barrier
OCT	optical coherence tomography
ON	optic nerve
ONC	optic nerve crush
ONH	optic nerve head
ONOO-	oxidant—peroxynitrite
OS	Oxidative stress
ox-LDL	oxidized LDL
PBS	phosphate-buffered saline
PFA	paraformaldehyde
PGI2	prostacyclin
PK	protein kinase
PON	paraoxonase
PPD	p-phenylenediamine
RECs	retinal endothelial cells

RGCs	retinal ganglion cells
RNFL	retinal nerve fiber layer
RNS	reactive nitrogen species
ROO•	peroxyl radicals
ROS	Reactive oxygen species
RPE	retinal pigment epithelium
SC	Schlemm's canal
SMD	standard mean deviation
SOD	superoxide dismutase
TLR	Toll-like receptor
TM	Trabecular meshwork
TNFR	tumor necrosis factor receptor
TNF-α	tumor necrosis factor-alpha
TPX	thioredoxin peroxidase
VCAM-1	vascular cell adhesion molecule 1
VEGF	vascular endothelial growth factor
VSMCs	vascular smooth muscle cells
WHO	World Health Organization
XO	xanthine oxidase

1. Deutsche Zusammenfassung

Oxidativer Stress (OS), ein Ungleichgewicht zwischen freien Radikalen/reaktiven Sauerstoffspezies (ROS) und Antioxidantien, löst biologische Reaktionen aus und steht in Verbindung mit Erkrankungen des Zentralnervensystems (ZNS). NADPH-Oxidase (NOX) ist eine wesentliche Quelle für endotheliale ROS, die die Blut-Retina-Schranke beeinträchtigt und zum Verlust von retinalen Ganglienzellen (RGCs) sowie zur Degeneration im Zusammenhang mit Glaukom beiträgt. Die Hemmung von NOX2 verringert signifikant oxidativen Stress, Immunfehlregulation und Schäden an der internen Blut-Retina-Schranke (iBRB) sowie an der neurovaskulären Einheit und schützt vor dem Verlust von RGCs und der Degeneration des Sehnervs in Glaukommodellen. Die Studie zeigte, dass von NOX2 abgeleitete ROS proinflammatorische Signalwege über Endothelin-1 (ET-1) fördern, was wiederum die ERK1/2-Signalwegaktivierung anregt und Mikroglia in Richtung eines proinflammatorischen M1-Phänotyps verschiebt. Folglich wird NOX2 als entscheidendes Ziel für neuroprotektive Therapien bei Glaukom identifiziert, dessen Hemmung Schutz gegen Schäden an der iBRB und der neurovaskulären Einheit bietet und den Verlust von RGCs sowie die Degeneration des Sehnervs mindert.

2. Summary

The imbalance between antioxidants and free radicals/reactive oxygen species (ROS) characterizes oxidative stress (OS), which induces biological responses and is linked to diseases in the central nervous system (CNS). NADPH oxidase (NOX) fulfills a critical function in producing endothelial ROS, compromising the blood-retinal barrier and depleting retinal ganglion cells (RGCs) and degeneration associated with glaucoma. Inhibition of NOX2 markedly diminishes oxidative stress, immune dysregulation, and damage to the internal blood-retinal barrier (iBRB) and the neurovascular unit, safeguarding against RGC loss and optic nerve deterioration in glaucoma models. The study revealed that NOX2-derived ROS facilitates pro-inflammatory signaling via endothelin-1 (ET-1), activating the ERK1/2 signaling pathway and shifting microglia toward a pro-inflammatory M1 phenotype. Consequently, NOX2 is identified as a critical target for neuroprotective treatments in glaucoma, with its inhibition offering protection against damage to the iBRB and neurovascular unit and mitigating RGC loss and optic nerve degeneration.

3. INTRODUCTION

3.1. Pathogenesis of glaucoma

Glaucoma, an optic neuropathy affecting nearly 60 million people [1], is considered the second leading cause of irreversible blindness worldwide, and its prevalence is expected to increase to over 112 million in the future [1-3]. Glaucoma is mainly categorized into open-angle or closed-angle subtypes, where the closed-angle type refers to the juxtaposition of iris trabecular contacts or adhesions, leading to trabecular meshwork obstruction and elevated intraocular pressure (IOP). Thus, elevated IOP is recognized as a significant risk factor for glaucoma, a disease marked by ongoing deterioration of the retinal ganglion cells (RGCs) and optic nerve (ON) papillary depression. Visual field defects in glaucoma patients are primarily linked to the loss of RGCs, positioning glaucoma alongside neurodegenerative conditions like Alzheimer's and Parkinson's, which stem from deficiencies in neuronal function and survival [4]. Additionally, the loss of RGCs in glaucoma is a progressive condition; even with effective IOP management, numerous patients still experience ongoing RGC and visual impairments [5,6]. Recent research supports the view that glaucoma involves complex degenerative mechanisms affecting the RGCs and ON, influenced by a variety of molecular pathways [7,8].

To date, the specific mechanisms leading to RGC death in glaucoma remain unclear; however, there is increasing evidence that various programmed cell death mechanisms significantly contribute to the demise of RGCs in this condition. Several contributors to the progression of glaucoma have been identified (Figure 1) [9], including aging [10], oxidative stress and endoplasmic reticulum (ER) stress [11], vascular factors [12], neurotrophic factor deprivation [13], and glutamate excitotoxicity [14]. Moreover, recent findings suggest that chronic neuroinflammation also holds a crucial role in the pathological development of glaucoma [15,16].

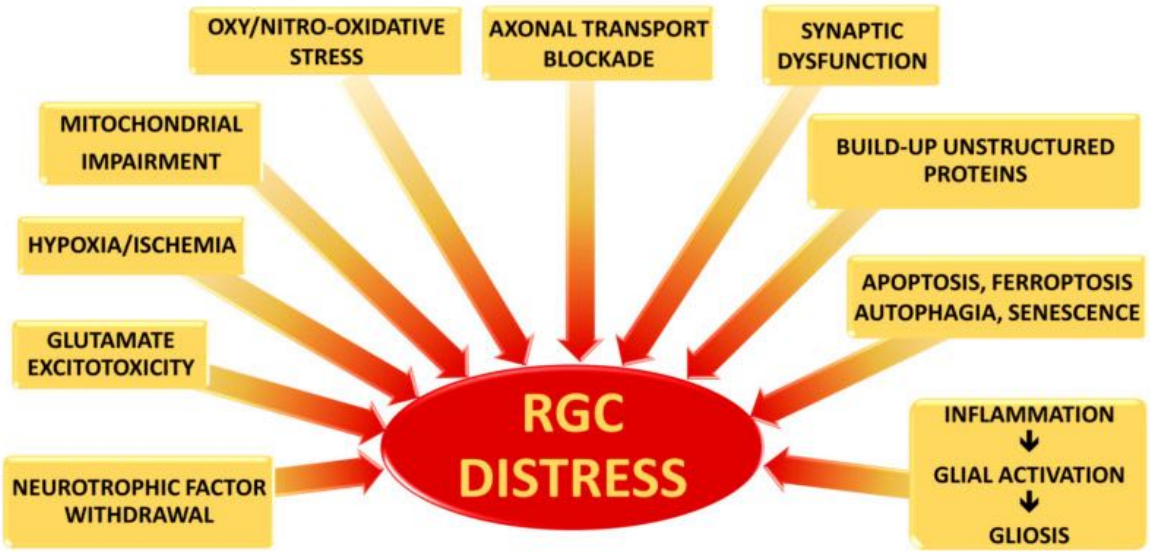

Figure 1 Various risk factors lead to RGC impairment in glaucoma, which includes a spectrum of mechanisms responsible for RGC harm.
Among these are shortages in neurotrophic factors, glutamate-induced excitotoxicity, lack of oxygen, ischemic conditions, mitochondrial impairment, oxidative and nitrosative pressures, interruptions in axonal transport, and disturbances in synaptic communication. Additional factors are the accumulation of misfolded proteins, programmed cell death, additional mechanisms of cell mortality that could precipitate early aging, and an inflammatory cascade that triggers the stimulation of glial cells, resulting in gliosis. Pathways initiated by such hazards often display significant interlinking, collectively exacerbating RGC distress in a way that becomes irreversible. Image from *Vernazza et al., 2021* [9].

3.2. Oxidative stress and neuroinflammation are key contributors to glaucoma.

Typically, various stimuli trigger different molecular cascade reactions that mediate regulated death pathways, leading to diverse immune outcomes. The RGC may also suffer damage under nonphysiological conditions, such as hypoxia, leading to impaired mitochondrial function or oxidative stress. Additionally, while specific defense systems are designed to counteract these risks, their effectiveness can vary based on the retinal microenvironment, potentially leading to glial cell activation instead of damage limitation, thereby causing progressive deterioration of retinal function [17,18]. Increasing evidence points to oxidative stress, coupled with inflammation in the eye, serves as principal elements that propel the pathogenic underpinnings of neurodegeneration in normal-tension glaucoma (NTG) and high-tension glaucoma (HTG) [19-21].

Reactive oxygen species (ROS), including free radicals such as superoxide anion (O_2^-), hydroxyl radical, lipid radical, and nitric oxide (NO), are central to oxidative stress. ROS production unfolds in three phases: initially maintained by mitochondrial responses to respiration inhibition, followed by activation through xanthine oxidase from ATP depletion, and finally through stimulation of nicotinamide adenine dinucleotide phosphate (NADPH) oxidase, which is dependent on calcium [22]. Oxidative stress arises from a disproportion of free radicals relative to antioxidants, which could potentially result in tissue damage. Consequently, it is identified as a key mechanism that drives cell death in neurodegenerative diseases, including glaucoma [23].

The retina is a complex structure with multiple specialized cell populations, including photoreceptors, interneurons, and ganglion cells, both pigmented and non-pigmented. It also includes three subtypes of neuroglia, each with multiple functions (Figure 2) [24-27]. During glaucomatous neurodegeneration, oxidative stress initiates an immune response. ROS boosts

the capability of glial cells to present antigens, subsequently serving as co-stimulants during this process [23]. Furthermore, substantial accumulations of ROS prompt damaged cells to release inflammatory cytokines, including tumor necrosis factor-alpha (TNF-α) and interleukins (ILs), along with vascular endothelial growth factor (VEGF) along with diverse chemokines [28,29]. In glaucoma, exogenous or self-antigens and elevated IOP trigger neuroinflammation via Toll-like receptor (TLR) and tumor necrosis factor receptor (TNFR) signaling routes. This activation leads to glial NF-κB activation and the formation of inflammatory vesicles [30-34].

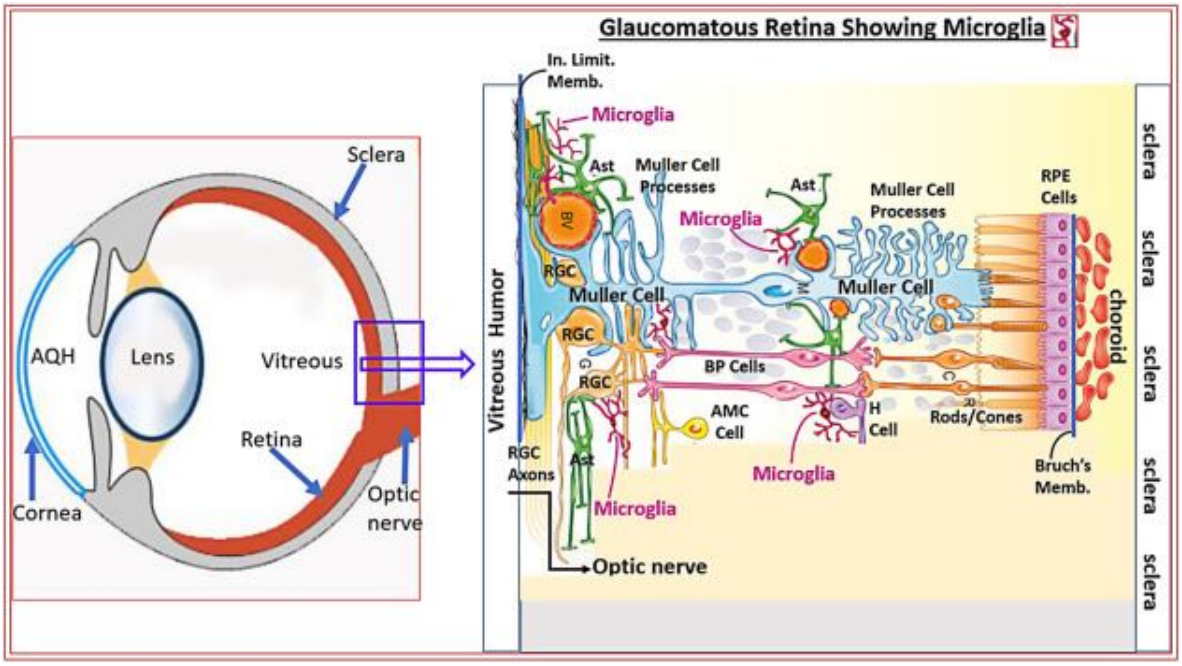

Figure 2 This figure details the various retinal cells and their interconnections, explicitly focusing on their positioning relative to the lamina cribrosa and the ONH.
The presence of activated microglia is highlighted as an example of the cellular changes that occur during the progression of diseases such as ocular hypertension (OHT), primary open-angle glaucoma (POAG), and NTG (refer to Figure 4). Key abbreviations include AMC, which corresponds to amacrine cells; Ast., which corresponds to astrocytes; BP, which corresponds to bipolar cells; H, which refers to horizontal cells; and Memb, which refers to the membrane. Image from *Najam A. Sharif et al., 2023* [35].

Significantly, during glaucomatous neurodegeneration, an alternative aspect of oxidative stress-induced glial dysfunction is its role in triggering aberrant immune responses [36]. In glaucoma eyes, glial cells are subjected to oxidative stress, which induces the generation of intrinsic ROS or exogenous ROS in the extracellular environment that can potentially damage these cells. Cerebral glial cells exhibit a plethora of antioxidant activities, such as superoxide dismutase, catalase, glutathione peroxidase, glutathione reductase, and NADPH regen-erase [37]. While glial cells can endure glaucomatous tissue stress, their immunomodulatory function

is altered. Therefore, alterations in glial cell function induced by oxidative stress are crucial for understanding their varying roles in supporting or impairing RGCs. Figure 3 shows that dysfunction in glial cells induced by oxidative stress could potentially exacerbate damage to neurons by promoting further decline of RGCs within glaucoma [23]. A substantial body of data suggests that glial cells can become neurodestructive under glaucomatous stress by emitting more neurotoxic substances, such as TNF-α and NO, linked to oxidative damage [23]. It is evident that upon release by glial cells, neurotoxic agents can facilitate neurodegeneration, possibly serving as a nonspecific method to eliminate damaged cells [38,39]. To gain a deeper insight into the complex cellular reactions to stress in glaucoma-affected tissues, including neuronal death alongside the retention and activation of glial cells [23]. Laboratory research utilizing primary cultures of RGCs and glial cells demonstrates that their variable responses to glaucomatous stimuli partly stem from the unique regulation and functioning of diverse signaling molecules, thought to determine these cells' outcomes 23. The molecules of signaling under discussion encompass those associated with mitogen-activated protein kinases (MAPKs), including ERK, JNK, and p38 kinases, in addition to nuclear factor kappa B (NF-κB) [40]. These in vitro results align with the observed differences in MAPK activity within glaucomatous human eyes among RGCs and glial cells [41] and support in vivo studies showing that MAPK is crucial in determining the fate of RGCs following ON injury [42]. The unique signaling molecule activation patterns among RGCs may be related to the comparative resilience of glial cells to glaucomatous damage and numerous other factors.

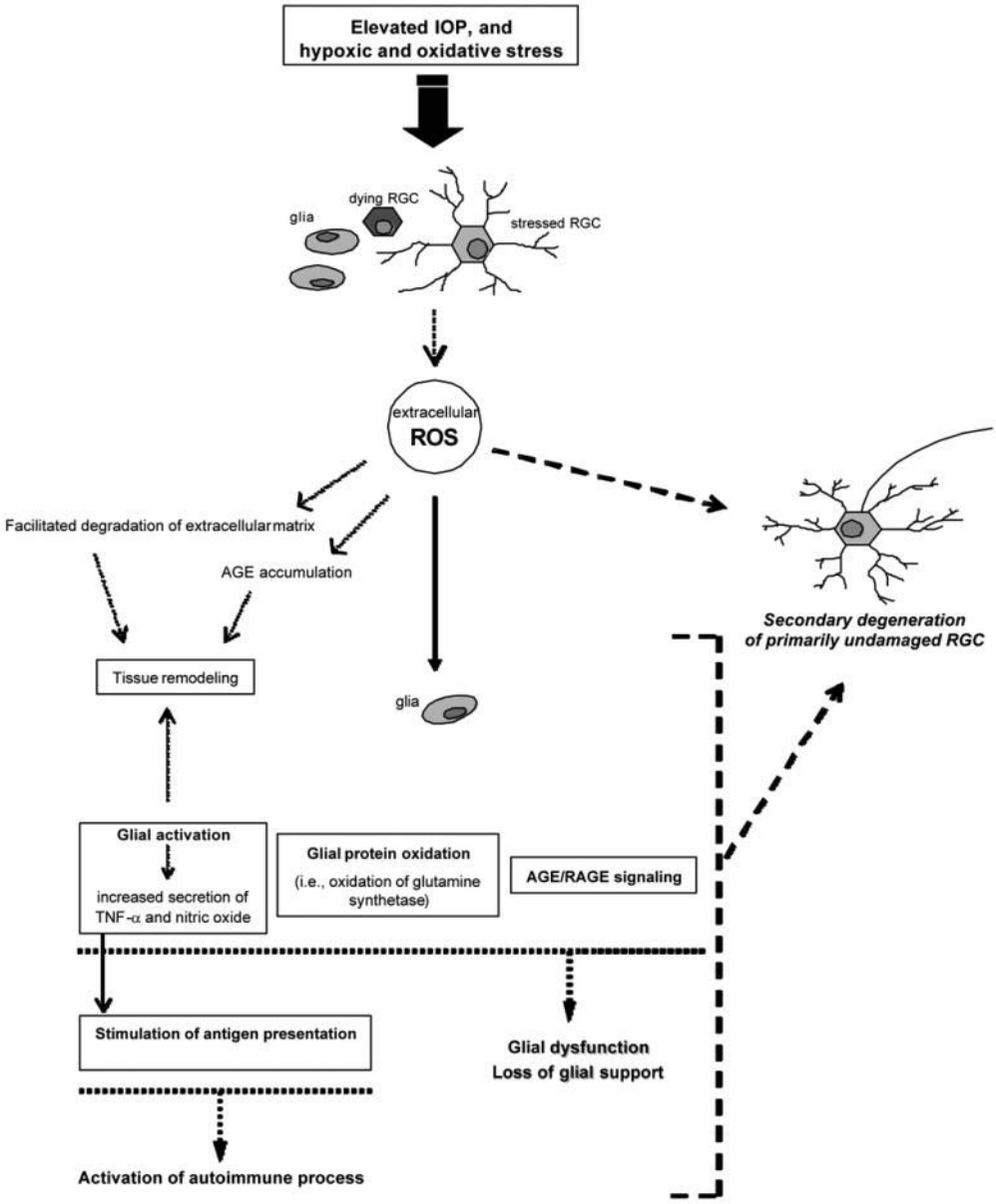

Figure 3 Besides the neurodegenerative injury caused by intracellular ROS, the ROS that stressed cells release into the extracellular environment can also promote secondary degeneration of RGCs.

ROS emitted by neighboring cells can be directly cytotoxic to primarily undamaged RGCs. Oxidative stress-induced activation of glial cells, glial fibrillary acidic protein oxidation, and signaling mediated by advanced glycation end-products and their receptors (AGE/RAGE) may compromise the supportive role of glial cells towards RGCs. Enhanced ROS production boosts the antigen-presenting capabilities of glial cells, potentially leading to aberrant activation of the immune system, thereby accelerating the progression of neurodegenerative diseases within glaucoma. Image from *Gülgün Tezel et al., 2006* [23].

Typically, neuroglials are relatively stable in the resting state, which maintains homeostasis of the internal environment, including sustaining the blood-brain/blood-retinal barrier, reprocessing neurotransmitters, and maintaining vascular perfusion while conserving synaptic integrity [35]. To accomplish these tasks, they are interlinked with capillary networks, neuronal soma, and RGC axonal tracts within the retina, extending into the posterior segment of the ON (Figure 4A) [43-45]. The blood-retinal barrier (BRB) is a complex neurovascular structure composed of an internal retinal vascular endothelium and an external retinal pigment epithelium. These components are connected by specific tight junctions that effectively prevent the accumulation of extracellular fluids, functioning similarly to the blood-brain barrier (BBB) [46]. The BRB plays a crucial role in maintaining the retina as an immunologically privileged site by preventing the infiltration of systemic immune and inflammatory components [47]. Additionally, local immunosuppression within the eye is primarily facilitated by the blood-aqueous barrier, the BRB, and immunosuppressive cytokines and neuropeptides that rapidly clear immune cells entering the retina due to apoptosis [48].

However, an increase in the production of inflammatory mediators, such as the complement system and cytokines (e.g., TNF-α), can compromise the efficacy of the BRB, leading to edema through the compression of surrounding cells and subsequently disrupting cellular functions [49]. In response to acute or chronic inflammatory triggers, more pro-inflammatory mediators can infiltrate ischemic tissues through gaps between endothelial cells (i.e., the BRBs), inducing rapid microglial/monocyte infiltration and neuroglial proliferation, further exacerbating the pathological state of the tissue [29]. These findings underscore the importance of maintaining BRB integrity in preventing and treating retinal diseases.

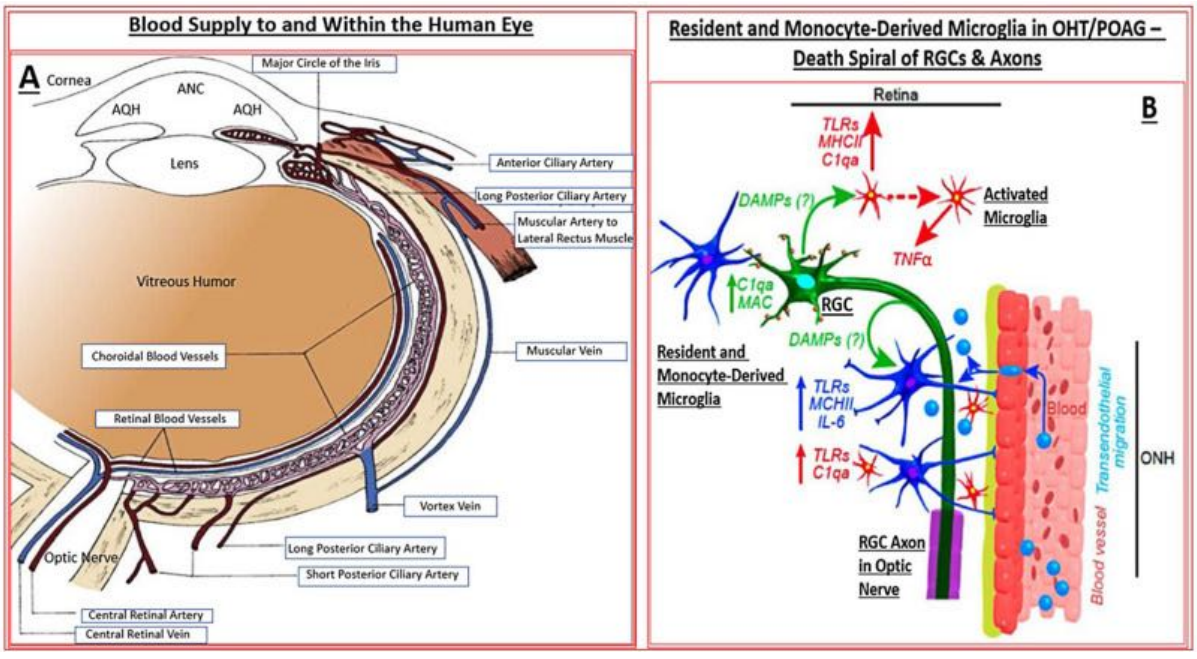

Figure 4 (A) outlines the blood supply to various ocular structures. (B) The illustrations focus on the ONH and LC areas, demonstrating how the optic nerve at the LC reacts to increased IOP in the eye's ANC.
Monocytes migrate from the retinal, choroidal circulation and traverse endothelial cells, penetrating through the RPE layer and transforming into activated microglia. These activated microglia join the resident population and instigate significant damage within the retina by releasing cytokines, chemokines, and other cytotoxic substances. This process triggers the activation of the complement system and the deposition of the MAC, leading to the death of RGCs and their axons. A similar cascade of inflammatory and immune responses occurs in the ON, disrupting the retina and brain connection. These reactions can ultimately lead to impaired vision or complete vision loss. This pathway highlights the critical roles that immune cell migration and activation play in the pathogenesis of neurodegenerative diseases within the visual system. Image from *Najam A. Sharif et al., 2023* [35].

In addition, damage to the BBB and BRB could also occur during aging, mediating inflammatory or immune responses. Although such damage is not observed in all cases of aging, significant evidence indicates that T lymphocyte infiltration induces microglia activation, which subsequently contributes to the deterioration of RGCs amid age-related neurodegeneration, such as glaucoma [50]. Neuroinflammatory responses mediated by retinal glial cells are crucial in the degeneration of RGCs and the ON in glaucoma [24,51]. Hence, RGC loss is associated with microglia activation in IOP-induced ON injury and optic nerve crush (ONC) models [52,53]. Cytokines and chemokines released by activated neuroglia recruit additional immune cells from the dilated vasculature to the injury site, involving monocytes and leukocytes, participate in orchestrating retinal inflammatory signals (Figure 4B), and the inflammatory response is amplified [35], which plays a pivotal role in exacerbating RGC damage in glaucoma [52-54] (Figure 5). Thus, the timing of changes in glial cells and the pattern of RGC degeneration is critical for developing neuroprotective therapies to manage the neuroinflammatory process triggered by RGC death.

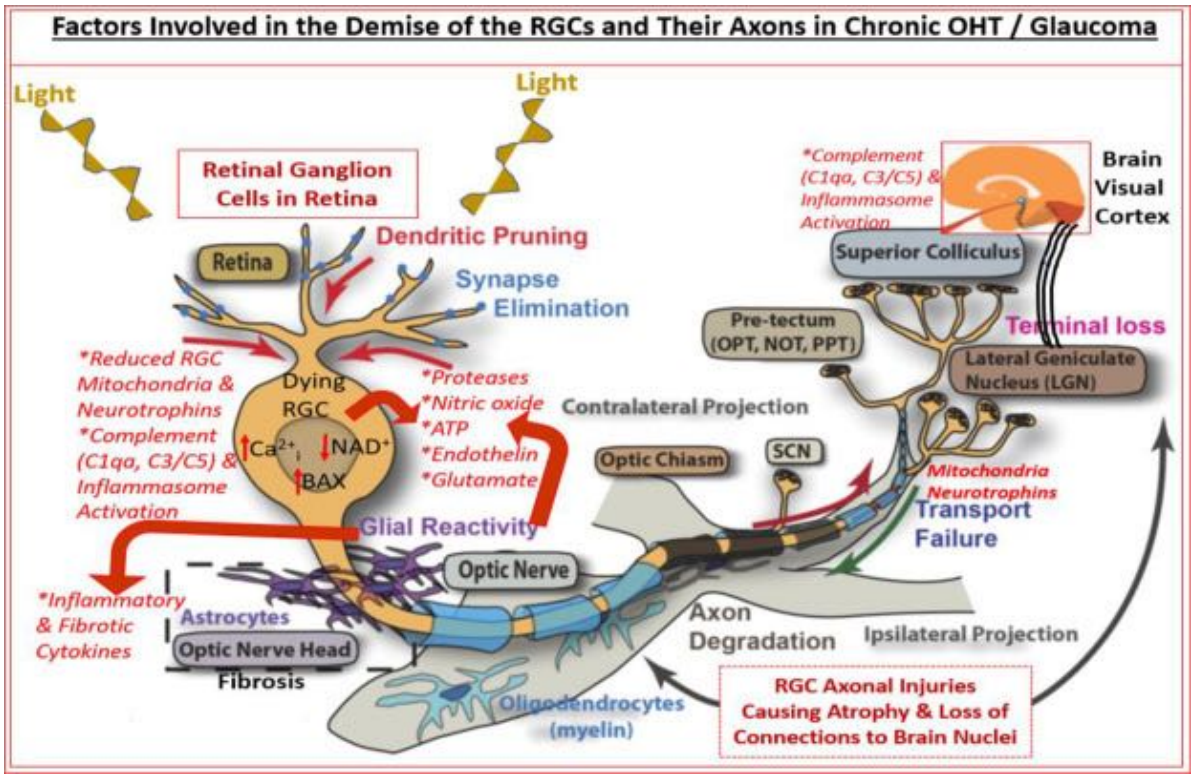

Figure 5 During chronic OHT and glaucoma progression, a series of complex harmful events affect individual RGCs and their axons, leading to their dysfunction and eventual death. Image from *Najam A. Sharif et al., 2023* [35].

3.3. Family members of NADPH oxidases.

NADPH oxidase (NOX), often referred to as the master ROS-producing enzyme, is uniquely involved in the production of ROS and is extensively expressed across both vascular and nonvascular cells [55]. NADPH oxidase is recognized as a critical source of oxidative stress in various retinal ocular disorders, including glaucoma, ischemic retinopathy, and age-related macular degeneration [56,57,58]. This enzyme family includes seven members: NOX1, NOX2 (previously referred to as gp91 ^{phox}), NOX3, NOX4, NOX5, and the dual oxidase proteins Duox1 and Duox2, each with unique activation mechanisms (Figure 6) [59].

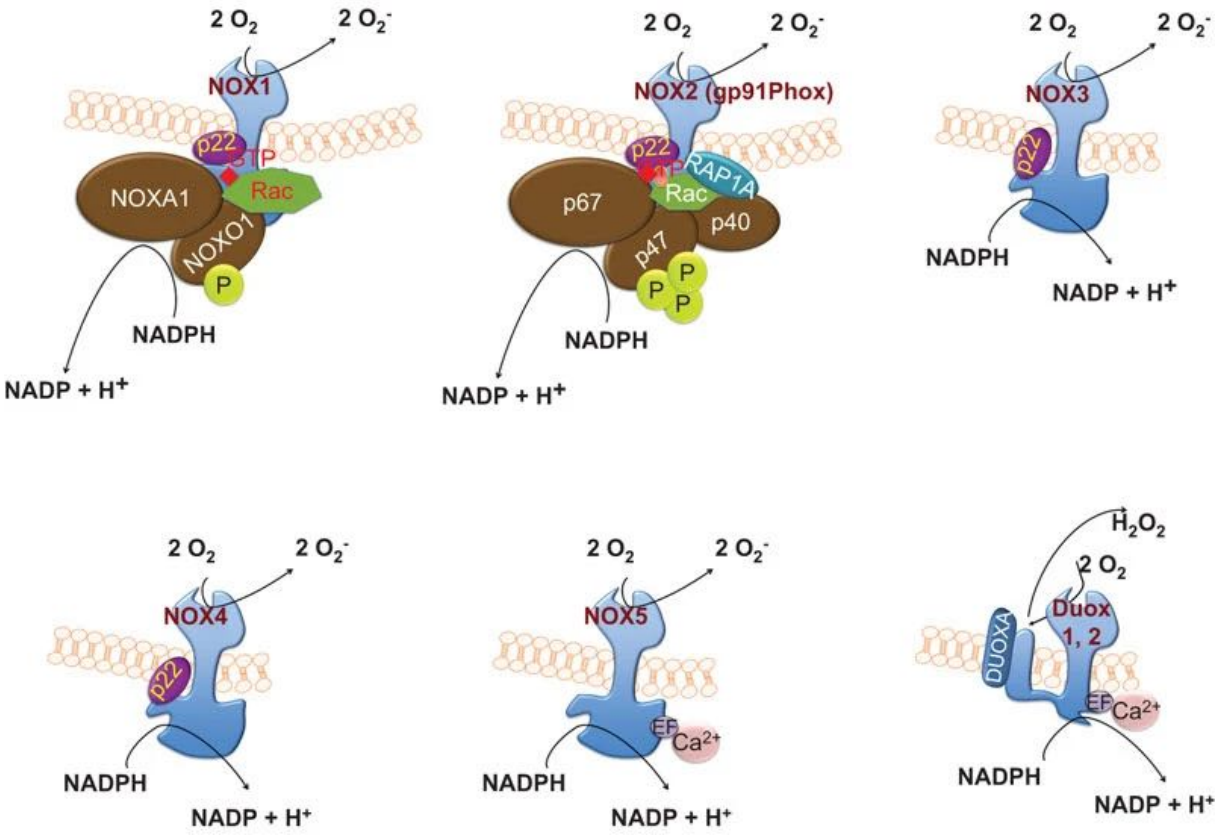

Figure 6 Assembly and activation of NOX enzymes:
The activation of NOX1 and NOX2 entails the phosphorylation of NOXO1 and p47 [phox], respectively, followed by the translocation of the entire multidomain complex—comprising p40 [phox], p67 [phox], and Rac—from the cytosol to the membrane. This process facilitates the transfer of electrons from the substrate to oxygen. Like NOX1 and NOX2, NOX3 also depends on p22 [phox], though it does not interact with Rac. The activation of NOX4 similarly requires p22 [phox]. In contrast, the activation of NOX5 and Duox is dependent on calcium. Image from *Panday, A. et al., 2015* [59].

NOX2, commonly referred to as gp91 [phox], contains six transmembrane domains [60]. It forms a constitutive association with p22 [phox], which stabilizes the NOX2 complex [61]. Activation of NOX2 necessitates the translocation and binding of phosphorylated p47 [phox], which then allows additional cytosolic components, such as p67 phox and p40 [phox], to interact with the NOX2/p22 [phox] complex [62-64]. Upon assembly of the complex, the GTPase Rac initially interacts with NOX2, followed by its interaction with p67 [phox], forming an activated complex. This activated complex generates superoxide by transferring electrons from cytosolic NADPH to oxygen in the phagosome or extracellular space [65,66].

NOX1 was discovered as the first homolog of NOX2, with which it shares 60% amino acid sequence identity [67,68]. Studies have indicated that this protein is membrane-bound and may

be localized within caveolae [69,70]. The identification of NOX Organizer 1 (NOXO1), a homolog of p47 [phox], and NOX Activator 1 (NOXA1), a homolog of p67 [phox], further supports the dependence of NOX1 activity on cytosolic subunits [70-72]. The activation of NOX1 depends on the membrane subunit p22 [phox], cytosolic subunits, and Rac GTPase. NOX3 shares 56% amino acid identity with NOX2 [73,74]. Like NOX1 and NOX2, NOX3 also relies on p22 [phox]; however, the specific role of p22 [phox] in NOX3 function is not yet fully understood [74,75]. Additionally, some studies suggest that NOXO1 and NOXA1 are essential for NOX3 activation, although the participation of p47 [phox] and p67 [phox] under physiological conditions has not been definitively established, the role of Rac in NOX3 activation remains a subject of debate [73,74,76].

NOX4 has about 39% sequence homology with NOX2 [77,78]. The activity of NOX4 is primarily dependent on p22 [phox] [79], but unlike other NOX enzymes, it does not require cytosolic subunits [80]. Furthermore, the involvement of Rac in the activation of NOX4 remains questionable [81]. NOX5 comprises five isoforms: α, β, γ, δ [82], and a fifth isoform known as NOX5ε or NOX5-S [83]. Isoforms NOX5 α–δ have an extended intracellular N-terminal domain that includes EF-hand regions responsible for Ca^{2+} binding [82,84]. The fifth isoform, however, lacks the EF-hand regions and structurally resembles NOX1-4 [83]. The NOX5 α–δ isoforms do not rely on p22 [phox] or cytosolic subunits for activation; instead, they depend on cytosolic calcium due to the presence of Ca2+ binding domains [75]. In contrast, the NOX5ε isoform, which does not contain the Ca^{2+} binding domain, depends on cAMP response element-binding protein for its activation [85].

Dual oxidases (Duox1 and Duox2), also referred to as thyroid oxidases, share roughly 50% amino acid identity with NOX2 [86,87] and have been recognized as glycosylated proteins found in the plasma membrane and endoplasmic reticulum [87-89]. The retention of Duox proteins in the endoplasmic reticulum depends on the maturation factors DuoxA1 and DuoxA2 [90]. The immature, partially glycosylated form of Duox2 generates O_2, while the mature form produces H_2O_2 [91]. Although research suggests a direct physical interaction between Duox proteins and p22 [phox], there is no conclusive evidence to determine if p22 [phox] is necessary for their activation [87,91,92]. Moreover, Duox proteins can be activated by Ca^{2+} without the need for cytosolic activators or organizer subunits [91].

NOX family members not only control normal physiological processes but also contribute to the development of pathologies related to infections, vascular disorders, and compromised immune responses caused by environmental factors. The NOX1, NOX2, and NOX4 have been most extensively researched in the context of ocular pathology [93].

3.4. Expression of NADPH oxidase mediates pathophysiologic alterations in glaucoma.

High IOP in animals is commonly induced through photocoagulation targeting trabecular meshwork structures or cauterization applied to external scleral veins [94]. Studies have shown that following laser photocoagulation, NOX2 co-localizes with activated microglia at the optic nerve head (ONH) in mice, where ROS generated by NOX2 disrupt axonal transport [95]. In models where high IOP is induced by unilateral scleral episcleral vein cauterization, there is an associated activation of astrocytes and microglia in the retina, along with an increase in NOX2 mRNA expression [96]. This supports NOX2's role in retinal inflammation.

Despite evaluations of NOX2 expression in two high IOP models, the interactions between NOX2 and microglial activation require further investigation [95,96]. Intriguingly, NOX2 in microglia is suggested to encourage polarization to an M1-like phenotype after traumatic brain injury, which is crucial for the inflammatory response [97]. The deletion of the NOX2 gene is noted to reduce this M1-like activation [98], highlighting NOX2's significant role in neuroinflammation. Given that microglial activation can exacerbate RGC damage in glaucoma [27], understanding whether NOX2 influences microglial polarization in glaucoma models is critical.

Additionally, NOX2 expression has been detected in the small arterioles of the retina in mice models with high IOP [99]. In these models, NOX2 (but not NOX1) mRNA levels are elevated, contributing to ROS production that impairs endothelium-dependent relaxation of retinal vessels under high IOP conditions [99]. Similar to microvascular networks in the brain, NOX2 is implicated in angiotensin II-induced endothelial dysfunction [100] and promotes leukocyte migration across the endothelium [101], facilitating the entry of pro-inflammatory cytokines into the ONH during inflammation. Such neuroinflammation and RGC degeneration further drive glaucoma progression [102].

These findings underline the role of NOX2 in promoting inflammation and endothelial dysfunction under high IOP conditions, emphasizing its importance in the pathogenesis of glaucoma.

3.5. Gene targeting or pharmacological inhibition of NADPH oxidase offers significant potential to protect against RGC loss

The concept of "neuroprotection" represents a therapeutic strategy to prevent or slow down the neurodegenerative processes in glaucoma, particularly the progression of RGC death [103]. Addressing the complex pathways in the apoptotic cascade is crucial for protecting RGCs

[104,105]. The imbalance between the generation of ROS and inadequate antioxidant defense may compromise the integrity of RGCs, ultimately leading to RGC apoptosis, either directly or indirectly [106-109]. Consequently, enhancing antioxidant activity presents a promising approach to neuroprotection, especially since oxidative stress, such as mitochondrial dysfunction, is a common element across all forms of glaucoma [110]. While antioxidants are currently being tested in clinical trials for glaucoma and animal studies, high doses are typically required to counteract the elevated ROS levels in these disease states [111]. Therefore, targeting the origins of ROS generation appears to be more effective as an alternative approach to control oxidative stress.

Pharmacological inhibition of NADPH oxidase is one strategy for blocking one of the primary sources of ROS. This approach has been extensively explored in retinal diseases like ischemic retinopathy and inflammation [112-114]. Pharmacological targeting of NOX enzymes in glaucoma models is limited, primarily focusing on non-selective inhibitors like apocynin, with studies in NOX2-deficient mice showing beneficial effects [115]. GKT137831, a dual inhibitor of NOX1 and NOX4, stands out as the first inhibitor recognized and classified by the World Health Organization (WHO) [116]. GKT137831 has been investigated for its potential protection in models of ischemic ocular disorders, inflammation in the retina mimicking diabetic conditions, and cultured retinal endothelial cells [114,117-119]. Similarly, GSK2795039, a small molecule targeting NOX2, has shown efficacy in animal models of inflammation and inflammatory cells such as neutrophils and monocytes in culture [120,121]. Before inducing traumatic brain injury in mice, administration of GSK2795039 effectively suppressed NOX2-dependent production of ROS in neurons located in the injured cerebral cortex, thereby promoting cell viability, improving neurological outcomes, and protecting the blood-brain barrier up to 24 hours post-injury [122]. Collectively, this evidence highlights that NOX2 inhibition has neuroprotective effects.

Therefore, elucidating the role of NOX2 gene-targeted deletion or pharmacologic intervention in glaucoma animal models provides a sufficient and necessary medical requirement. The present study investigated whether loss of RGC is associated with NOX2 activation in glaucoma, whether inhibition or deletion of NOX2 is neuroprotective in glaucoma animal models, and its underlying molecular mechanisms.

4. Oxidative Stress, Vascular Endothelium, and the Pathology of Neurodegeneration in Retina

antioxidants

MDPI

Review

Oxidative Stress, Vascular Endothelium, and the Pathology of Neurodegeneration in Retina

Xin Shi †, Panpan Li †, Hanhan Liu and Verena Prokosch *

Department of Ophthalmology, Faculty of Medicine and University Hospital of Cologne, University of Cologne, 50937 Cologne, Germany; shixinsx123@gmail.com (X.S.); panpanlimed@gmail.com (P.L.); hanhan.liu@uk-koeln.de (H.L.)

* Correspondence: verena.prokosch@uk-koeln.de; Tel.: +49-6131-173326

† These authors contributed equally to this work.

Abstract: Oxidative stress (OS) is an imbalance between free radicals/ROS and antioxidants, which evokes a biological response and is an important risk factor for diseases, in both the cardiovascular system and central nervous system (CNS). The underlying mechanisms driving pathophysiological complications that arise from OS remain largely unclear. The vascular endothelium is emerging as a primary target of excessive glucocorticoid and catecholamine action. Endothelial dysfunction (ED) has been implicated to play a crucial role in the development of neurodegeneration in the CNS. The retina is known as an extension of the CNS. Stress and endothelium dysfunction are suspected to be interlinked and associated with neurodegenerative diseases in the retina as well. In this narrative review, we explore the role of OS-led ED in the retina by focusing on mechanistic links between OS and ED, ED in the pathophysiology of different retinal neurodegenerative conditions, and how a better understanding of the role of endothelial function could lead to new therapeutic approaches for neurodegenerative diseases in the retina.

Keywords: oxidative stress; endothelium; neurodegeneration; retina

Citation: Shi, X.; Li, P.; Liu, H.; Prokosch, V. Oxidative Stress, Vascular Endothelium, and the Pathology of Neurodegeneration in Retina. *Antioxidants* **2022**, *11*, 543. https://doi.org/10.3390/antiox11030543

Academic Editor: Michele C. Madigan

Received: 6 January 2022
Accepted: 10 March 2022
Published: 12 March 2022

1. Introduction

Oxygen, which plays a crucial role for living organisms, is also considered a double-edged sword. It can be actively involved in signal transduction, gene transcription, and multiple cellular activities, but it also generates harmful effects on biomolecules in the form of free radicals. Highly reactive atoms or molecules with one or more unpaired electrons in their outer shells can form radicals when oxygen interacts with certain molecules [1], such as the hydroxyl radicals (HO•), superoxide radical anion ($\bullet O_2^-$), hydroperoxyl radicals ($HO_2\bullet$), and peroxyl radicals (ROO•). Free radicals can behave as oxidants or reducers in cells by accepting or losing an electron [2]. Reactive oxygen species (ROS) and reactive nitrogen species (RNS) refer to reactive free radicals and nonradical derivatives of oxygen and nitrogen, respectively. ROS/RNS can be produced by all aerobic cells [3]. "ROS" stands for both oxygen free radicals and nonradicals (H_2O_2, $1O_2$, etc.) that can be conveniently converted to free radicals [4–7]. ROS/RNS are not only associated with energy extraction, immune defense, and signaling processes but may also generate harmful effects [8]. Under normal circumstances, homeostasis ROS act as secondary messengers in various intracellular signaling pathways of the cardiovascular system [9]. Nevertheless, once the production of ROS/RNS and other oxidants exceeds the antioxidant defense, they may trigger cellular oxidative stress (OS) [10]. OS may contribute to subsequent oxidative modifications or damage to lipids, proteins, and DNA, with deleterious consequences for metabolism and cardiovascular disease [9], which is considered to be responsible for the pathogenesis of numerous age-related neurodegenerative diseases. ROS contribute significantly to the degeneration of neuronal cells by regulating the function of biomolecules. ROS involved in neurodegeneration includes hydrogen peroxide (H_2O_2), superoxide anions

(O_2^-), and highly reactive HO•. O_2^- is generated by adding an electron to oxygen, and several mechanisms exist to generate superoxide in vivo [11]. Moreover, electron transport chains in the inner membrane of mitochondria reduce oxygen to water. During this process, free radical intermediates are produced, which are usually tightly bound to the components of the transport chain. However, some electrons keep leaking into the mitochondrial matrix, which leads to the formation of superoxide [12,13]. In addition, the vascular endothelium probably produces O_2^- continuously to neutralize nitric oxide, other cells generate superoxide to regulate cell growth and differentiation, and phagocytes produce superoxide during oxidative bursts [14,15]. The results of a systematic review and meta-analysis of randomized controlled trials indicated that markers of oxidative stress were increased in glaucoma overall (effect size = 1. 64; 95% CI 1.20–2.09), which ranged from an effect size of 1.29 (95% CI 0.84–1.74) in serum to 2.62 (95% CI 1.60–3.65) in aqueous humor. Although antioxidative stress markers in serum were decreased (effect size = −0.41; 95% CI −0.72 to −0.11), several were increased in the aqueous humor (superoxide dismutase, effect size = 3.53; 95% CI 1.20–5.85; glutathione peroxidase, effect size = 6.60; 95% CI 3.88–9.31). In addition, the increase in some antioxidant markers is probably a protective response of the eye to oxidative stress [16].

Endothelial cells (ECs) form the innermost lining of the vasculature. In the retina, ECs tightly interact with other cells within the neurovascular system to regulate blood–retina barrier integrity, neurovascular coupling, immune signaling, and neuronal metabolism [17–21]. While endothelial function plays a key role in the homeostasis of retinal neurons, the endothelial function can be impacted by increased OS [22–24]. Special receptors on EC membranes initiate intracellular signal cascades in response to agonists that activate specific receptors or changes in cell surface shear stress caused by changes in blood flow rate. Gap junctions allow crosstalk between adjacent ECs, thereby allowing the transmission of intracellular reactions. Once activated, these cascades trigger the release of potent vasodilator substances, such as nitric oxide (NO) and prostaglandins and vasoconstrictors, such as endothelin and endothelium-derived vasoconstrictors [25–27]. At low concentrations, ROS act as vasodilators, but at high concentrations, it may result in vascular dysfunction [28]. Systemic oxidative stress is associated with reduced ocular hemodynamic flow [29], which is linked to vascular permeability. Significantly higher endothelin-1 blood levels have been found in patients with POAG [30]. The association of nitric oxide with glaucoma has been previously reported [31]. Therefore, this review focuses on the impact of OS on endothelial function and the roles of endothelial dysfunction (ED) in retinal neurodegenerative diseases.

2. The Role of Endothelial Function in Human Diseases

Endothelial cells are located in the intimal layer of the vascular wall, making up about 1.5% of the total body weight [32–34]. Over the years, the endothelium has been recognized as more than a simple barrier to boundary the vascular wall [32,35]. As the innermost layer of blood vessels, the endothelium is considered to be a dynamic, adaptive interface between the blood circulation and the internal environment. The vascular endothelial cells are subjected to hemodynamic forces [36]. At the same time, ECs also send out various necessary signals and regulate vascular permeability by producing many messengers, which have good biological functions [37,38]. The biomechanical signals from blood and surrounding tissues provide selective barriers for the permeability of macromolecular substances while separating blood components from vascular wall matrix and tissues. Depending on the needs of the tissue, endothelium regulates vascular tension and changes vascular diameter by releasing vasodilator molecules, such as prostacyclin (PGI2) and vasoconstrictor molecules, such as endothelin and thromboxane A2 [39]. In addition, ECs also regulate blood fluidity by secreting anticoagulants, procoagulants, and fibrinolytic substances, control angiogenesis by producing angiogenic growth factors, and regulate acute and chronic by expression of cytokines, chemokines, and adhesion molecules. The endothelium responds to hemodynamics through mechanical sensors [40]. Moreover, ECs

can also reduce intracellular apoptosis by integrating neurohumoral and inducing adaptive signaling pathways [41]. On all counts, the endothelium has anti-inflammatory and anti-coagulant effects, contributes to the anti-thrombus formation, and controls permeability, endothelium and muscle growth (reshaping blood vessel), and vasoconstriction.

3. Endothelium Dysfunction

The endothelium plays a significant role in regulating vascular tone through the synthesis and release of a range of endothelium-derived diastolic factors, including the vasodilators prostaglandins, NO, and endothelium-dependent hyperpolarizing (EDH) factors, as well as endothelium-derived contractile factors [42,43]. Endothelium dysfunction is defined as an imbalance in the production of vasodilators and vasoconstrictors, which predisposes the vascular system to a prothrombotic and proatherogenic phenotype [44]. ED is primarily caused by reduced production or weakened activity of endothelial-derived relaxing factors, which are associated with a multitude of diseases, including atherosclerosis, diabetes, coronary artery disease, hypertension, hypercholesterolemia, and hyperhomocysteinemia (HHcy) [45,46]. ED has a multitude of distinguishing features, including disruption of vascular tone, redox imbalance, increased inflammatory response within the vessel wall [47], vasoconstriction (due to the impaired activity of vasodilator mediators), overexpression of leukocyte and platelet adhesion molecules, platelet activation (the secretion of active substances, increased von Willebrand factor and tissue factor), mitosis, pro-oxidation, impaired coagulation (anticoagulant factors such as heparin decreased), atherosclerosis, and thrombosis [44,48–50].

NO has a multi-biological regulatory role, including vascular smooth muscle cell relaxation and proliferation, leukocyte adhesion, angiogenesis, platelet aggregation, thrombosis, vascular tone, and hemodynamics, as well as inhibiting the production and/or activity of other vasoactive factors such as prostaglandins and endothelin-1 (ET-1) in response to vasoconstrictors [51]. When the NO-mediated reaction is functionally impaired, PGI2 and/or EDH contribute to functional compensation. Subsequently, as the ability of ECs to release NO gradually decreases, the production and activity of endothelium-derived cyclic oxygenase-dependent contractile factor (EDCF) and/or ET-1 becomes prominent, facilitating vasoconstriction. Simultaneously, due to the weakened protective effect of NO, the expression of endothelial cell adhesion molecules (e.g., vascular cell adhesion molecule 1 (VCAM-1), intercellular adhesion molecule 1 (ICAM-1)) is enhanced, which promotes leukocyte adhesion and infiltration. All these factors would result in the failure of the endothelium to perform its basic activities (i.e., regulation of vasodilation and/or cellular redox homeostasis), as well as decreased NO production is associated with damage to vascular smooth muscle dilation [52] (Figure 1).

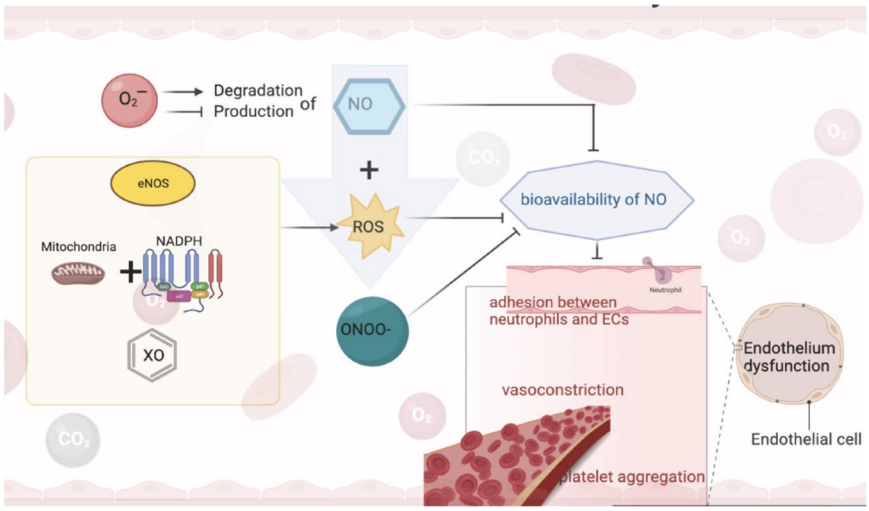

Figure 1. NO and endothelium dysfunction.

4. Oxidative Stress and Endothelium Dysfunction

Oxidative stress (OS) occurs when there is an imbalance between ROS production and the antioxidant defense system [53]. NO is the primary endothelial regulator of local vascular tone, which is essential for maintaining vascular homeostasis in the endothelium. NO bioavailability decreased due to O_2^--reducing NO production and/or increasing NO degradation, which marks the beginning of ED [54]. The free form of NO is hazardous to biomolecules. In addition, xanthine oxidase (XO), nicotinamide adenine dinucleotide phosphate (NADPH) oxidase, and uncoupled endothelial NO synthase (eNOS) as potential sources of enzymes may be responsible for increased ROS [55]. Mitochondria [56] react with membrane-related NADPH oxidase [57] to produce ROS. The increase in ROS production will dwindle the bioavailability of NO, thus promoting vasoconstriction, weakening the inhibition of platelet aggregation, as well as inducing the adhesion between neutrophils and ECs, while NO reacts with ROS to produce a strong oxidant—peroxynitrite (ONOO-). When NO reacts to peroxynitrite, NO no longer has normal physiological functions. These changes will provoke ED and perhaps cause alteration in intracellular signal pathways and transcription factor-mediated gene expression in ECs. OS caused by reduced NO production or increased ROS plays an important role in ED [58,59]. OS increases the phosphorylation of tyrosine kinases, such as focal adhesion kinase, post protein, and p130 cas in ECs, accompanied by increased stress fiber formation and neutrophil-endothelial cell adhesion [60,61]. Therefore, increased ROS and RNS levels and vascular OS is associated with ED [62,63]. The persistence of this condition probably induces endothelial contraction and death, increased permeability, and exposure of basement membrane components, which further amplifies the situation of vascular inflammation [48,62,64], causing significant damage to cells.

Vascular ROS act as significant intracellular signaling messengers, which could regulate vascular contractility, cell growth, and vascular remodeling [65]. Under normal physiological conditions, the majority of hazardous ROS are eliminated by the cellular antioxidant system. However, OS can trigger the pathogenesis of associated cardiovascular diseases [66]. Increased ROS production in blood vessels may result in pathologies associated with hypercholesterolemia, hypertension, diabetes, and aging [57]. It is well known that excess ROS contribute to lipid peroxidation and oxidative modifications of proteins and nucleic acids, which can cause ED [67]. OS and correlated oxidative damage are mediators of vascular damage and inflammation in numerous cardiovascular diseases, particularly in the setting of complications such as hypertension, hyperlipidemia, and diabetes [68,69]. The main source of OS in the arterial wall is NADPH oxidase (NOX) [70], which is involved in the production of ROS and the scavenging of NO [71]. In the endothelium, increased levels of ROS will reduce the bioavailability of NO, leading to vasoconstriction and ED. Other sources of ROS in the vascular wall include the mitochondrial respiratory chain and other enzymatic reactions, such as cyclooxygenases (COX), xanthine oxidase (XO), lipoxygenases (LOX), cytochrome P450, and dysfunctional eNOS [72–74]. Furthermore, the blood vessel wall is enriched with multiple enzymes, which could alleviate the ROS overload and act as an antioxidant defense system. These bio-enzymes include superoxide dismutase (SOD), catalase, glutathione peroxidase (GPx), hemoglobin oxygenase (HO), thioredoxin peroxidase (TPX), paraoxonase (PON) [72,75,76]. OS can be responsible for the oxidation of low-density lipoprotein (LDL), which inhibits the release of endothelium-derived NO or closely related molecules even more than natural or unoxidized LDL [24]. In addition, oxidized LDL (ox-LDL) exerts a multitude of biological effects, such as cytotoxicity to ECs, chemotaxis to monocytes, and the accumulation of inflammatory cells and ROS in the vascular system [77,78].

Interestingly, studies have confirmed that correcting hypercholesterolemia or treating cell cultures and experimental animals with SOD or SOD simulants can reduce vascular $O_2\bullet$-levels and restore endothelial function [79]. It has been reported that XO inhibitors hydroxypurinol or allopurinol can improve ED in hypercholesterolemia [80]. Therefore, XO may become a significant source of ROS production in vascular ECs and is related to ED

in some vascular diseases. Moreover, the reduction of NO-dependent dilation induced by OS and alterations in vascular smooth muscle function directly contribute to microvascular dysfunction in major depressive disorder (MDD) [81].

La Favor et al. [82] exploited a novel microdialysis technique that allows simultaneous measurement of ROS levels and microvascular endothelial function in vivo. They discovered that elevated levels of NADPH oxidase-derived ROS in obese subjects were associated with microvascular ED, such as impaired acetylcholine-induced increases in blood flow. Interestingly, Gray et al. [83] demonstrated that NADPH oxidase 4-derived H_2O_2 provides vasoprotective effects in a mouse model of diabetic atherosclerosis. However, Gutterman's laboratory has proposed a new mechanism for microvascular dysfunction, in which various atherosclerotic conditions and metabolic disorders lead to the conversion of endothelium-dependent relaxing mediators from NO to H_2O_2 (ceramide-induced reduction in mitochondrial telomerase activity has been shown to cause this conversion) [84,85]. As a consequence, the pathological levels of H_2O_2 act similar to a double-edged sword, which results in microvascular dysfunction and the development of coronary artery diseases [86]. Deficiency of eNOS caveolin-1 negative regulator or overexpression of eNOS will disrupt the physiological balance of EDH factors (e.g., NO, H_2O_2) in the microcirculation, which contributes to the overproduction of endothelial NO in mice with cardiovascular lesions [87]. Among the redox-regulated proteins, endothelial thioredoxin reductase 2 has been demonstrated to play a role in maintaining the healthy endothelial function [88], while peroxisome proliferator receptor-γ coactivator 1α is also considered to be a principal regulator of endothelial function, including the prevention of OS, inflammation, and atherosclerosis [89].

Hyperhomocysteinemia (HHcy) is an independent risk factor for cerebrovascular, cardiovascular, and peripheral arterial disease [90]. HHcy-related ED is a complex mechanism, whereby HHcy increases ROS production by a variety of mechanisms (e.g., HHcy autoxidation), which induces OS and an inflammatory state triggering the secondary cardiovascular disease, including atherosclerosis, hypertension, and neurodegeneration [91]. HHcy could cause an imbalance between antioxidant and oxidative enzymes by inhibiting SOD or activating NADPH oxidase [92]. Furthermore, auto-oxidation of the free thiol group of HHcy will generate H_2O_2, ROS, HO•, and O_2^-, with which NO could react to compose ONOO-, thereby reducing the bioavailability of NO [93]. Both in vitro and in vivo experiments have reported that HHcy can block GPx activity and HO-1, which promote ROS accumulation and exacerbate damage to ECs [94,95]. In addition, high plasma levels of HHcy induced apoptosis in ECs, due to endoplasmic reticulum stress, and increased ROS production and HHcy–thiolactone production [96].

Cells perceive and respond to the mechanical properties and cues of the microenvironment [96,97]. For example, this "mechanical sensing" allows vascular ECs to change the morphology, function, and gene expression in response to shear stress [98,99]. Mechanical stress, such as periodic tensile or shear stress, also stimulates NADPH oxidase activity in ECs [100,101]. However, elevated blood pressure (BP) itself can trigger damage to endothelial function and vascular remodeling [102]. The chronic presence of high BP was found to elicit increased arterial superoxide production by activating directly a protein kinase (PK) C-dependent NADPH oxidase pathway but also, in part, via activation of the local renin–angiotensin system [103].

5. The Role of Endothelial Dysfunction in Neurodegenerative Diseases in Central Nervous System

ED plays a key role in the pathogenesis of insufficient blood supply to various organs and tissues, including the brain [104], heart [105], and eyes [106], resulting in increased blood pressure [107,108] and insulin resistance [109]. Many neurodegenerative diseases have been shown to have pathological changes in ED, such as atherosclerosis, cancer, sepsis, Alzheimer's disease (AD), and multiple sclerosis [110]. ED, at the junction of blood vessels and peripheral nerves, is involved in a variety of diseases through different mechanisms,

including decreased levels of NO, increased expression of pro-inflammatory factors, and changes in endothelial cell permeability [111]. ECs in the brain form the blood–brain barrier (BBB), which strictly regulates the solute exchange between the vascular lumen and brain parenchyma. The destruction of BBB leads to the accumulation of blood-derived neurotoxic proteins (such as fibrinogen, thrombin, hemoglobin, ferritin, and free iron) in the brain parenchyma, which leads to neurodegenerative changes [112,113]. The patients and animal models of AD have demonstrated that the decrease in BBB tension is due to Aβ accumulation, leading to dysfunction of ECs and decreased expression of tight junction proteins in brain ECs [114–118]. Recently, some studies have shown that brain microvascular ECs produce amyloid-β peptide, which is perhaps a potential endothelium-dependent pathway that participates in Aβ deposition [119]. A potential pathway is the activation of proinflammatory cytokines induced by stress, which have been shown to induce the expression of adhesion molecules on the surface of vascular ECs [120].

6. The Pivotal Role of Endothelium Underlying Pathophysiology of Neurodegenerative Diseases in Retina

The central retinal artery provides nutrition and oxygen for neurons in the retina [121]. ECs are arranged in the lumen of microvessels as physical barriers between blood and surrounding tissues and play key roles in regulating retinal homeostasis [122]. Pericytes wrap around retinal capillaries and regulate the function of ECs [123]. In addition to maintaining the structural support of the vascular wall, peripheral cell coverage also regulates the expression of tight junction protein in adjacent ECs [123]. The basement membrane separates pericytes from ECs; however, the pores in this membrane matrix allow the formation of intercellular junctions between pericytes and ECs [124,125]. Outer blood–retinal barrier (oBRB) composed of retinal pigment epithelium (RPE) and internal BRB (IBRB) consisting of ECs protect retinal nerve cells from harmful molecules in circulation [126]. Tight junctions between adjacent RPE cells and ECs play regulatory roles in the strict control of fluid and solute crossing the blood–retinal barrier, which prevents toxic molecules and plasma components from entering the retina [126]. In a recently conducted meta-analysis investigating levels of oxidative stress markers and antioxidants in patients suffering from conical cornea for the first time, the authors reviewed 36 articles, published until 1 June 2020, with a total of 1328 conical cornea patients and 1208 healthy controls. Compared with healthy controls, patients with keratitis presented with an overall increase in oxidative stress markers (standard mean deviation (SMD) = 0.94; 95% confidence interval (95% CI) 0.55–1.33), accompanied by a decrease in antioxidants (−0.63, −0.89 to −0.36), which resulted in a significant decrease in total antioxidant capacity/status (−1.65, −2.88 to −0.43). Moreover, oxidative stress markers were found to increase in stromal cells, while antioxidants were reduced in endothelial cells [127]. In order to achieve normal visual function, highly coordinated activities of neurons, glial cells, microglia, and microvessels are essential. Ocular blood flow is adjusted by NO secreted by ECs and efferent nitroergic neurons. ED impairs ocular hemodynamics by reducing the bioavailability of NO and increasing the production of ROS. On the other hand, the production of NO by inducible nitric oxide synthase (iNOS) under the action of inflammatory mediators leads to neurodegeneration and cell apoptosis, which initiate serious eye diseases (Figure 2).

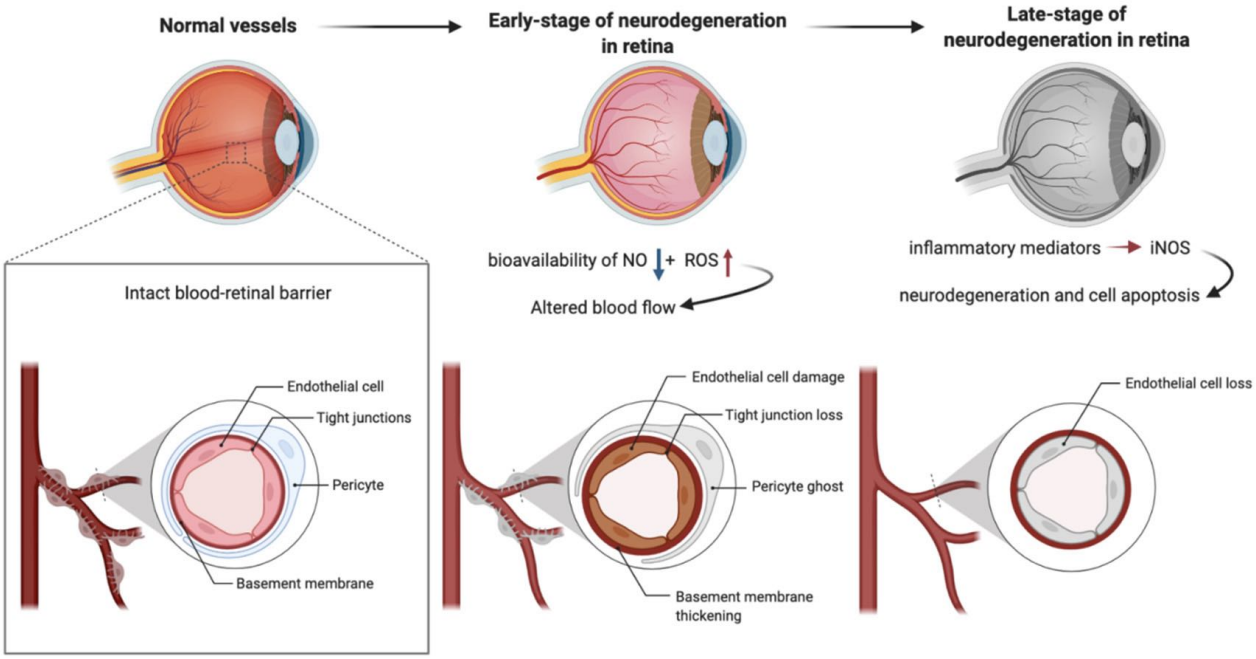

Figure 2. Endothelium and neurodegenerative diseases in retina.

The endothelium-derived NO possesses multiple complex physiological functions, such as inducing vasodilation, reducing vascular resistance, decreasing blood pressure, inhibiting platelet aggregation and adhesion, inhibiting leukocyte adhesion and migration, reducing smooth muscle hyperplasia, and preventing atherosclerosis. Shear stress, vascular endothelial growth factor (VEGF), insulin, or bradykinin can induce the phosphorylation of eNOS through phosphatidylinositol-3 (PI3) kinase and downstream serine/threonine–protein kinase Akt (protein kinase B), which leads to the enhancement of NO synthesis [128–130]. In the bovine retina, shear stress stimulates NO release from bovine retinal ECs monolayer [131]. VEGF increases retinal endothelial cell permeability through an eNOS dependent caveolae cell transport mechanism [132] or directly increases NO release from bovine choroidal ECs [133]. Michelson et al. [134] demonstrated that NOS-dependent vascular tension in retinal arteries and capillaries of patients with early hypertension is impaired. iNOS elicited a large amount of NO production is related to inflammatory response, as well as increased OS caused by hyperglycemia and ED, which is involved in the pathological changes in the retina and associated tissues in glaucoma and diabetic retinopathy. In a double-blind crossover study of healthy male subjects, Dallinger et al. [135] revealed that infusion of L-arginine (rather than D-arginine) increased choroidal pulsatile blood flow, mean ophthalmic artery velocity, and renal plasma flow, and that insulin infusion enhances vasodilation of L-arginine. They concluded that this stereo-specific vasodilation may be due to the promotion of membrane transport of L-arginine, which enhances the formation of intracellular NO or increases the bioavailability of NO. Intravenous injection of L-arginine can reduce mean arterial pressure and increase choroidal blood flow and retinal vein blood flow in healthy volunteers [136].

In healthy conditions, most ECs remain static and participate in the maintenance of barrier function and tissue homeostasis [137]. However, hyperglycemia induces OS in retinal endothelial cells (RECs), which further activates and interferes with a variety of metabolic pathways, leading to the self-perpetuating cycle of harmful OS and promoting the development of DR [138,139]; the ultimate consequence is to reduce the integrity of the blood–retinal barrier [140]. The OS of REC induced by hyperglycemia results from mitochondrial dysfunction [141]. Under the condition of hyperglycemia, the excessive production of mitochondrial ROS leads to mitochondrial disruption and dysfunction, which changes REC metabolism into hyperglycemia and reduces the ability of REC to maintain DR barrier function and tissue homeostasis [142,143]. Delles et al. [144] propose

that retinal vascular endothelial function is impaired in young patients with early primary hypertension, but angiotensin AT1 receptor blockade can improve its function. However, several studies have shown that vitamins could affect the process of common eye diseases. Vitamins A, B9, C, and E are well-known antioxidants that prevent age-related eye diseases, for instance, cataracts and age-related macular degeneration [145,146]. A meta-analysis reported that dietary intake of vitamins A and C was beneficially correlated with OAG; however, the results of studies on the levels of vitamins in blood failed to provide a definitive relationship with OAG [147].

7. Schlemm's Canal and Glaucoma

Elevated intraocular pressure (IOP) is a major risk factor of retinal ganglion cell degeneration in glaucoma, which is caused by increased resistance to the outflow of aqueous humor (AH). Trabecular meshwork (TM) and Schlemm's canal (SC) endothelial are key regulators of outflow resistance. In glaucomatous eyes, the TM–SC pathway is damaged by accumulated oxidative stress arising from the microenvironment, vascular dysregulation, and aging [148]. As the final filtration barrier of the AH outflow pathway, stiffness of SC endothelia are crucial to the regulation of aqueous humor outflow resistance and control of IOP [149]. Schlemm's canal endothelial cells share morphological characteristics and cell marker expression with both lymphatic and venous endothelial cells [150]. Similar to that of other ECs, Schlemm's canal ECs also respond to changes in substrate stiffness or architecture. In particular, glaucomatous SC cells have an exaggerated and possibly pathological response to increased substrate stiffness, compared with normal SC cells [149]. They alter their expression of genes implicated in outflow obstruction and glaucoma in response to changes in substrate stiffness, particularly connective tissue growth factor (CTGF), an agent which has been shown to cause ocular hypertension and glaucomatous optic neuropathy in mice [151].

Thus, targeting SC cell stiffness seems to be a promising antiglaucoma therapy to decrease outflow resistance at the location responsible for regulating the majority of outflow resistance. Drugs targeting Rho-kinase inhibition, actin depolymerization, and nitric oxide were recently introduced to reduce SC cell stiffness and reduce IOP [152–155].

8. Conclusions

It is widely accepted that endothelial dysfunction plays a crucial role in the development of neurodegeneration. There is a potential pathological link between oxidative stress, endothelial function, and neurodegenerative diseases of the retina. A better understanding of the roles of endothelial function may provide new treatments for retinal neurodegenerative diseases.

Author Contributions: Writing—original draft preparation, X.S., P.L., and H.L.; writing—review and editing, X.S., P.L., and H.L.; visualization, X.S. and P.L.; supervision, V.P. All authors have read and agreed to the published version of the manuscript.

Funding: This research was funded by Deutsche forschungsgemeinschaft, Grant Number PR1569/1-1.

Acknowledgments: The authors gratefully acknowledge scholarship financial support from the China Scholarship Council.

Conflicts of Interest: The authors declare no conflict of interest.

References

1. Chandrasekaran, A.; Idelchik, M.D.P.S.; Melendez, J.A. Redox control of senescence and age-related disease. *Redox Biol.* **2017**, *11*, 91–102. [CrossRef] [PubMed]
2. Lobo, V.; Patil, A.; Phatak, A.; Chandra, N. Free radicals, antioxidants and functional foods: Impact on human health. *Pharmacogn. Rev.* **2010**, *4*, 118–126. [CrossRef] [PubMed]
3. Powers, S.K.; Ji, L.L.; Kavazis, A.N.; Jackson, M.J. Reactive Oxygen Species: Impact on Skeletal Muscle. *Compr. Physiol.* **2011**, *1*, 941–969. [CrossRef] [PubMed]

4. Aikens, J.; Dix, T.A. Perhydroxyl radical (HOO) initiated lipid peroxidation: The role of fatty acid hydroperoxides. *J. Biol. Chem.* **1991**, *266*, 15091–15098. [CrossRef]
5. Halliwell, B.; Gutteridge, J.M. *Free Radicals in Biology and Medicine*, 3rd ed.; Oxford University Press: Oxford, UK, 1999.
6. Dröge, W. Free Radicals in the Physiological Control of Cell Function. *Physiol. Rev.* **2002**, *82*, 47–95. [CrossRef] [PubMed]
7. Chiurchiù, V.; Maccarrone, M. Chronic Inflammatory Disorders and Their Redox Control: From Molecular Mechanisms to Therapeutic Opportunities. *Antioxid. Redox Signal.* **2011**, *15*, 2605–2641. [CrossRef]
8. Genestra, M. Oxyl radicals, redox-sensitive signalling cascades and antioxidants. *Cell. Signal.* **2007**, *19*, 1807–1819. [CrossRef]
9. Sies, H. Hydrogen peroxide as a central redox signaling molecule in physiological oxidative stress: Oxidative eustress. *Redox Biol.* **2017**, *11*, 613–619. [CrossRef]
10. Sena, C.M.; Leandro, A.; Azul, L.; Seiça, R.; Perry, G. Vascular Oxidative Stress: Impact and Therapeutic Approaches. *Front. Physiol.* **2018**, *9*, 1668. [CrossRef]
11. Barbacanne, M.A.; Souchard, J.P.; Darblade, B.; Iliou, J.P.; Nepveu, F.; Pipy, B.; Bayard, F.; Arnal, J.F. Detection of superoxide anion released extracellularly by endothelial cells using cytochrome c reduction, ESR, fluorescence and lucigenin-enhanced chemiluminescence techniques. *Free Radic. Biol. Med.* **2000**, *29*, 388–396. [CrossRef]
12. Vidrio, E.; Jung, H.; Anastasio, C. Generation of hydroxyl radicals from dissolved transition metals in surrogate lung fluid solutions. *Atmos. Environ.* **2008**, *42*, 4369–4379. [CrossRef] [PubMed]
13. Murphy, E.; Steenbergen, C. Mechanisms Underlying Acute Protection from Cardiac Ischemia-Reperfusion Injury. *Physiol. Rev.* **2008**, *88*, 581–609. [CrossRef] [PubMed]
14. Bortoletto, P.; Lyman, K.; Camacho, A.; Fricchione, M.; Khanolkar, A.; Katz, B.Z. Chronic Granulomatous Disease. *Pediatr. Infect. Dis. J.* **2015**, *34*, 1110–1114. [CrossRef] [PubMed]
15. Tsao, P.S.; Heidary, S.; Wang, A.; Chan, J.R.; Reaven, G.M.; Cooke, J.P. Protein kinase C-epsilon mediates glucose-induced superoxide production and MCP-1 expression in endothelial cells. *FASEB J.* **1998**, *12*, 512.
16. D'Azy, C.B.; Pereira, B.; Chiambaretta, F.; Dutheil, F. Oxidative and Anti-Oxidative Stress Markers in Chronic Glaucoma: A Systematic Review and Meta-Analysis. *PLoS ONE* **2016**, *11*, e0166915. [CrossRef]
17. Attwell, D.; Buchan, A.M.; Charpak, S.; Lauritzen, M.J.; MacVicar, B.A.; Newman, E.A. Glial and neuronal control of brain blood flow. *Nature* **2010**, *468*, 232–243. [CrossRef]
18. Daneman, R.; Zhou, L.; Kebede, A.A.; Barres, B.A. Pericytes are required for blood–brain barrier integrity during embryogenesis. *Nature* **2010**, *468*, 562–566. [CrossRef]
19. Hall, C.N.; Reynell, C.; Gesslein, B.; Hamilton, N.B.; Mishra, A.; Sutherland, B.A.; O'Farrell, F.M.; Buchan, A.M.; Lauritzen, M.; Attwell, D. Capillary pericytes regulate cerebral blood flow in health and disease. *Nature* **2014**, *508*, 55–60. [CrossRef] [PubMed]
20. Sweeney, M.; Ayyadurai, S.; Zlokovic, B.V. Pericytes of the neurovascular unit: Key functions and signaling pathways. *Nat. Neurosci.* **2016**, *19*, 771–783. [CrossRef]
21. Sweeney, M.D.; Kisler, K.; Montagne, A.; Toga, A.W.; Zlokovic, B.V. The role of brain vasculature in neurodegenerative disorders. *Nat. Neurosci.* **2018**, *21*, 1318–1331. [CrossRef]
22. Ando, J.; Yamamoto, K. Effects of Shear Stress and Stretch on Endothelial Function. *Antioxid. Redox Signal.* **2011**, *15*, 1389–1403. [CrossRef] [PubMed]
23. Breslin, J.W.; Kurtz, K.M. Lymphatic Endothelial Cells Adapt Their Barrier Function in Response to Changes in Shear Stress. *Lymphat. Res. Biol.* **2009**, *7*, 229–237. [CrossRef] [PubMed]
24. Ogita, H.; Liao, J.K. Endothelial function and oxidative stress. *Endothelium* **2004**, *11*, 123–132. [CrossRef] [PubMed]
25. Faraci, F.; Heistad, D.D. Regulation of the Cerebral Circulation: Role of Endothelium and Potassium Channels. *Physiol. Rev.* **1998**, *78*, 53–97. [CrossRef] [PubMed]
26. Golding, E.M.; Marrelli, S.P.; You, J.; Bryan, R.M. Endothelium-derived hyperpolarizing factor in the brain: A new regulator of cerebral blood flow? *Stroke* **2002**, *33*, 661–663. [CrossRef] [PubMed]
27. Wolburg, H.; Noell, S.; Mack, A.; Wolburg-Buchholz, K.; Fallier-Becker, P. Brain endothelial cells and the glio-vascular complex. *Cell Tissue Res.* **2008**, *335*, 75–96. [CrossRef] [PubMed]
28. Faraci, F.M. Reactive oxygen species: Influence on cerebral vascular tone. *J. Appl. Physiol.* **2006**, *100*, 739–743. [CrossRef] [PubMed]
29. Himori, N.; Kunikata, H.; Shiga, Y.; Omodaka, K.; Maruyama, K.; Takahashi, H.; Nakazawa, T. The association between systemic oxidative stress and ocular blood flow in patients with normal-tension glaucoma. *Graefe's Arch. Clin. Exp. Ophthalmol.* **2015**, *254*, 333–341. [CrossRef]
30. López-Riquelme, N.; Villalba, C.; Tormo, C.; Belmonte, A.; Fernandez, C.; Torralba, G.; Hernández, F. Endothelin-1 levels and biomarkers of oxidative stress in glaucoma patients. *Int. Ophthalmol.* **2015**, *35*, 527–532. [CrossRef]
31. Nathanson, J.A.; McKee, M. Alterations of ocular nitric oxide synthase in human glaucoma. *Investig. Ophthalmol. Vis. Sci.* **1995**, *36*, 1774–1784.
32. Triggle, C.R.; Samuel, S.M.; Ravishankar, S.; Marei, I.; Arunachalam, G.; Ding, H. The endothelium: Influencing vascular smooth muscle in many ways. *Can. J. Physiol. Pharmacol.* **2012**, *90*, 713–738. [CrossRef] [PubMed]
33. Florey, L. The endothelial cell. *Br. Med. J.* **1966**, *2*, 487–490. [CrossRef] [PubMed]
34. Michiels, C. Endothelial cell functions. *J. Cell. Physiol.* **2003**, *196*, 430–443. [CrossRef] [PubMed]
35. Virchow, R. Der ateromatose prozess der arterien. *Wien. Med. Wochenschr.* **1856**, *6*, 825–827.

36. Furchgott, R.F.; Zawadzki, J.V. The obligatory role of endothelial cells in the relaxation of arterial smooth muscle by acetylcholine. *Nature* **1980**, *288*, 373–376. [CrossRef] [PubMed]
37. Levick, J.R. *An Introduction to Cardiovascular Physiology*; Hodder Arnold: London, UK, 2009; p. 607.
38. Plutzky, J. The vascular biology of atherosclerosis. *Am. J. Med.* **2003**, *115*, 55–61. [CrossRef] [PubMed]
39. Wang, M.; Hao, H.; Leeper, N.J.; Zhu, L. Thrombotic Regulation from the Endothelial Cell Perspectives. *Arter. Thromb. Vasc. Biol.* **2018**, *38*, e90–e95. [CrossRef] [PubMed]
40. Chiu, J.J.; Chien, S. Effects of Disturbed Flow on Vascular Endothelium: Pathophysiological Basis and Clinical Perspectives. *Physiol. Rev.* **2011**, *91*, 327–387. [CrossRef] [PubMed]
41. Boulanger, C.M. Endothelium. *Arter. Thromb. Vasc. Biol.* **2016**, *36*, e26–e31. [CrossRef] [PubMed]
42. Vanhoutte, P.M.; Shimokawa, H.; Feletou, M.; Tang, E.H.C. Endothelial dysfunction and vascular disease—a 30th anniversary update. *Acta Physiol.* **2017**, *219*, 22–96. [CrossRef] [PubMed]
43. Shimokawa, H. Williams Harvey Lecture: Importance of coronary vasomotion abnormalities—from bench to bedside. *Eur. Heart J.* **2014**, *35*, 3180–3193. [CrossRef]
44. Dhananjayan, R.; Koundinya, K.S.S.; Malati, T.; Kutala, V.K. Endothelial Dysfunction in Type 2 Diabetes Mellitus. *Indian J. Clin. Biochem.* **2016**, *31*, 372–379. [CrossRef]
45. Cheng, H.M.; Koutsidis, G.; Lodge, J.; Ashor, A.; Siervo, M.; Lara, J. Tomato and lycopene supplementation and cardiovascular risk factors: A systematic review and meta-analysis. *Atherosclerosis* **2017**, *257*, 100–108. [CrossRef] [PubMed]
46. Liao, J.K. Linking endothelial dysfunction with endothelial cell activation. *J. Clin. Investig.* **2013**, *123*, 540–541. [CrossRef]
47. Ooi, B.K.; Chan, K.G.; Goh, B.H.; Yap, W.H. The Role of Natural Products in Targeting Cardiovascular Diseases via Nrf2 Pathway: Novel Molecular Mechanisms and Therapeutic Approaches. *Front. Pharmacol.* **2018**, *9*, 1308. [CrossRef] [PubMed]
48. Rajendran, P.; Rengarajan, T.; Thangavel, J.; Nishigaki, Y.; Sakthisekaran, D.; Sethi, G.; Nishigaki, I. The Vascular Endothelium and Human Diseases. *Int. J. Biol. Sci.* **2013**, *9*, 1057–1069. [CrossRef] [PubMed]
49. Haybar, H.; Shahrabi, S.; Rezaeeyan, H.; Shirzad, R.; Saki, N. Endothelial Cells: From Dysfunction Mechanism to Pharmacological Effect in Cardiovascular Disease. *Cardiovasc. Toxicol.* **2019**, *19*, 13–22. [CrossRef] [PubMed]
50. Verma, S.; Anderson, T.J. Fundamentals of Endothelial Function for the Clinical Cardiologist. *Circulation* **2002**, *105*, 546–549. [CrossRef] [PubMed]
51. Valko, M.; Leibfritz, D.; Moncol, J.; Cronin, M.T.; Mazur, M.; Telser, J. Free radicals and antioxidants in normal physiological functions and human disease. *Int. J. Biochem. Cell Biol.* **2007**, *39*, 44–84. [CrossRef] [PubMed]
52. Kvietys, P.R.; Granger, D.N. Role of reactive oxygen and nitrogen species in the vascular responses to inflammation. *Free Radic. Biol. Med.* **2012**, *52*, 556–592. [CrossRef] [PubMed]
53. Aprioku, J.S. Pharmacology of Free Radicals and the Impact of Reactive Oxygen Species on the Testis. *J. Reprod. Infertil.* **2013**, *14*, 158–172. [PubMed]
54. Incalza, M.A.; D'Oria, R.; Natalicchio, A.; Perrini, S.; Laviola, L.; Giorgino, F. Oxidative stress and reactive oxygen species in endothelial dysfunction associated with cardiovascular and metabolic diseases. *Vasc. Pharmacol.* **2018**, *100*, 1–19. [CrossRef] [PubMed]
55. Dohi, Y.; Thiel, M.A.; Bühler, F.R.; Lüscher, T.F. Activation of endothelial L-arginine pathway in resistance arteries. Effect of age and hypertension. *Hypertension* **1990**, *16*, 170–179. [CrossRef] [PubMed]
56. Brownlee, M. Biochemistry and molecular cell biology of diabetic complications. *Nature* **2001**, *414*, 813–820. [CrossRef] [PubMed]
57. Guzik, T.J.; Harrison, D.G. Vascular NADPH oxidases as drug targets for novel antioxidant strategies. *Drug Discov. Today* **2006**, *11*, 524–533. [CrossRef] [PubMed]
58. Cai, H.; Harrison, D.G. Endothelial Dysfunction in Cardiovascular Diseases: The Role of Oxidant Stress. *Circ. Res.* **2000**, *87*, 840–844. [CrossRef] [PubMed]
59. Dijhorst-Oei, L.T.; Stores, E.S.; Koomans, H.A.; Rabelink, T.J. Acute stimultaneous stimulation of nitric oxide and oxygen radicals by angiotensin II in humans in vivo. *J Cardiovasc. Pharm.* **1999**, *33*, 420–424. [CrossRef] [PubMed]
60. Gozin, A.; Franzini, E.; Andrieu, V.; Da Costa, L.; Rollet-Labelle, E.; Pasquier, C. Reactive oxygen species activate focal adhesion kinase, paxillin and p130cas tyrosine phosphorylation in endothelial cells. *Free Radic. Biol. Med.* **1998**, *25*, 1021–1032. [CrossRef]
61. Vepa, S.; Scribner, W.M.; Parinandi, N.L.; English, D.; Garcia, J.G.; Natarajan, V. Hydrogen peroxide stimulates tyrosine phosphorylation of focal adhesion kinase in vascular endothelial cells. *Am. J. Physiol.* **1999**, *277*, L150–L158. [CrossRef] [PubMed]
62. Loscalzo, J. Oxidative stress in endothelial cell dysfunction and thrombosis. *Pathophysiol. Haemost. Thromb.* **2002**, *32*, 359–360. [CrossRef]
63. Daiber, A.; Oelze, M.; Wenzel, P.; Dias Wickramanayake, J.M.; Schuhmacher, S.; Jansen, T.; Lackner, K.J.; Torzewski, M.; Münzel, T. Nitrate tolerance as a model of vascular dysfunction: Roles for mitochondrial aldehyde dehydrogenase and mitochondrial oxidative stress. *Pharmacol. Rep.* **2009**, *61*, 33–48. [CrossRef]
64. Wagner, D.D.; Frenette, P.S. The vessel wall and its interactions. *Blood* **2008**, *111*, 5271–5281. [CrossRef]
65. Xu, S.; Touyz, R.M. Reactive oxygen species and vascular remodelling in hypertension: Still alive. *Can. J. Cardiol.* **2006**, *22*, 947–951. [CrossRef]
66. Senoner, T.; Dichtl, W. Oxidative Stress in Cardiovascular Diseases: Still a Therapeutic Target? *Nutrients* **2019**, *11*, 2090. [CrossRef] [PubMed]

67. Stadtman, E.R. Metal ion-catalyzed oxidation of proteins: Biochemical mechanism and biological consequences. *Free Radic. Biol. Med.* **1990**, *9*, 315–325. [CrossRef]
68. Higashi, Y.; Noma, K.; Yoshizumi, M.; Kihara, Y. Endothelial Function and Oxidative Stress in Cardiovascular Diseases. *Circ. J.* **2009**, *73*, 411–418. [CrossRef] [PubMed]
69. Tousoulis, D.; Andreou, I.; Antoniades, C.; Tentolouris, C.; Stefanadis, C. Role of inflammation and oxidative stress in endothelial progenitor cell function and mobilization: Therapeutic implications for cardiovascular diseases. *Atherosclerosis* **2008**, *201*, 236–247. [CrossRef] [PubMed]
70. Soccio, M.; Toniato, E.; Evangelista, V.; Carluccio, M.; De Caterina, R. Oxidative stress and cardiovascular risk: The role of vascular NAD(P)H oxidase and its genetic variants. *Eur. J. Clin. Investig.* **2005**, *35*, 305–314. [CrossRef]
71. De Caterina, R. Endothelial dysfunctions: Common denominators in vascular disease. *Curr. Opin. Lipidol.* **2000**, *11*, 9–23. [CrossRef]
72. Li, H.; Horke, S.; Förstermann, U. Oxidative stress in vascular disease and its pharmacological prevention. *Trends Pharmacol. Sci.* **2013**, *34*, 313–319. [CrossRef] [PubMed]
73. Münzel, T.; Camici, G.G.; Maack, C.; Bonetti, N.R.; Fuster, V.; Kovacic, J.C. Impact of Oxidative Stress on the Heart and Vasculature. *J. Am. Coll. Cardiol.* **2017**, *70*, 212–229. [CrossRef] [PubMed]
74. Corre, I.; Paris, F.; Huot, A.J. The p38 pathway, a major pleiotropic cascade that transduces stress and metastatic signals in endothelial cells. *Oncotarget* **2017**, *8*, 55684–55714. [CrossRef] [PubMed]
75. Lee, R.; Margaritis, M.; Channon, K.; Antoniades, C. Evaluating Oxidative Stress in Human Cardiovascular Disease: Methodological Aspects and Considerations. *Curr. Med. Chem.* **2012**, *19*, 2504–2520. [CrossRef] [PubMed]
76. Förstermann, U.; Xia, N.; Li, H. Roles of Vascular Oxidative Stress and Nitric Oxide in the Pathogenesis of Atherosclerosis. *Circ. Res.* **2017**, *120*, 713–735. [CrossRef]
77. Levitan, I.; Volkov, S.; Subbaiah, P.V. Oxidized LDL: Diversity, Patterns of Recognition, and Pathophysiology. *Antioxid. Redox Signal.* **2010**, *13*, 39–75. [CrossRef] [PubMed]
78. Ou, H.C.; Chou, F.P.; Sheen, H.M.; Lin, T.M.; Yang, C.H.; Sheu, W.H.H. Resveratrol, a polyphenolic compound in red wine, protects against oxidized LDL-induced cytotoxicity in endothelial cells. *Clin. Chim. Acta* **2006**, *364*, 196–204. [CrossRef] [PubMed]
79. Ohara, Y.; Peterson, T.E.; Sayegh, H.S.; Subramanian, R.R.; Wilcox, J.N.; Harrison, D.G. Dietary correction of hypercholesterolemia in the rabbit normalizesendothelial superoxide anion production. *Circulation* **1995**, *92*, 898–903. [CrossRef]
80. Mervaala, E.M.; Cheng, Z.J.; Tikkanen, I.; Lapatto, R.; Nurminen, K.; Vapaatalo, H.; Muller, D.N.; Fiebeler, A.; Ganten, U.; Ganten, D.; et al. Endothelial dysfunction and xanthine oxidoreductase activity in rats with human renin and angiotensinogen genes. *Hypertension* **2001**, *37*, 414–418. [CrossRef]
81. Greaney, J.L.; Saunders, E.; Santhanam, L.; Alexander, L.M. Oxidative Stress Contributes to Microvascular Endothelial Dysfunction in Men and Women With Major Depressive Disorder. *Circ. Res.* **2019**, *124*, 564–574. [CrossRef] [PubMed]
82. La Favor, J.D.; Dubis, G.S.; Yan, H.; White, J.D.; Nelson, M.A.; Anderson, E.J.; Hickner, R. Microvascular Endothelial Dysfunction in Sedentary, Obese Humans is Mediated by NADPH Oxidase. *Arter. Thromb. Vasc. Biol.* **2016**, *36*, 2412–2420. [CrossRef]
83. Gray, S.P.; Di Marco, E.; Kennedy, K.; Chew, P.; Okabe, J.; El-Osta, A.; Calkin, A.C.; Biessen, E.A.; Touyz, R.M.; Cooper, M.E.; et al. Reactive Oxygen Species can Provide Atheroprotection via NOX4-Dependent Inhibition of Inflammation and Vascular Remodeling. *Arter. Thromb. Vasc. Biol.* **2016**, *36*, 295–307. [CrossRef] [PubMed]
84. Freed, J.K.; Beyer, A.M.; Logiudice, J.A.; Hockenberry, J.C.; Gutterman, D.D. Ceramide Changes the Mediator of Flow-Induced Vasodilation from Nitric Oxide to Hydrogen Peroxide in the Human Microcirculation. *Circ. Res.* **2014**, *115*, 525–532. [CrossRef] [PubMed]
85. Durand, M.J.; Zinkevich, N.S.; Riedel, M.; Gutterman, D.D.; Nasci, V.; Salato, V.K.; Hijjawi, J.B.; Reuben, C.F.; North, P.E.; Beyer, A.M. Vascular Actions of Angiotensin 1–7 in the Human Microcirculation. *Arter. Thromb. Vasc. Biol.* **2016**, *36*, 1254–1262. [CrossRef]
86. Gutterman, D.D.; Chabowski, D.S.; Kadlec, A.O.; Durand, M.J.; Freed, J.K.; Ait-Aissa, K.; Beyer, A. The Human Microcirculation. *Circ. Res.* **2016**, *118*, 157–172. [CrossRef] [PubMed]
87. Godo, S.; Sawada, A.; Saito, H.; Ikeda, S.; Enkhjargal, B.; Suzuki, K.; Tanaka, S.; Shimokawa, H. Disruption of Physiological Balance between Nitric Oxide and Endothelium-Dependent Hyperpolarization Impairs Cardiovascular Homeostasis in Mice. *Arter. Thromb. Vasc. Biol.* **2016**, *36*, 97–107. [CrossRef] [PubMed]
88. Kirsch, J.; Schneider, H.; Pagel, J.I.; Rehberg, M.; Singer, M.; Hellfritsch, J.; Chillo, O.; Schubert, K.M.; Qiu, J.; Pogoda, K.; et al. Endothelial Dysfunction, and a Prothrombotic, Proinflammatory Phenotype is Caused by Loss of Mitochondrial Thioredoxin Reductase in Endothelium. *Arter. Thromb. Vasc. Biol.* **2016**, *36*, 1891–1899. [CrossRef] [PubMed]
89. Kadlec, A.O.; Chabowski, D.S.; Ait-Aissa, K.; Gutterman, D.D. Role of PGC-1α in Vascular Regulation. *Arter. Thromb. Vasc. Biol.* **2016**, *36*, 1467–1474. [CrossRef] [PubMed]
90. Ganguly, P.; Alam, S.F. Role of homocysteine in the development of cardiovascular disease. *Nutr. J.* **2015**, *14*, 6. [CrossRef] [PubMed]
91. Kumar, A.; Palfrey, H.A.; Pathak, R.; Kadowitz, P.J.; Gettys, T.W.; Murthy, S.N. The metabolism and significance of homocysteine in nutrition and health. *Nutr. Metab.* **2017**, *14*, 1–12. [CrossRef] [PubMed]
92. Liu, H.H.; Shih, T.S.; Huang, H.R.; Huang, S.C.; Lee, L.H.; Huang, Y.C. Plasma Homocysteine is Associated with Increased Oxidative Stress and Antioxidant Enzyme Activity in Welders. *Sci. World J.* **2013**, *2013*, 1–8. [CrossRef] [PubMed]

93. Weiss, N. Mechanisms of Increased Vascular Oxidant Stress in Hyperhomocysteinemia and Its Impact on Endothelial Function. *Curr. Drug Metab.* **2005**, *6*, 27–36. [CrossRef] [PubMed]
94. Mani, M.; Golmohammadi, T.; Khaghani, S.; Zamani, Z.; Azadmanesh, K.; Meshkani, R.; Pasalar, P. Homocysteine Induces Heme Oxygenase-1 Expression via Transcription Factor Nrf2 Activation in HepG2 Cells. *Iran. Biomed. J.* **2013**, *17*, 93–100. [CrossRef]
95. Handy, D.; Zhang, Y.; Loscalzo, J. Homocysteine Down-regulates Cellular Glutathione Peroxidase (GPx1) by Decreasing Translation. *J. Biol. Chem.* **2005**, *280*, 15518–15525. [CrossRef] [PubMed]
96. Solon, J.; Levental, I.; Sengupta, K.; Georges, P.C.; Janmey, P.A. Janmey Fibroblast adaptation and stiffness matching to soft elastic substrates. *Biophys. J.* **2007**, *93*, 4453–4461. [CrossRef] [PubMed]
97. Byfield, F.J.; Wen, Q.; Levental, I.; Nordstrom, K.; Arratia, P.E.; Miller, R.T.; Janmey, P.A. Janmey Absence of filamin A prevents cells from responding to stiffness gradients on gels coated with collagen but not fibronectin. *Biophys. J.* **2009**, *96*, 5095–5102. [CrossRef]
98. Ando, J.; Yamamoto, K. Vascular mechanobiology: Endothelial cell responses to fluid shear stress. *Circ. J.* **2009**, *73*, 1983–1992. [CrossRef] [PubMed]
99. Birukova, A.A.; Tian, X.; Cokic, I.; Beckham, Y.; Gardel, M.L.; Birukov, K.G. Endothelial barrier disruption and recovery is controlled by substrate stiffness. *Microvasc. Res.* **2013**, *87*, 50–57. [CrossRef] [PubMed]
100. Hishikawa, K.; Luscher, T.F. Pulsatile stretch stimulates superoxide production in human aortic endothelial cells. *Circulation* **1997**, *96*, 3610–3616. [CrossRef] [PubMed]
101. De Keulenaer, G.W.; Chappell, D.C.; Ishizaka, N.; Nerem, R.M.; Alexander, R.W.; Griendling, K.K. Oscillatory and steady laminar shear stress differentially affect human endothelial redox state: Role of a superoxide-producing NADH oxidase. *Circ. Research.* **1998**, *82*, 1094–1101. [CrossRef] [PubMed]
102. Van de Voorde, J.; Vanheel, B.; Leusen, I. Depressed endothelium-dependent relaxation in hypertension: Relation to increased blood pressure and reversibility. *Pflügers Arch. Eur. J. Physiol.* **1988**, *411*, 500–504. [CrossRef]
103. Ungvari, Z.; Csiszar, A.; Kaminski, P.M.; Wolin, M.S.; Koller, A. Chronic High Pressure-Induced Arterial Oxidative Stress: Involvement of Protein Kinase C-Dependent NAD(P)H Oxidase and Local Renin-Angiotensin System. *Am. J. Pathol.* **2004**, *165*, 219–226. [CrossRef]
104. Toda, N.; Ayajiki, K.; Okamura, T. Cerebral Blood Flow Regulation by Nitric Oxide: Recent Advances. *Pharmacol. Rev.* **2009**, *61*, 62–97. [CrossRef] [PubMed]
105. Toda, N.; Tanabe, S.; Nakanishi, S. Nitric Oxide-Mediated Coronary Flow Regulation in Patients with Coronary Artery Disease: Recent Advances. *Int. J. Angiol.* **2011**, *20*, 121–134. [CrossRef]
106. Toda, N.; Nakanishi-Toda, M. Nitric oxide: Ocular blood flow, glaucoma, and diabetic retinopathy. *Prog. Retin. Eye Res.* **2007**, *26*, 205–238. [CrossRef] [PubMed]
107. Dharmashankar, K.; Widlansky, M.E. Vascular Endothelial Function and Hypertension: Insights and Directions. *Curr. Hypertens. Rep.* **2010**, *12*, 448–455. [CrossRef] [PubMed]
108. Tang, E.H.C.; Vanhoutte, P.M. Endothelial dysfunction: A strategic target in the treatment of hypertension? *Pflügers Arch. Eur. J. Physiol.* **2010**, *459*, 995–1004. [CrossRef] [PubMed]
109. Steinberg, H.; Chaker, H.; Leaming, R.; Johnson, A.; Brechtel, G.; Baron, A.D. Obesity/insulin resistance is associated with endothelial dysfunction. Implications for the syndrome of insulin resistance. *J. Clin. Investig.* **1996**, *97*, 2601–2610. [CrossRef] [PubMed]
110. Aird, W.C. Spatial and temporal dynamics of the endothelium. *J. Thromb. Haemost.* **2005**, *3*, 1392–1406. [CrossRef] [PubMed]
111. Roberts, A.M.; Jagadapillai, R.; Vaishnav, R.A.; Friedland, R.P.; Drinovac, R.; Lin, X.; Gozal, E. Increased pulmonary arteriolar tone associated with lung oxidative stress and nitric oxide in a mouse model of Alzheimer's disease. *Physiol. Rep.* **2016**, *4*, e12953. [CrossRef]
112. Armulik, A.; Genové, G.; Mäe, M.; Nisancioglu, M.H.; Wallgard, E.; Niaudet, C.; He, L.; Norlin, J.; Lindblom, P.; Strittmatter, K.; et al. Pericytes regulate the blood-brain barrier. *Nature* **2010**, *468*, 557–561. [CrossRef]
113. Bell, R.D.; Winkler, E.A.; Sagare, A.P.; Singh, I.; LaRue, B.; Deane, R.; Zlokovic, B.V. Pericytes Control Key Neurovascular Functions and Neuronal Phenotype in the Adult Brain and during Brain Aging. *Neuron* **2010**, *68*, 409–427. [CrossRef] [PubMed]
114. Marco, S.; Skaper, S.D. Amyloid beta-peptide1-42 alters tight junction protein distribution and expression in brain microvessel endothelial cells. *Neurosci. Lett.* **2006**, *401*, 219–224. [CrossRef]
115. Janota, C.; Lemere, C.A.; Brito, M.A. Dissecting the Contribution of Vascular Alterations and Aging to Alzheimer's Disease. *Mol. Neurobiol.* **2015**, *53*, 3793–3811. [CrossRef] [PubMed]
116. Wan, W.; Chen, H.; Li, Y. The potential mechanisms of Abeta-receptor for advanced glycation end-products nteraction disrupting tight junctions of the blood-brain barrier in Alzheimer's disease. *Int. J. Neurosci.* **2014**, *124*, 75–81. [CrossRef] [PubMed]
117. Chen, W.; Chan, Y.; Wan, W.; Li, Y.; Zhang, C. Abeta1-42 induces cell damage via RAGE-dependent endoplasmic reticulum stress in bEnd.3 cells. *Exp. Cell Res.* **2018**, *362*, 83–89. [CrossRef] [PubMed]
118. Sole, M.; Esteban-Lopez, M.; Taltavull, B.; Fabregas, C.; Fado, R.; Casals, N.; Rodriguez-Alvarez, J.; Minano-Molina, A.J.; Unzeta, M. Blood-brain barrier dysfunction underlying Alzheimer's disease is induced by an SSAO/VAP-1-dependent cerebrovascular activation with enhanced Abeta deposition. *Biochim. Biophys. Acta Mol. Basis Dis.* **2019**, *1865*, 2189–2202. [CrossRef] [PubMed]

119. Kitazume, S.; Tachida, Y.; Kato, M.; Yamaguchi, Y.; Honda, T.; Hashimoto, Y.; Wada, Y.; Saito, T.; Iwata, N.; Saido, T.; et al. Brain Endothelial Cells Produce Amyloid β from Amyloid Precursor Protein 770 and Preferentially Secrete the O-Glycosylated Form. *J. Biol. Chem.* **2010**, *285*, 40097–40103. [CrossRef] [PubMed]
120. Song, Y.; Manson, J.E.; Tinker, L.; Rifai, N.; Cook, N.R.; Hu, F.B.; Hotamisligil, G.S.; Ridker, P.M.; Rodriguez, B.L.; Margolis, K.L.; et al. Circulating Levels of Endothelial Adhesion Molecules and Risk of Diabetes in an Ethnically Diverse Cohort of Women. *Diabetes* **2007**, *56*, 1898–1904. [CrossRef] [PubMed]
121. Sun, Y.; Smith, L.E.H. Retinal vasculature in development and diseases. *Annu. Rev. Vis. Sci.* **2018**, *4*, 101–122. [CrossRef]
122. Chou, J.; Rollins, S.; A Fawzi, A. Role of Endothelial Cell and Pericyte Dysfunction in Diabetic Retinopathy: Review of Techniques in Rodent Models. *Adv. Exp. Med. Biol.* **2014**, *801*, 669–675. [CrossRef]
123. Lechner, J.; O'Leary, O.E.; Stitt, A.W. The pathology associated with diabetic retinopathy. *Vis. Res.* **2017**, *139*, 7–14. [CrossRef] [PubMed]
124. Kur, J.; Newman, E.A.; Chan-Ling, T. Cellular and physiological mechanisms underlying blood flow regulation in the retina and choroid in health and disease. *Prog. Retin. Eye Res.* **2012**, *31*, 377–406. [CrossRef] [PubMed]
125. Klaassen, I.; Van Noorden, C.J.; Schlingemann, R.O. Molecular basis of the inner blood-retinal barrier and its breakdown in diabetic macular edema and other pathological conditions. *Prog. Retin. Eye Res.* **2013**, *34*, 19–48. [CrossRef]
126. Sim, R.; Hernández, C. Neurodegeneration in the diabetic eye: New insights and therapeutic perspectives. *Trends Endocrinol. Metab.* **2014**, *25*, 23–33. [CrossRef] [PubMed]
127. Navel, V.; Sapin, V.; Henrioux, F.; Blanchon, L.; Labbé, A.; Chiambaretta, F.; Baudouin, C.; Dutheil, F. Oxidative and antioxidative stress markers in dry eye disease: A systematic review and meta-analysis. *Acta Ophthalmol.* **2022**, *100*, 45–57. [CrossRef] [PubMed]
128. Dimmeler, S.; Fleming, I.; Fisslthaler, B.; Hermann, C.; Busse, R.; Zeiher, A.M. Activation of nitric oxide synthase in endothelial cells by Akt-dependent phosphorylation. *Nature* **1999**, *399*, 601–605. [CrossRef] [PubMed]
129. Fulton, D.; Gratton, J.P.; McCabe, T.J.; Fontana, J.; Fujio, Y.; Walsh, K.; Franke, T.F.; Papapetropoulos, A.; Sessa, W.C. Regulation of endothelium-derived nitric oxide production by the protein kinase Akt. *Nature* **1999**, *399*, 597–601. [CrossRef] [PubMed]
130. Harris, M.B.; Ju, H.; Venema, V.J.; Liang, H.; Zou, R.; Michell, B.J.; Chen, Z.P.; Kemp, B.E.; Venema, R.C. Reciprocal Phosphorylation and Regulation of Endothelial Nitric-oxide Synthase in Response to Bradykinin Stimulation. *J. Biol. Chem.* **2001**, *276*, 16587–16591. [CrossRef] [PubMed]
131. Lakshminarayanan, S.; Gardner, T.W.; Tarbell, J.M. Effect of shear stress on the hydraulic conductivity of cultured bovine retinal microvascular endothelial cell monolayers. *Curr. Eye Res.* **2000**, *21*, 944–951. [CrossRef]
132. Feng, Y.; Venema, V.J.; Venema, R.C.; Tsai, N.; A Behzadian, M.; Caldwell, R. VEGF-induced permeability increase is mediated by caveolae. *Investig. Ophthalmol. Vis. Sci.* **1999**, *40*, 157–167.
133. Uhlmann, S.; Friedrichs, U.; Eichler, W.; Hoffmann, S.; Wiedemann, P. Direct Measurement of VEGF-Induced Nitric Oxide Production by Choroidal Endothelial Cells. *Microvasc. Res.* **2001**, *62*, 179–189. [CrossRef] [PubMed]
134. Michelson, G.; Warntges, S.; Harazny, J.; Oehmer, S.; Delles, C.; Schmieder, R.E. Effect of nos inhibition on retinal arterial and capillary circulation in early arterial hypertension. *Retina* **2016**, *26*, 437–444. [CrossRef]
135. Dallinger, S.; Sieder, A.; Strametz, J.; Bayerle-Erder, M.; Wolzt, M.; Schmetterer, L. Vasodilator effects of L-arginine are stereospecifific and augmented by insulin in humans. *Am. J. Physiol.* **2003**, *284*, E1106–E1111.
136. Garhöfer, G.; Resch, H.; Lung, S.; Weigert, G.; Schmetterer, L. Intravenous Administration of L-Arginine Increases Retinal and Choroidal Blood Flow. *Am. J. Ophthalmol.* **2005**, *140*, 69-e1. [CrossRef]
137. de Zeeuw, P.; Wong, B.W.; Carmeliet, P. Metabolic Adaptations in Diabetic Endothelial Cells. *Circ. J.* **2015**, *79*, 934–941. [CrossRef] [PubMed]
138. Kowluru, R.A.; Kanwar, M.; Kennedy, A. Metabolic Memory Phenomenon and Accumulation of Peroxynitrite in Retinal Capillaries. *Exp. Diabetes Res.* **2007**, 1–7. [CrossRef]
139. Li, C.; Miao, X.; Li, F.; Wang, S.; Liu, Q.; Wang, Y.; Sun, J. Oxidative Stress-Related Mechanisms and Antioxidant Therapy in Diabetic Retinopathy. *Oxidative Med. Cell. Longev.* **2017**, *2017*, 1–15. [CrossRef]
140. Cho, M.J.; Yoon, S.J.; Kim, W.; Park, J.; Lee, J.; Park, J.G.; Cho, Y.L.; Kim, J.H.; Jang, H.; Park, Y.J.; et al. Oxidative stress-mediated TXNIP loss causes RPE dysfunction. *Exp. Mol. Med.* **2019**, *51*, 1–13. [CrossRef] [PubMed]
141. Busik, J.V.; Mohr, S.; Grant, M.B. Hyperglycemia-Induced Reactive Oxygen Species Toxicity to Endothelial Cells Is Dependent on Paracrine Mediators. *Diabetes* **2008**, *57*, 1952–1965. [CrossRef]
142. Trudeau, K.; Molina, A.J.; Guo, W.; Roy, S. High Glucose Disrupts Mitochondrial Morphology in Retinal Endothelial Cells: Implications for Diabetic Retinopathy. *Am. J. Pathol.* **2010**, *177*, 447–455. [CrossRef]
143. Madsen-Bouterse, S.; Mohammad, G.; Kanwar, M.; Kowluru, R.A. Role of Mitochondrial DNA Damage in the Development of Diabetic Retinopathy, and the Metabolic Memory Phenomenon Associated with Its Progression. *Antioxid. Redox Signal.* **2010**, *13*, 797–805. [CrossRef] [PubMed]
144. Delles, C.; Michelson, G.; Harazny, J.; Oehmer, S.; Hilgers, K.F.; Schmieder, R.E. Impaired Endothelial Function of the Retinal Vasculature in Hypertensive Patients. *Stroke* **2004**, *35*, 1289–1293. [CrossRef]
145. Mares, J.A. High-dose Antioxidant Supplementation and Cataract Risk. *Nutr. Rev.* **2004**, *62*, 28–32. [CrossRef] [PubMed]
146. Evans, J. Antioxidant supplements to prevent or slow down the progression of AMD: A systematic review and meta-analysis. *Eye* **2008**, *22*, 751–760. [CrossRef] [PubMed]

147. Ramdas, W.D.; Schouten, J.; Webers, C.A.B. The Effect of Vitamins on Glaucoma: A Systematic Review and Meta-Analysis. *Nutrients* **2018**, *10*, 359. [CrossRef] [PubMed]
148. Wang, N.; Chintala, S.K.; Fini, M.E.; Schuman, J.S. Activation of a tissue-specific stress response in the aqueous outflow pathway of the eye defines the glaucoma disease phenotype. *Nat. Med.* **2001**, *7*, 304–309. [CrossRef] [PubMed]
149. Stamer, W.D.; Braakman, S.T.; Zhou, E.H.; Ethier, C.R.; Fredberg, J.J.; Overby, D.R.; Johnson, M. Biomechanics of Schlemm's canal endothelium and intraocular pressure reduction. *Prog. Retin. Eye Res.* **2015**, *44*, 86–98. [CrossRef] [PubMed]
150. Dautriche, C.N.; Tian, Y.; Xie, Y.; Sharfstein, S.T. A Closer Look at Schlemm's Canal Cell Physiology: Implications for Biomimetics. *J. Funct. Biomater.* **2015**, *6*, 963–985. [CrossRef] [PubMed]
151. Junglas, B.; Kuespert, S.; Seleem, A.A.; Struller, T.; Ullmann, S.; Bosl, M.; Bosserhoff, A.; Kostler, J.; Wagner, R.; Tamm, E.R.; et al. Fuchshofer Connective tissue growth factor causes glaucoma by modifying the actin cytoskeleton of the trabecular meshwork. *Am. J. Pathol.* **2012**, *180*, 2386–2403. [CrossRef] [PubMed]
152. Stack, T.; Vahabikashi, A.; Johnson, M.; Scott, E. Modulation of Schlemm's canal endothelial cell stiffness via latrunculin loaded block copolymer micelles. *J. Biomed. Mater. Res. A* **2018**, *106*, 1771–1779. [CrossRef]
153. Tanna, A.P.; Johnson, M. Rho Kinase Inhibitors as a Novel Treatment for Glaucoma and Ocular Hypertension. *Ophthalmology* **2018**, *125*, 1741–1756. [CrossRef] [PubMed]
154. Stack, T.; Vincent, M.; Vahabikashi, A.; Li, G.; Perkumas, K.M.; Stamer, W.D.; Johnson, M.; Scott, E. Targeted Delivery of Cell Softening Micelles to Schlemm's Canal Endothelial Cells for Treatment of Glaucoma. *Small* **2020**, *16*, e2004205. [CrossRef] [PubMed]
155. Krauss, A.H.; Impagnatiello, F.; Toris, C.B.; Gale, D.C.; Prasanna, G.; Borghi, V.; Chiroli, V.; Chong, W.; Carreiro, S.T.; Ongini, E. Ocular hypotensive activity of BOL-303259-X, a nitric oxide donating Prostaglandin F2α agonist, in preclinical models. *Exp. Eye Res.* **2011**, *93*, 250–255. [CrossRef] [PubMed]

5. Pathological high intraocular pressure induces glial cell reactive proliferation contributing to neuroinflammation of the blood-retinal barrier via the NOX2/ET-1 axis-controlled ERK1/2 pathway

Shi et al. Journal of Neuroinflammation (2024) 21:105
https://doi.org/10.1186/s12974-024-03075-x

Journal of Neuroinflammation

RESEARCH Open Access

Pathological high intraocular pressure induces glial cell reactive proliferation contributing to neuroinflammation of the blood-retinal barrier via the NOX2/ET-1 axis-controlled ERK1/2 pathway

Xin Shi[†], Panpan Li[†], Marc Herb[2,3], Hanhan Liu[1], Maoren Wang[4], Xiaosha Wang[1], Yuan Feng[1], Tim van Beers[5], Ning Xia[6], Huige Li[6,7] and Verena Prokosch[1*]

Abstract

Background NADPH oxidase (NOX), a primary source of endothelial reactive oxygen species (ROS), is considered a key event in disrupting the integrity of the blood-retinal barrier. Abnormalities in neurovascular-coupled immune signaling herald the loss of ganglion cells in glaucoma. Persistent microglia-driven inflammation and cellular innate immune system dysregulation often lead to deteriorating retinal degeneration. However, the crosstalk between NOX and the retinal immune environment remains unresolved. Here, we investigate the interaction between oxidative stress and neuroinflammation in glaucoma by genetic defects of NOX2 or its regulation via gp91ds-tat.

Methods Ex vivo cultures of retinal explants from wildtype C57BL/6J and *Nox2* $^{-/-}$ mice were subjected to normal and high hydrostatic pressure (Pressure 60 mmHg) for 24 h. In vivo, high intraocular pressure (H-IOP) was induced in C57BL/6J mice for two weeks. Both Pressure 60 mmHg retinas and H-IOP mice were treated with either gp91ds-tat (a NOX2-specific inhibitor). Proteomic analysis was performed on control, H-IOP, and treatment with gp91ds-tat retinas to identify differentially expressed proteins (DEPs). The study also evaluated various glaucoma phenotypes, including IOP, retinal ganglion cell (RGC) functionality, and optic nerve (ON) degeneration. The superoxide (O_2^-) levels assay, blood-retinal barrier degradation, gliosis, neuroinflammation, enzyme-linked immunosorbent assay (ELISA), western blotting, and quantitative PCR were performed in this study.

Results We found that NOX2-specific deletion or activity inhibition effectively attenuated retinal oxidative stress, immune dysregulation, the internal blood-retinal barrier (iBRB) injury, neurovascular unit (NVU) dysfunction, RGC loss, and ON axonal degeneration following H-IOP. Mechanistically, we unveiled for the first time that NOX2-dependent

[†]Xin Shi and Panpan Li contributed equally to this work and shared the first authorship.

*Correspondence:
Verena Prokosch
verena.prokosch@uk-koeln.de

Full list of author information is available at the end of the article

ROS-driven pro-inflammatory signaling, where NOX2/ROS induces endothelium-derived endothelin-1 (ET-1) overexpression, which activates the ERK1/2 signaling pathway and mediates the shift of microglia activation to a pro-inflammatory M1 phenotype, thereby triggering a neuroinflammatory outburst.

Conclusions Collectively, we demonstrate for the first time that NOX2 deletion or gp91ds-tat inhibition attenuates iBRB injury and NVU dysfunction to rescue glaucomatous RGC loss and ON axon degeneration, which is associated with inhibition of the ET-1/ERK1/2-transduced shift of microglial cell activation toward a pro-inflammatory M1 phenotype, highlighting NOX2 as a potential target for novel neuroprotective therapies in glaucoma management.

Keywords NADPH oxidase 2, Deletion, Pharmacological inhibition, Oxidative stress, Neurodegeneration, Neuroinflammation, Vascular dysfunction, Glaucoma

Background

Glaucoma, a heterogeneous group of disorders, is characterized by the loss of retinal ganglion cells (RGCs) and the axons, ultimately contributing to defects in the visual field. Glaucoma is considered the principal cause of irreversible blindness and is estimated to affect more than 111.8 million people by the year 2040 [1]. To date, the pathogenesis of glaucoma remains unclear, where multiple pathophysiological factors and pathways, which regulate mechanical, vascular, and immune responses, are considered critical events responsible for RGC apoptosis [2]. Besides, there is a potential pathological link between oxidative stress, endothelial function, and glaucoma [3]. Reactive oxygen species (ROS) function as vasodilators at low concentrations, while high concentrations may lead to vascular dysfunction [4]. Oxidative stress, induced by ROS overproduction, is associated with reduced ocular hemodynamics [5] and increased intraocular pressure (IOP) [6–8], possibly accounting for abnormal vascular permeability, which might explain the underlying mechanisms of these risk elements in the development of glaucoma. Ocular vascular dysregulation is another pathological feature of glaucoma, the underlying mechanism of which remains unclear. The phenomenon is probably attributed partially to autoregulation and endothelial dysfunction influenced by high IOP (H-IOP), which appears to be connected to oxidative stress [9].

The family of superoxide-generating enzymes, nicotinamide adenine dinucleotide phosphate (NADPH) oxidase (NOX), is considered to be a primary contributor to oxidative stress in various human pathologies [10]. NOX2, the primary NOX isoform of phagocytes, consists of membrane-bound ($gp91^{phox}$, $p22^{phox}$) and cytoplasmic ($p40^{phox}$, $p47^{phox}$, and $p67^{phox}$) subunits [11, 12]. NADPH oxidase enzymes, act as an emerging source of oxidative stress in glaucoma, whose induction plays a key role in the progression of glaucoma [13]. Patients with glaucoma suffer compromised endothelial cells (ECs) function [14] and increased plasma and aqueous humor levels of endothelin-1 (ET-1) [15–17], which could lead to NOX activation [18]. Based on studies, under the circumstances of IOP, NOX2-dependent ROS production is associated with reduced endothelium-dependent relaxation of the retinal vasculature [19]. NOX2-derived "signaling ROS" are primarily involved in immune regulation and mediate protection against autoimmunity as well as maintenance of self-tolerance [20]. In the recent two decades, genetic NOX2 deletion has been investigated to clarify the impact of NOX2-derived ROS on disease development and progression. Pharmacological inhibition is also one of the methods commonly applied to investigate the contribution of NADPH oxidase, which has been extensively explored in animal models of vascular disorders [21]. However, in animal models of glaucoma, investigations of NOX2 are considerably limited [22], especially as the exact molecular mechanisms and potential effects on vascular endothelium and multiple downstream cytokines are unclear. Therefore, it is of high medical need to assess the effects of genetic deletion or pharmacological interventions with NOX2 in the animal models of glaucoma. The present study aimed to analyze the loss of RGC, whether it is associated with NOX2 activation in glaucoma, and whether suppressing or deleting NOX2 has a neuroprotective role in the animal model of glaucoma and the potential mechanisms.

Materials and methods

Laboratory animals

All animal experiments were conducted in accordance with the EU Animal Experimentation Directive 2010/63/EU and the Association for Research in Vision and Ophthalmology (ARVO) guidelines. In this study, the implemented animal protocol was scrutinized and approved by the government agency responsible for animal welfare in the state of North Rhine-Westphalia (Landesamt für Natur, Umwelt und Verbraucherschutz Nordrhein-Westfalen, Germany). The experiments were performed in C57BL/6J male mice (8–9 weeks old), *Nox2* $^{-/-}$ ($gp91^{phox-/-}$) and age-matched wildtype (WT) mice. The standard mouse housing conditions were: 12 h light/dark cycle, 22 ± 2 °C, 55 ± 10% humidity, and free access to food and water.

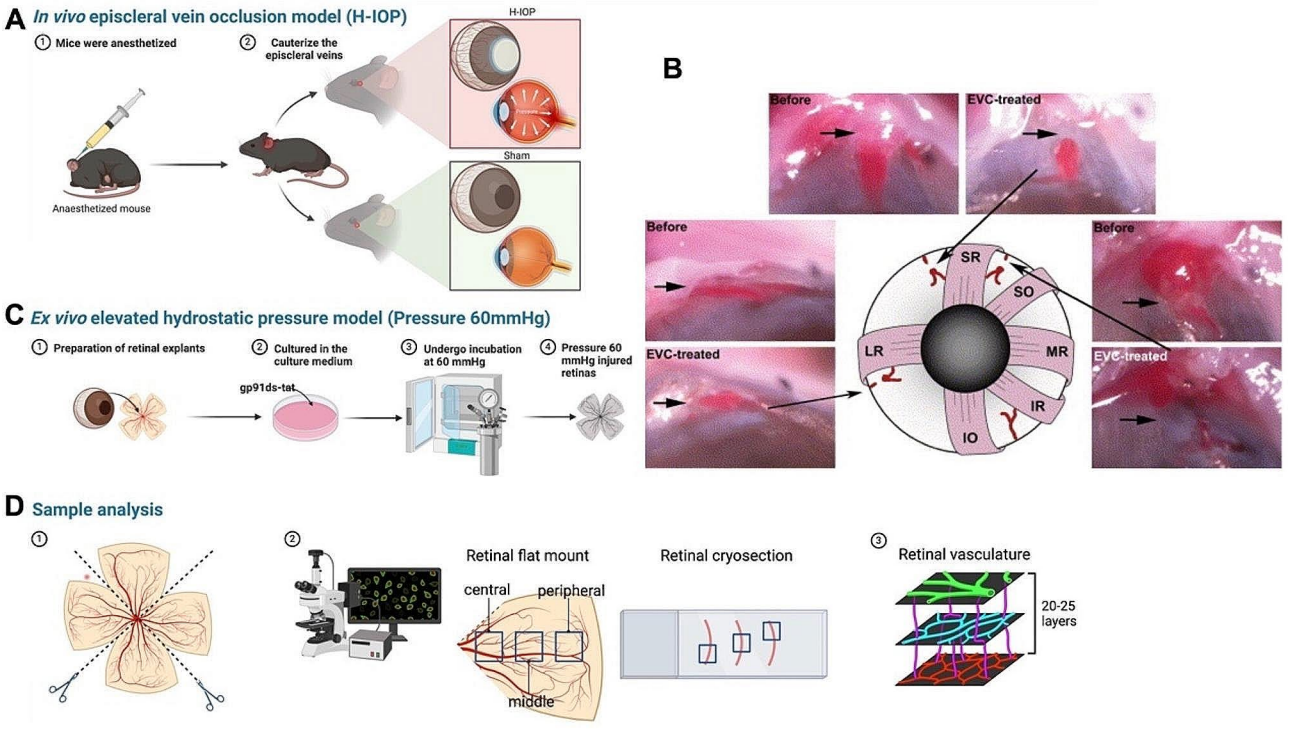

Fig. 1 Schematic diagram of the construction of mouse glaucoma model and analysis of retinal samples. (**A**) The overview of in vivo H-IOP mouse model construction. (**B**) The schematic diagram of episcleral vein cautery. Image from Ruiz-Ederra et al., 2005 [23]. The illustration of the mouse eye depicts episcleral veins (red) relative to extraocular muscles, with three veins marked by cauterization interruptions. Pre- and post-cauterization (EVC-treated) images of these veins are provided, with arrows pointing to cauterization sites. (**C**) The overview of ex vivo retinal explants Pressure 60 mmHg model construction and inhibition of gp91ds-tat. (**D**) The overview of the retina sample preparation and the imaging and analysis of the retinal flat mount and cryosection. Abbreviations: EVC, episcleral vein occlusion; IO, inferior oblique; IR, inferior rectus; LR, lateral rectus; MR, medial rectus; SO, superior oblique; SR, superior rectus

In vivo episcleral vein occlusion model (H-IOP)

All animals received episcleral vein occlusion surgeries in their right eyes (H-IOP) and sham surgeries in their left eyes (Sham) (Fig. 1A). The glaucoma mouse model was induced by occlusion of the three episcleral veins in their right eyes [19, 23]. Briefly, mice were anesthetized using a ketamine (100 mg/kg) and xylazine (10 mg/kg) solution via intraperitoneal injection. We also applied one drop of the 4 mg/mL oxybuprocain hydrochloride (Novesine® 0.4% Eyedrops, OmniVision®, OmniVision GmbH, Puchheim, Germany) onto the scathe ocular surface for local anesthesia. A cut was made across the conjunctiva and Tenon's capsule at the limbal edge of the right eye under an operating microscope. Two relaxing incisions were made at the edges of the initial incisions, and the tissue was recessed posteriorly to expose the underlying extraocular superior and lateral rectus muscles. These muscles were gently pulled aside with a suture, bringing the episcleral veins into view. After surgical isolation, microforceps were positioned under the episcleral veins adjacent to the lateral and superior rectus and to the superior oblique muscles. A hand-held ophthalmic thermal cautery device (Fine Science Tools GmbH, Heidelberg, Germany) was employed to cauterize each vein until venous congestion was noticeable, indicating blockage without any leakage (Fig. 1B, the Image from *Ruiz-Ederra et al., 2005*). Great care was taken to minimize blood loss and avoid damage to the conjunctiva and the underlying sclera. Finally, the conjunctiva was put back to its original location, and ofloxacin ointment was given onto the ocular surface to prevent inflammation. Sham surgery was conducted similarly but without causing damage to the episcleral veins. Euthanasia via cervical dislocation was performed on the mice at three distinct post-operative intervals: 4 days, 8 days, and 2 weeks.

IOP monitoring

The IOP of the mice was monitored using a TonoLab rebound tonometer (iCare, Vantaa, Finland) in animals once every two days [24, 25]. All measurements were conducted between 9:00 a.m. to 12:00 p.m. for comparability. After six consecutive measurements, the tonometer generated a mean IOP. We took 5 sets of measurements and averaged these IOP values.

Ex vivo elevated hydrostatic pressure model (Pressure 60 mmHg)

The C57BL/6J, *Nox2* $^{-/-}$, and WT mice were euthanized by cervical dislocation. Eyes were immediately enucleated and transferred to Petri dishes containing ice-cold phosphate-buffered saline (PBS) (Carl Roth,1108.1), followed by peeling out the intact retina and dissecting the vitreous humor. The retinal explants were divided equally into four segments, ensuring that the ganglion cells were facing upward, and placed in Mixed Cellulose Ester (MCE) Membrane Filters (Advantec, A045R047Z-P). The retinal explants were transferred to lumox culture dishes 35 (Sarstedt, Nümbrecht, Germany). Retinal tissues were cultured in the standard culture medium, Dulbecco's Modified Eagle's Medium/Nutrient Mixture F-12 (DMEM/F12; Gibco BRL, Eggenstein, Germany) supplemented with 10 µg/mL porcine insulin, 100 U/mL penicillin, 100 µg/mL streptomycin. To minimize variability, retinal tissues were randomly assigned to the control and Pressure 60 mmHg groups.

For the Pressure 60 mmHg model, retinal explants undergo incubation for 8,16,24 h in a tailor-made pressure incubator chamber at a hydrostatic pressure of 60 mmHg, which simulates intraocular conditions under abnormally elevated IOP. Pressure incubation chambers with lids and non-directional valves allow access to 5% CO_2 in the incubator at 37 °C for constant monitoring of internal air pressure employing manometers. Control retinas were cultured in the incubator with humidified 5% CO_2 at 37 °C under normal atmospheric pressure (Fig. 1C).

gp91ds-tat pharmacological intervention for experimental glaucoma models

The peptide gp91ds-tat (YGRKKRRQRRRCSTRIRRQL-NH2), a NOX2-specific inhibitor, interferes with NADPH oxidase assembly by targeting a sequence essential for binding $gp91^{phox}$ with $p47^{phox}$ [26, 27]. HIV-tat peptide, an amino acid sequence internalized by all cells, is linked to the $gp91^{phox}$ sequence to facilitate cell entry [28]. For the Pressure 60 mmHg model, the retinal explants from C57BL/6J mice were incubated by adding different concentrations of gp91ds-tat (Anaspec, San Jose, CA, USA) in the standard culture medium for 24 h (Fig. 1C). Control or Pressure 60 mmHg retinas were incubated in the standard culture medium (Vehicle). For the in vivo H-IOP model, the different concentrations of gp91ds-tat (dissolved in normal saline) were injected intraperitoneally (10 ml/kg) 30 min after the H-IOP surgery and once every two days until the end of the experiment. Sham and H-IOP mice were injected with normal saline (Vehicle) (10 ml/kg). The mice were euthanized by cervical dislocation after two weeks. The preparation of retinal explants was performed as described above.

Immunostaining of retinal flat mounts and cryosections

Each retina was divided into four equal sections along the dotted line in the schematic of Fig. 1D-1. Then, each quarter of the retinal explants from different mice served as an independent sample of each group, which was subjected to immunostaining for different markers and preparation of frozen sections. Retinal explants were fixed in 4% paraformaldehyde (PFA) (Histofix, Roth, Karlsruhe, Germany) for 30 min after rinsing with PBS. Subsequently, the retinas were rinsed twice with PBS for 10 min and dehydrated in 30% sucrose solution at 4 °C for 24 h to be analyzed further. After washing 3 times (10 min each) in PBS, the retinas were incubated in a buffer solution containing 1% BSA and 0.3% Triton-X-100 in PBS for 2 h at room temperature. Then, the retinas were incubated overnight at 4 °C with the primary antibody (Table 1). Next, the retinas were washed with PBS and placed with the secondary antibody in 1% BSA and 0.3% Triton-X-100 in PBS for 2 h at room temperature. Afterward, the retinas were rinsed with PBS three times and mounted on slides.

After fixation, the retinas were embedded in an optimal cutting temperature (OCT) compound (Sakura Finetek, Torrance, CA, USA) for cryostat sectioning. Retinal explants were cut vertically to a thickness of 12 µm by a Leica CM3050S cryostat (Leica Microsystems, Buffalo Grove, IL), collected onto gelatin-coated slides, and stored frozen until immunohistochemical processing. The retinal sections were washed with PBS for 5 min over 3 times. Then, the retina was blocked with 3% Normal goat serum and 0.1% Triton X-100 in PBS for 60 min, followed by primary antibodies (Table 1) at 4 °C for overnight incubation. After washing with PBS for 5 min 3 times, ensure that all procedures are performed in the dark and apply the secondary antibody 1:1000 in PBS for 2 h. Sections were rinsed with PBS. Finally, the retinal flat mounts and cryosection slides were mounted with VECTASHIELD® mounting medium with DAPI (BIOZOL Diagnostica Vertrieb GmbH, Eching, Germany) and covered with a coverslip.

Imaging and analysis of retinal flat mounts and cryosections

Images were captured using a Zeiss Imager M.2 equipped with an Apotome.2 (Carl Zeiss; Jena, Germany). As detailed in Fig. 1D-2, three areas—central, middle, and peripheral—were imaged under a 20X magnification for each quarter of the retinal flat mount. Similarly, for retinal cryosections, the Zeiss Imager M.2 with an Apotome.2 was employed to photograph the central, middle, and peripheral regions of three consecutive sections from each sample, using a 20X objective.

Glia-vascular unit interactions in the retinal flat mounts were examined using a Leica SP8 confocal

Table 1 Antibodies used for histological analyses

Marker	Company	Dilution	Secondary antibody
Brn3a (mouse)	Millipore, MAB1585, Lot#3,684,607, EMD Millipore Corporation, Temecula, CA, USA	1:200	goat anti-mouse IgG H + L (Alexa Flour 488; ab150113, Abcam, Cambridge, UK)
Iba1 (rabbit)	019-19741, FUJIFILM Wako Pure Chemical Corporation	1:500	goat anti-rabbit IgG H + L (Alexa Flour 594; ab150080, Abcam, Cambridge, UK)
CD31 (mouse)	MEC13.3, BD	1:200	goat anti-mouse IgG H + L (Alexa Flour 488; ab150113, Abcam, Cambridge, UK)
NOX2 (rabbit)	ab129068, Abcam, Cambridge, UK	1:200	goat anti-rabbit IgG H + L (Alexa Flour 594; ab150080, Abcam, Cambridge, UK)
ET-1 (mouse)	NB300-526, Novus Biologicals, Littleton, USA	1:200	goat anti-mouse IgG H + L (Alexa Flour 488; ab150113, Abcam, Cambridge, UK)
GAFP (rabbit)	#Z0334, Agilent (DAKO)	1:200	donkey anti-rabbit IgG H + L (Alexa Flour 647; ab150075, Abcam, Cambridge, UK)
Isolectin GS-IB4	Alexa Fluor 488 conjugate, Invitrogen	1:500	-
α-SMA	ab202368 Abcam, Cambridge, UK Alexa Fluor® 594 Anti-alpha smooth muscle Actin antibody (1A4)	1:200	-
p-ERK1/2 (rabbit)	#9101, Cell Signaling	1:300	goat anti-rabbit IgG H + L (Alexa Flour 594; ab150080, Abcam, Cambridge, UK)

laser-scanning microscope (Leica, Wetzlar, Germany) at 20X magnification. Additionally, CD31 immunolabeled retinal flat mounts were observed with a Leica SP8 confocal microscope. Z-stack images, comprising 20–25 layers for each area (Fig. 1D-3), were compiled along the Z-axis to produce a 2D representation of the retinal vasculature.

Image analysis was conducted using ImageJ2 2.3.0 (http://rsb.info.nih.gov/ij/), NIH, Bethesda, MD, USA. Quantitative assessments of various markers, including RGCs count et al., were performed. The mean count from the three regions of a quarter-section of the retina provided a measure of overall retinal changes, which was then utilized for further statistical evaluation.

Culture and stimulation of primary microglia

As described previously [29], primary microglia were isolated from C57BL/6J neonatal mouse pups (P0). Cell suspension was plated on cell culture dishes (Nunc) coated with Poly-D-Lysine (#A003E stock 1 mg/ml (use 50ng/ml in PBS)) in PM Medium (Neurobasal-A, 10% horse serum, B27, P/S/G). Primary Microglia at passage 2 or 3 were used for experiments. Cells were stimulated with 100nM ET-1 (E7764, Sigma-Aldrich) and inhibited with 20 μm MEK (PD98059) for 20 min and 24 h starting at 3 days in vitro (DIV). For Immunostaining, primary microglia grown on slides were treated and then washed with PBS, followed by fixation with 4% PFA for 30 min. The immunostaining protocol for primary microglia follows the same procedure as used for the retinal flat-mount.

Quantification of cytosolic ROS

Retinas were also homogenized in lysis buffer as previously described [30]. Lysates were centrifuged at 1500 g for 3 min, and the supernatant was exposed to 20 μM 2,7-dichlorofluorescein derivative 6-carboxy-2,7-dichlorodihydrofluorescein diacetate, di(acetoxymethyl ester) (referred to as DCF throughout this manuscript) for 30 min at 37 °C. Fluorescence was measured using a plate reader (Tecan infinite 200Pro) (ex/em=485/535 nm).

Quantification of superoxide (O_2^-)

O_2^- levels were measured in frozen sections of unfixed retinas by staining with the fluorescent dye dihydroethidium (DHE) [19, 31–33]. Immediately after thawing, tissue sections were incubated with 1 μM of DHE for 30 min at 37 °C. The slides were mounted with VectaShield mounting medium (Vector Laboratories, Burlingame, CA) and covered with a coverslip. Photographs of retinal cross-sections were taken using a Leica SP8 confocal laser scanning microscope (Leica, Wetzlar, Germany). As described previously, the staining intensity of blood vessels and individual retinal layers was measured using ImageJ software (NIH, http://rsb.info.nih.gov/ij/).

Assessment of optic nerve degeneration

Optic nerve (ON) degeneration was assessed by p-phenylenediamine (PPD)-stained ON cross sections, as previously described [34, 35]. The semi-thin cross sections of ON were taken from 1.0 mm posterior to the eyeballs. In brief, the ON was separated from the eyeball and fixed overnight in a phosphate-buffered 3% glutaraldehyde/paraformaldehyde mixture at 4 °C. Following overnight treatment in 1% osmium tetroxide at 4 °C, ON were rinsed in 0.1 M phosphate buffer and 0.1 M sodium-acetate buffer, then dehydrated in graded ethanol concentrations. After embedding ON in resin (Eponate-12; Ted Pella), 1 µm sections were cut and stained in 1% PPD for 10 min. The sections were imaged under a Zeiss Axio Imager Z1 Microscope (Zeiss, Oberkochen, Germany) with a Zeiss Plan-ACHROMAT 100×Lens (Zeiss, Oberkochen, Germany). Image Acquisition was performed using a Canon EOS 6D Mk II camera (Canon, Krefeld, Germany) and CanonEOS Utility Software (Canon, Krefeld, Germany). Following a protocol similar to that of retinal cryosection imaging, three fields (including one central and two peripheral) were imaged from three sequential cross-sections for each ON, utilizing a 100× magnification. ON axon numbers were counted manually with ImageJ software (http://rsb.info.nih.gov/ij/, NIH, Bethesda, MD, USA), and the average numbers were calculated as axon density per square millimeter of ON and then multiplied by cross-sectional area to calculate the total number of axons per ON [31].

Western blotting

Tissues were processed for Western blotting as previously described [36]. In brief, the retinal tissues and primary microglia were washed twice with cold PBS and incubated in 100 µL lysis buffer (T-PER Tissue Protein Extraction Reagent + 2% protease inhibitor) per whole retina explants on ice. After 15 min of incubation, the retina and cell lysates were dissected and sonicated for 1 min in an ultrasonic bath on ice and then centrifuged at 1000 g for 8 min. The supernatants were collected for further analysis. The BCA Protein Assay Kit (Pierce, Rockford, IL, USA) determined each lysate's protein concentration per the manufacturer's instructions. From each retina lysate, 20 µg of protein was loaded onto a Novex NuPAGE 12% Bis-Tris polyacrylamide gel (Thermo Fisher, USA). The gel electrophoresis was run using NuPAGE running buffer MES at room temperature with a voltage of 130 V for 60 min. After electrophoresis, the proteins were transferred to polyvinylidene fluoride membranes (Bio-Rad, Gladesville, Australia) using a dry transfer system (Bio-Rad, Hercules, CA, USA), and a standard transfer buffer (with 20% methanol), a voltage of 20 V was applied for 7 min. For immunoblotting, membranes were incubated with the appropriate antisera ET-1 (1:1000, NB300-526, Novus Biologicals, Littleton, USA), $p47^{phox}$ (1:1000, sc-17,845, Santa Cruz Biotechnology), $gp91^{phox}$ (1:1000, sc-130,543, Santa Cruz Biotechnology), polyclonal antibodies recognizing phospho-JNK (Thr183/185) (1:1000; catalog no. 9251), phospho-ERK1/2 (Thr202/204) (1:1000; catalog no. 9101) and phospho-p38 MAPK (Thr180/182) (1:1000; catalog no. 4511) overnight at 4 °C, and labeling was carried out using a multi-step detection procedure. First, appropriate biotinylated secondary antibodies were reacted with membranes, and then streptavidin-peroxidase conjugates were applied. Blots were developed with a 0.016% solution of 3-amino-9-ethyl carbazole in 50 mM sodium acetate (pH 5) containing 0.05% Tween-20 and 0.03% H_2O_2. Images were acquired from labeled blots and analyzed for densitometry using the software program ImageJ2 2.3.0. Densitometry values were then normalized for β-actin (1:10000, ab6276, Abcam).

MS measurement

Proteins were extracted from the retinal tissue of these individuals using the detergent sodium dodecyl sulfate (SDS), which is the most efficient reagent for lysing tissue and cells to achieve complete protein extraction [37]. Subsequently, DIA-MS proteomics analysis was performed with a high-resolution, high-quality precision LTQ-Orbitrap Elite mass spectrometer. The continuum MS data were collected by an ESI-LTQ Orbitrap XL-MS system (Thermo Scientific, Bremen, Germany) and searched against the UniProt database with MaxQuant software version 1.5.3.30 (Max Planck Gesellschaft, Germany). Due to the random nature of "Birdshot" label-free quantitative proteomics, protein identification or abundance data are sometimes missing in some samples [38]. 40 A target-decoy-based false discovery rate (FDR) was set to 0.01 for the identification of peptides and proteins, the minimum peptide length was 6 amino acids, and the minimum unique peptides were set at 2. Fold changes of the label-free quantitation (LFQ) intensities were calculated to identify the significantly differentially expressed proteins (DEPs). We performed differential expression analysis on the quantitative proteomics data targeting the H-IOP relative to the control |Student's T-test Difference| ≥ 0.5 change threshold and -Log *P*-value > 1.3. To outline the DEPs profiles of the transcripts, generating volcano maps via the R ggplot2 package and performing hierarchical cluster analysis via the Manhattan distance metric and the Ward minimum variance method from the heatmap package in R. Principal component analysis (PCA), implemented in the prcomp function of R, was conducted to abstract the main characteristics of the data, which served as an indicator of the overall state of the data.

Gene ontology and kyoto encyclopedia of genes and genomes pathway analysis

Gene Ontology (GO; http://geneontology.org/) analysis is based on three annotated ontologies, including the exploration of molecular function (MF), cellular components (CC), and biological processes (BP), which originate from DEPs targeting genes. Simultaneously, the Kyoto Encyclopedia of Genes and Genomes (KEGG; http://www.kegg.jp/) analysis was performed to assess the biological functions and enrichment pathways of the DE genes. GO and KEGG analyses were performed by assigning R packages based on hypergeometric distributions.

Enzyme-linked immunosorbent assay (ELISA)

The concentration of cytokines in total retinal and primary microglia lysates was measured by ELISA. Tissue samples were sonicated in PBS supplemented with protease and phosphatase inhibitors (Complete protease inhibitor cocktail, Roche). Interleukin 1beta (IL-1β) (DY401), tumor necrosis factor-alpha (TNF-α) (DY410), and interleukin 6 (IL-6) (DY406) Quantikine® ELISA's were purchased from R&D Systems.

Quantification of gene expression by quantitative PCR

Messenger RNA for the pro-oxidant enzymes, the NOX enzymes (*Nox1*, *Nox2*, *p47* ^{phox}, *Nox4*), for the vascular endothelial growth factor-A (*Vegf-a*), for the antioxidant redox enzymes, heme oxygenase 1 (*Ho-1*), and glutathione peroxidases 1 (*Gpx1*), for the cytokines, *Tnf-α*, *IL-1β*, superoxide dismutase type 2 (*Sod2*), and for the nitric oxide synthase (NOS) isoforms, *eNos*, *iNos*, and *nNos*, was quantified in the whole retinal explants as described before [39]. Tissue samples were homogenized (FastPrep; MP Biomedicals, Illkirch, France). RNA was isolated using peqGOLD TriFast™ (PEQLAB), and cDNA was generated with the High-Capacity cDNA Reverse Transcription Kit (Applied Biosystems, Darmstadt, Germany). Quantitative real-time RT-PCR (qPCR) reactions were performed on a StepOnePlus™ Real-Time PCR System (Applied Biosystems) using SYBR® Green JumpStart™ Taq ReadyMix™ (Sigma-Aldrich, Munich, Germany) and 20 ng cDNA. Relative mRNA levels of target genes were quantified using the comparative threshold (CT) normalized to the housekeeping gene TATA-binding protein (*Tbp*). The qPCR primer sequences are shown in Table 2.

Statistics

Details of the statistical test used for each experiment are in figure legends, along with n and *p*-value. All data is represented as mean ± SEM. Statistical analysis was performed using GraphPad Prism 9 (GraphPad Software, La Jolla, California, USA).

Results

H-IOP injury-induced glaucomatous RGC loss and neurodegeneration H-IOP injury provoked up-regulation of NOX2 expression accompanying O_2^- over-production in the retina

To elucidate the effect of H-IOP on glaucoma, we first assessed the survival of the Brn3a-positive RGC by establishing a corresponding model ex vivo explant cultures (Pressure 60 mmHg) and in vivo (H-IOP). Compared with the control group (0 mmHg, 24 h), Pressure 60 mmHg induced retinal damage, resulting in a decrease in RGC survival from 16 h, peaking at 24 h with an RGC loss rate of 62.35% ($n=6$, $p<0.0001$) (Fig. 2A, B). In addition, we induced mice sustainability H-IOP by episcleral vein occlusion. IOP ascends to a maximum within six days post-H-IOP surgery with a mean value of 29.33 ± 0.20 mmHg ($p<0.0001$), which indicates successful induction of H-IOP glaucoma. By Day 14, the mean IOP progressively dropped to a mean value of 23.60 ± 0.23 mmHg ($p<0.0001$), which was still above the physiologic IOP value (13.43 ± 0.2275 mmHg) (Fig. 2C).

Table 2 Primer sequences used for quantitative PCR analysis

Gene	Accession number	Forward	Reverse
Nox1	NM_172203.1	GGAGGAATTAGGCAAAATGGATT	GCTGCATGACCAGCAATGTT
Nox2	NM_007807.2	CCAACTGGGATAACGAGTTCA	GAGAGTTTCAGCCAAGGCTTC
p47^{phox}	NM_001286037.1	AGAGCACGGATGGCACAAAG	CCGCGGGCTGTGGTT
Nox4	NM_015760.2	GGCTGGCCAACGAAGGGGTTAA	GAGGCTGCAGTTGAGGTTCAGGACA
Ho-1	NM_010442	GGTGATGCTGACAGAGGAACAC	TAGCAGGCCTCTGACGAAGTG
Vegf-a	NM_001025250.3	ACTTGTGTTGGGAGGAGGATGTC	AATGGGTTTGTCGTGTTTCTGG
Gpx1	NM_008160	CCCGTGCGCAGGTACAG	GGGACAGCAGGGTTTCTATGTC
Sod2	NM_013671	CCTGCTCTAATCAGGACCCATT	CGTGCTCCCACACGTCAAT
Tnf-α	NM_001278601.1	GCCTCTTCTCATTCCTGCTTG	CTGATGAGAGGGAGGCCATT
Il-1β	NM_008361	AAGGAGAACCAAGCAACGACAAAA	TGGGGAACTCTGCAGACTCAAACT
eNos	NM_008713	CCTTCCGCTACCAGCCAGA	CAGAGATCTTCACTGCATTGGCTA
iNos	NM_010927	CAGCTGGGCTGTACAAACCTT	CATTGGAAGTGAAGCGTTTCG
nNos	NM_008712	TCCACCTGCCTCGAAACC	TTGTCGCTGTTGCCAAAAAC
Tbp	NM_013684	CTTCGTGCAAGAAATGCTGAAT	CAGTTGTCCGTGGCTCTCTTATT

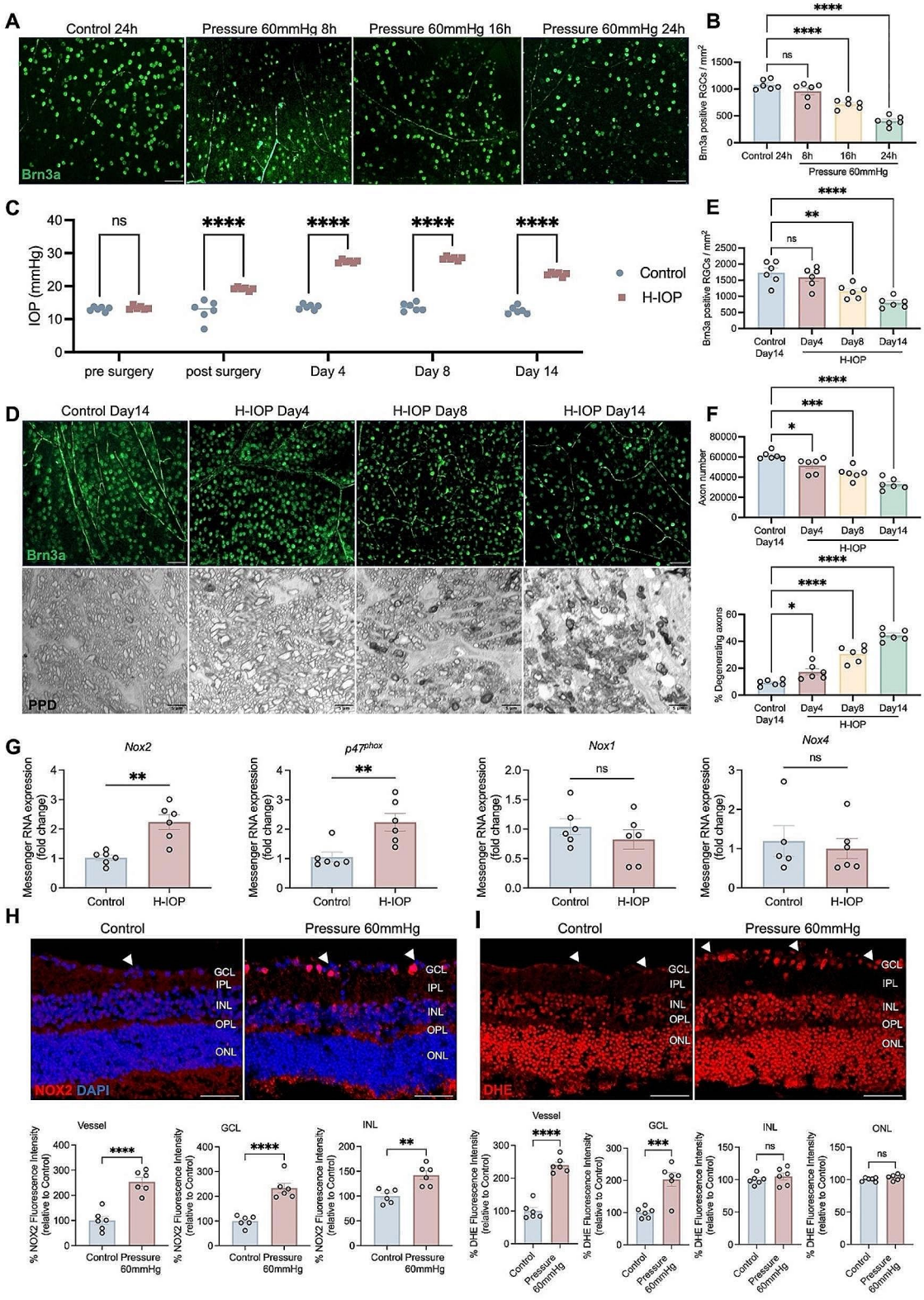

Fig. 2 (See legend on next page.)

(See figure on previous page.)

Fig. 2 Pathologically high intraocular pressure-induced glaucomatous RGC loss and neurodegeneration. (**A**) Representative images of flat mount retina immunostained with Brn3a after Pressure 60 mmHg. Scale bar, 50 μm. (**B**) Analysis of the number of Brn3a-positive RGCs at different times after Pressure 60 mmHg. Data are shown as mean ± SEM ($n=6$ in each group, one-way ANOVA with Tukey's multiple comparisons test, *$p<0.05$,**$p<0.01$, ***$p<0.001$, ****$p<0.0001$). (**C**) Time course of IOP before as well as 14 days after H-IOP surgery. Data are shown as mean ± SEM ($n=6$ in each group, two-way ANOVA with Šídák's multiple comparisons test, ****$p<0.0001$). (**D**) Representative images of flat mount retina immunostained with Brn3a and PPD-stained ON after H-IOP. Scale bar, 50 μm and 5 μm. (**E**) Analysis of the number of Brn3a-positive RGCs at different times after H-IOP. (**F**) Analysis of the number of axons and the percent of degenerating axons in the different groups. Data are shown as mean ± SEM ($n=6$ in each group, one-way ANOVA with Tukey's multiple comparisons test, *$p<0.05$,**$p<0.01$, ***$p<0.001$, ****$p<0.0001$). (**G**) Messenger RNA expression of Nox enzymes (Nox2, $p47^{phox}$, Nox1, Nox4) in H-IOP retinas. Data are presented as the fold-change after H-IOP versus control. Data are shown as mean ± SEM ($n=6$ in each group, Unpaired T-test, *$p<0.05$,**$p<0.01$, ***$p<0.001$, ****$p<0.0001$). (**H**) Representative images of retinal cross-sections immunostained with NOX2 after Pressure 60 mmHg (Scale bar, 50 μm) and the analysis of NOX2 fluorescence intensity in the retinal vessels and different retinal layers. (**I**) Representative images of retinal cross-sections immunostained with DHE staining after Pressure 60 mmHg. Scale bar, 50 μm. Analysis of DHE fluorescence intensity in the retinal vessels and different retinal layers. The white arrows point to cross-sections of retinal blood vessels. Data are presented as the percent fluorescence intensity of the Pressure 60 mmHg versus control. Data are shown as mean ± SEM ($n=6$ in each group, Unpaired T-test, **$p<0.01$, ****$p<0.0001$)

Correspondingly, RGCs declined from Day 8 and peaked at Day 14 ($803\pm66.20/mm^2$) compared to sham ($1734\pm141.7/mm^2$) ($n=6$, $p<0.0001$) (Fig. 2D, E). Furthermore, PPD staining of ON cross-sections indicated a reduction in the total number of myelinated axons induced by H-IOP injury from Day 4, scattered vacuole formation on Day 8, and a significant vesicle and glial scar formation on Day 14 (Fig. 2F). Interestingly, ON degeneration belongs to an early event in glaucoma that appears to pre-date the loss of RGC. In conclusion, these data confirm that the H-IOP will contribute to the loss of RGC and ON degeneration in a time-dependent manner. Inspired by the above results, Pressure 60 mmHg–24 h and H-IOP-14-day retinas were selected for follow-up experiments to ensure the reliability of the experimental glaucoma model.

Besides mitochondria, the NOX enzymes [40] have been identified as one of the major sources of oxidative stress in retinal eye diseases such as ischemic retinopathy and age-related macular degeneration [41]. Aiming to determine the potential role of NOX enzymes in H-IOP-induced glaucomatous damage, we analyzed the transcription levels of different *Nox* isoforms by qPCR. The results show that the transcription levels of *Nox2* and $p47^{phox}$ statistically increased in the retina after H-IOP injury (Fig. 2G). In contrast, the mRNA levels of *Nox1* or *Nox4* were not significantly altered. Consistent with H-IOP-induced retinal injury, in the ex vivo Pressure 60 mmHg model, we observed a robust increase in NOX2 immunoreactivity compared to the control, which was specifically localized to the retinal vessels, the ganglion cell layer (GCL) and the inner nuclear layer (INL) (Fig. 2H). Interestingly, DHE staining assays indicated that Pressure 60 mmHg damage strongly stimulated the overproduction of O_2^-, which highly overlapped with the strong fluorescence region of NOX2 (Fig. 2I). These data imply that H-IOP-induced retinal injury might be associated with NOX2-mediated oxidative stress.

The gp91ds-tat treatment modulates oxidative stress-driven pro-inflammatory signaling in H-IOP-injured retinas

To fully characterize the proteomic profiles associated with experimental glaucoma in mice, we performed proteomic analysis on retinal samples from control mice, H-IOP mice, and treated with gp91ds-tat mice ($n=4$). The PCA maps illustrated the overall reproducibility and individual heterogeneity of protein expression profiles between Control, H-IOP, and H-IOP retinas treated by gp91ds-tat (Fig. 3A). We identified 1174 DEPs in the H-IOP compared with Control, 1110 DEPs in the H-IOP with gp91ds-tat compared with H-IOP, and 34 DEPs in the H-IOP with gp91ds-tat compared with Control (Fig. 3B). As shown in Fig. 3C, by Venn analysis, we screened 635 co-DEPs between the data set of H-IOP compared with Control and H-IOP with gp91ds-tat compared with H-IOP. Subsequent KEGG secondary pathway enrichment analysis of the 635 DEPs revealed that the Immune system was the most highly enriched in the Organismal Systems category (Fig. 3D). NOX2-derived ROS can affect pro-inflammatory signaling [42]. As shown in Fig. 3D, the gp91ds-tat treatment effectively reduced the expression of most immune-related genes in H-IOP-injured retinas. KEGG enrichment analysis revealed the C-type lectin receptor signaling pathway, MAPK signaling pathway, and reactive oxygen species (Fig. 3E). Notably, GO enrichment analysis also revealed that experimental glaucoma involves multiple BP, CC, and MF, which intimately correlated with response to oxidative stress and inflammatory response (Fig. 3F).

NOX2 deficiency or pharmacological inhibition via gp91ds-tat salvages H-IOP injury-induced glaucomatous RGC loss and neurodegeneration but not IOP modulation

To further explore the contribution of NOX2 in glaucoma, we initially tracked changes in RGC applying *Nox2* $^{-/-}$ mice. Compared with WT retinas, the survival of RGCs in *Nox2* $^{-/-}$ retinas improved by 52% after 24 h at Pressure 60 mmHg (Fig. 4A, B). Meanwhile, intraperitoneal injection of gp91ds-tat in mice significantly attenuated H-IOP-induced Brn3a-positive RGC loss in

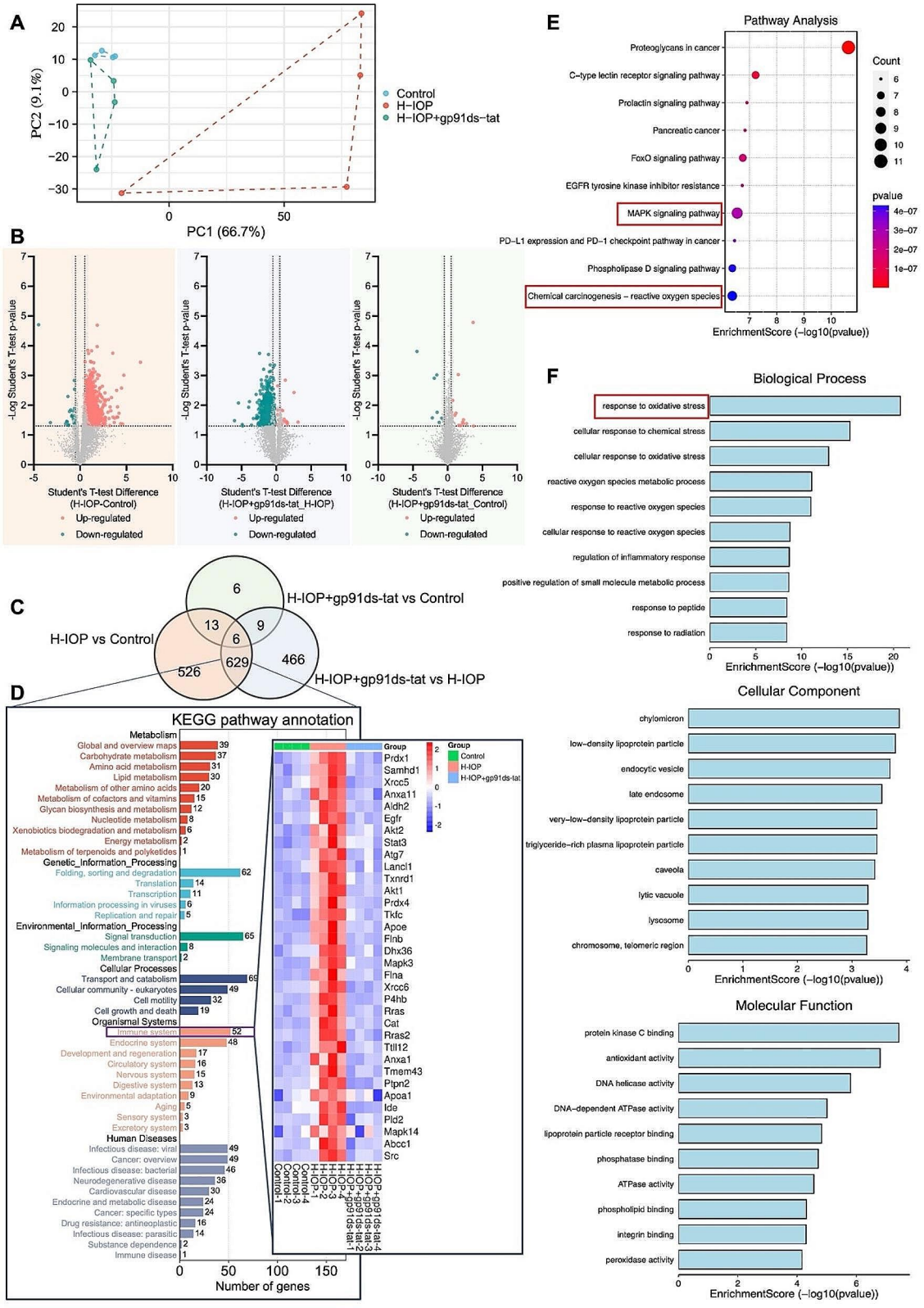

Fig. 3 (See legend on next page.)

(See figure on previous page.)

Fig. 3 gp91ds-tat treatment effectively modulates the expression of major immune-related genes in H-IOP injured retina. (**A**) Principal component analysis shows the clustering of proteins in different samples. (**B**) Volcano plot showing differentially expressed proteins between H-IOP and control group, H-IOP + gp91ds-tat and H-IOP, H-IOP + gp91ds-tat and control group. (**C**) The Venn diagram was created by the differentially expressed data of proteins. (**D**) The most enriched KEGG Level 2 pathways for the 635 co-differentially expressed proteins. Hierarchical clustering illustrates distinct expression differences of immune genes between the three groups and homogeneity between groups. (**E**) The 10 most enriched KEGG pathways for the differentially expressed proteins. The size of the symbol represents the number of genes, and the colors represent the *p*-value. (**F**) The 10 most enriched gene ontology terms for the parental genes of the differentially expressed immune genes. Enriched GO terms are on the vertical axis, and the number of annotated differentially expressed genes associated with each GO term is indicated on the horizontal axis

a dose-dependent manner but failed to modulate IOP (Fig. 4C-F). In addition, gp91ds-tat-treated effectively ameliorated H-IOP-induced ON degeneration, which included a 34% increase in the total number of axons (44,390±1843 vs. 33,220±2334, $n=6$, $p=0.0058$); and a 17% increase in the percentage of degenerated axons (27.33±3.879% versus 44.50±1.648%, $n=6$, $p=0.0006$) (Fig. 4E, G, H).

Finally, to support the knockout outcome by translational therapeutic approaches, we analyzed the RGC-protective effect of gp91ds-tat ex vivo. Treatment with 100μM, 300μM, and 500μM gp91ds-tat enhanced RGC survival by 62%, 95%, and 81%, respectively, compared to controls ($p<0.05$) (Fig. 4I, J). Therefore, 300μM gp91ds-tat was considered the optimal therapeutic dose under in vitro conditions and was set as the standard treatment for subsequent experiments (*** $p<0.001$). These data demonstrate that the absence of NOX2 and pharmacological inhibition effectively attenuates pathologically glaucomatous ON degeneration and reverses the loss of RGCs induced by H-IOP.

NOX2 deficiency or inhibition dampens O_2^- overproduction induced by H-IOP in the vascular and GCL of the retina

NOX2-mediated ROS are an essential source of oxidative stress, whose excessive accumulation leads to retinal damage [43]. By quantifying the superoxide produced in the retina by reacting with DCF, we identified that Pressure 60 mmHg significantly evoked WT retinal superoxide production, which could be prevented by *Nox2* $^{-/-}$ (Fig. 5A). The results support the hypothesis that NOX2-mediated ROS is a key event in oxidative stress in the Pressure 60 mmHg retina.

To further clarify the primary location of NOX2-mediated ROS production in the H-IOP retina, we co-stained DHE with CD31 in the retinal cryosection to delineate oxidative stress derived from EC (Fig. 5B). *Nox2* $^{-/-}$ or treatment with gp91ds-tat significantly suppressed the overproduction of O_2^- by EC, vasculature, and GCL at Pressure 60 mmHg (Fig. 5B-E). Notably, NOX2-mediated modulation of ROS was particularly prominent in the endothelium, where up to 2-fold excess O_2^- was almost entirely inhibited by *Nox2* $^{-/-}$ or gp91ds-tat. In contrast, there are no significant changes in other layers (Fig. 5E, *Additional file 1*). The data show that pathologically H-IOP-induced NOX2-mediated ROS overproduction dominantly derives from ECs, blood vessels, and GCL.

Next, we attempted to elucidate the substantial pharmacologic role of gp91ds-tat repression of the NOX2 enzyme activity in glaucoma. The gp91ds-tat strongly attenuated the immunoreactivity augmentation by Pressure 60 mmHg injury-mediated NOX2, which was selectively localized to the vessel sites, GCL and INL by immunofluorescence staining in retinal cryosections (Fig. 5F, G). In addition, the transcript levels of *Nox2* and *p47* ^{phox} were significantly reduced in the H-IOP retinas treated with gp91ds-tat compared to the vehicle (Fig. 5H). Western blot analysis also supports that gp91ds-tat effectively reduces the expression levels of $gp91^{phox}$ and $p47^{phox}$ (Fig. 5I, J). These data indicated that gp91ds-tat does not only inhibit the activation of NOX2 but also reduces its protein expression.

NOX2/ROS-activated glial cells involved in H-IOP-mediated blood-retinal barrier damage and inflammation

Next, we hypothesized that the NOX2/ROS-specific expression pattern in the endothelium and vasculature might be involved in the regulation of the internal blood-retinal barrier (iBRB), a physiological barrier regulating the movement of ions, proteins, and water in and out of the retina, which characterizes ECs arrayed on the inner retinal microvascular system [44]. Therefore, we visualized the three main components in iBRB: glial cells (marked with GFAP, Iba1), ECs (labeled with GS-IB4), and pericytes (marked with α-SMA) in the retinal flat mount to explore further the contribution of NOX2 to iBRB (Fig. 6A). The results showed a significant decrease in the percentage coverage of α-SMA and the ratio of α-SMA/GS-IB4 after H-IOP (Fig. 6B), implicating damage to the retinal vascular system and vascular permeability. Besides, we employed confocal microscopy to observe the interaction of astrocytes with vascular units, which indicated astrocyte activation, with a significant increase in the percentage of GFAP-positive area, characterized by a significant increase in the coverage of their protrusions encircling the blood vessels (Fig. 6C). Consistent with our hypothesis, inhibition of the NOX2 activity effectively alleviated GFAP activation and proliferation adhering to the vascular surface after H-IOP, reversing the retinal vasculature system damage typified by a significant rebound in the ratio of α-SMA/GS-IB4

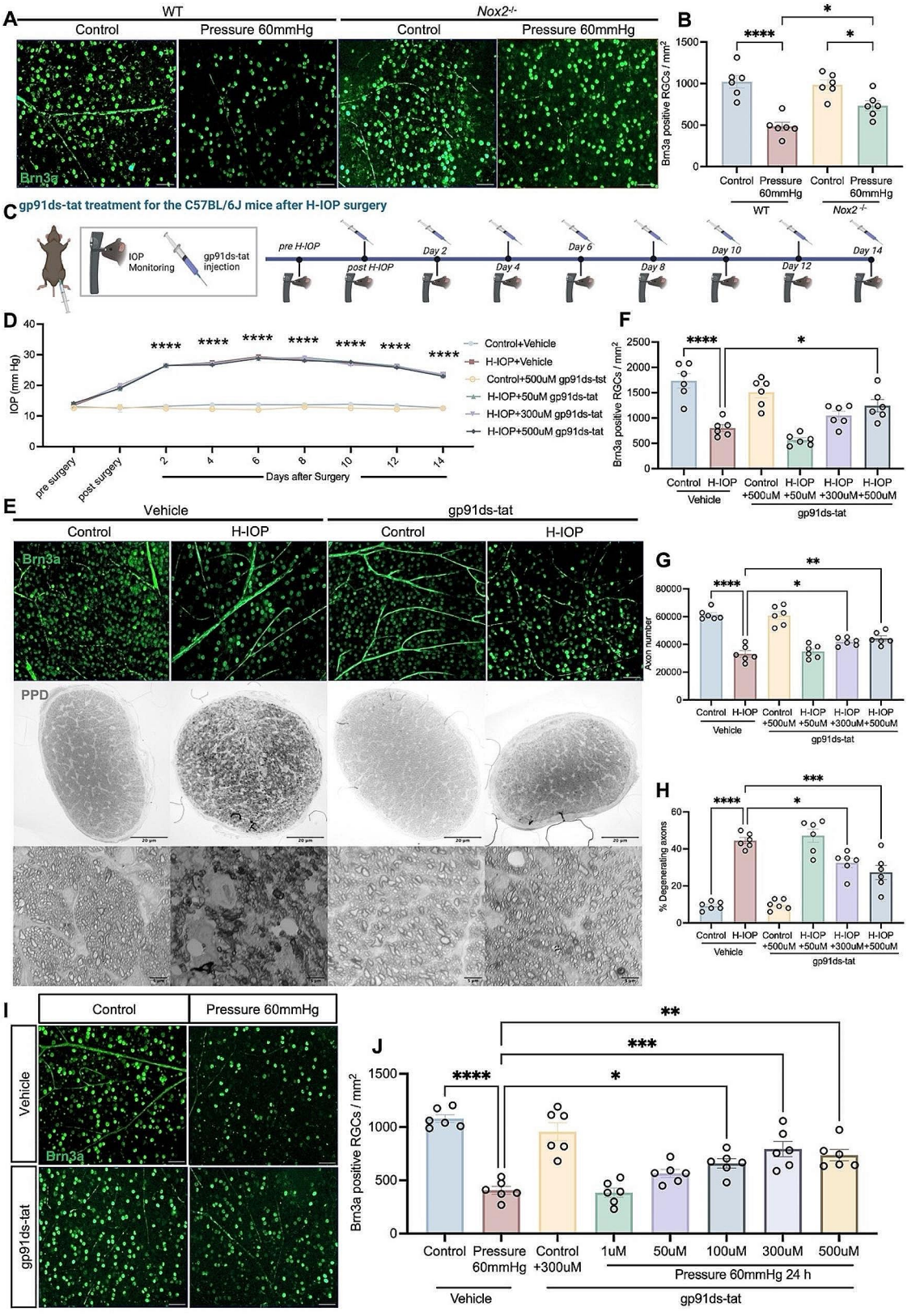

Fig. 4 (See legend on next page.)

(See figure on previous page.)

Fig. 4 Pharmacological inhibition of NOX2 attenuates Pathologically high intraocular pressure-induced glaucomatous RGC loss and ON degeneration but not IOP modulation. (**A**) Representative images of WT and Nox2$^{-/-}$ retinas immunostained with Brn3a after Pressure 60 mmHg 24 h. Scale bar, 50 μm. (**B**) Analysis of the number of Brn3a-positive RGCs in the different groups. Data are shown as mean ± SEM ($n = 6$ in each group, one-way ANOVA with Tukey's multiple comparisons test, *$p < 0.05$, **$p < 0.01$,***$p < 0.001$, ****$p < 0.0001$). (**C**) The timeline of C57BL/6J mice after H-IOP with gp91ds-tat treatment and IOP measurement. (**D**) IOP measurements revealed sustained significant IOP elevation in H-IOP mice with gp91ds-tat-injected compared to Veh-injected control mice. Data are shown as mean ± SEM ($n = 6$ in each group, two-way ANOVA with Tukey's multiple comparisons test, ****$p < 0.0001$). (**E**) Representative images of flat mount retina immunostained with Brn3a after H-IOP treated by 500μM gp91ds-tat. Scale bar, 50 μm. Representative images of PPD-stained ON after H-IOP treated by 500μM gp91ds-tat, at low (upper row, scale bar, 20 μm) and high (lower row, scale bar, 5 μm) magnification. (**F**) Analysis of the number of Brn3a-positive RGCs of retinas treated by different concentrations of gp91ds-tat after H-IOP in the different groups. (**G**) Analysis of the number of axons of ON treated by different concentrations of gp91ds-tat after H-IOP in the different groups. (**H**) Analysis of the percent of degenerating axons of ON treated by different concentrations of gp91ds-tat after H-IOP in the different groups. Data are shown as mean ± SEM ($n = 6$ in each group, one-way ANOVA with Tukey's multiple comparisons test, *$p < 0.05$, **$p < 0.01$,***$p < 0.001$, ****$p < 0.0001$). (**I**) Representative images of flat mount retina immunostained with Brn3a after Pressure 60 mmHg treated by 300μM gp91ds-tat. Scale bar, 50 μm. (**J**) Analysis of the number of Brn3a-positive RGCs of retinas treated by different concentrations of gp91ds-tat after Pressure 60 mmHg in the different groups. Data are shown as mean ± SEM ($n = 6$ in each group, one-way ANOVA with Tukey's multiple comparisons test, *$p < 0.05$, **$p < 0.01$,***$p < 0.001$, ****$p < 0.0001$)

as evidenced by the significant rebound in the ratio of α-SMA/GS-IB4. Notably, we also observed significant activation (Amoeba-like shape) of Iba1 + microglia induced by H-IOP to converge and aggregate around the vasculature (Fig. 6D, E). In contrast, gp91ds-tat treatment significantly inhibited the activated state of microglia and interrupted the chemotaxis and aggregation of perivascular microglia (Fig. 6D, E). These findings suggest that the NOX2-dependent glial-endothelial unit plays a pivotal role in the structure and function of iBRB.

Meanwhile, we observed a dramatic decrease in capillary coverage with the tendency of the vasculature to simplify and degenerate in the retinas under H-IOP (Fig. 6F). Interestingly, this substantial remodeling could be dramatically ameliorated by gp91ds-tat, characterized by a 36% increase in vascular area fraction, 59% main vessel diameter, and 39% in branch number points (Fig. 6G).

Mechanistically, NOX2/ROS is essential for the activation of glial cells, including Müller cells, astrocytes, and microglia, in which overactivation and gliosis are involved in vascular adhesion and pro-inflammatory responses, ultimately leading to the destruction of iBRB [45–47]. The retinas under Pressure 60 mmHg were observed to have an enormously increased and prolonged GFAP-positive process extending from the GCL to the INL, which effect was significantly inhibited in *Nox2* $^{-/-}$ retinas (Fig. 7A, B). Iba1 positive microglia are mainly migratory, increased in the GCL with an Amoeba-like shape, and a surge of amoeboid microglia with round bodies and scarce dendrites was detected after Pressure 60 mmHg. This microglia-reactive proliferation and infiltration could be dramatically alleviated by NOX2 deficiency (Fig. 7C, D).

Moreover, glial cell activation triggers an inflammatory response in the retinal vasculature by releasing pro-inflammatory mediators [48]. ELISA (Fig. 7E) and qPCR (Fig. 7F) results confirmed that inhibiting NOX2 activity could significantly reduce the H-IOP-induced surge in TNF-α, IL-1β, and IL-6 levels. In addition, we further examined the transcript levels of genes linked to angiogenesis and endothelial function by qPCR. The results indicated that H-IOP induces a significant elevation of *eNos* and *Ho-1*, which could be reversed by inhibiting NOX2 activity. In contrast, no significant differences in the mRNA levels of *Gpx1* and *Sod2*, hypoxia genes *Vegf-a*, *iNos*, and *nNos*, were found between the groups (Fig. 7G). Collectively, these data demonstrate that NOX2/ROS-activated glial cells facilitate iBRB damage and inflammation responses in glaucoma.

NOX2/ET-1 axis mediates microglia activation switching to M1 pro-inflammatory phenotype via ERK1/2 pathway contributing to iBRB inflammatory injury

Under pathophysiological conditions, intensified NOX2 activity promotes ET-1 production in ECs, which mediates pro-inflammatory microglia activation and neuroinflammation, involved in vascular disruption and disruption of the blood-brain barrier in neurodegenerative diseases [49–51]. To further explore the mechanism of NOX2 regulation of iBRB, we hypothesized that the NOX2/ET-1 axis regulates the proliferation of microglia (the principal mediator of neuroinflammation) via the MAPK signaling pathway mediating the inflammatory damage to the iBRB in pathologically H-IOP. We observed an effective attenuation of Pressure 60 mmHg-induced hyperimmunoreactivity of ET-1 in *Nox2* $^{-/-}$ retinas (Fig. 8A, B). Similarly, alterations in ET-1 immunoreactivity were verified in H-IOP retinas after our treatment with gp91ds-tat (Fig. 8C, D). Western blot analysis also demonstrated that Pressure 60 mmHg and H-IOP injury invokes a significant elevation in the protein level of ET-1 in retinal homogenates, which is reversible by genetic deletion of NOX2 and inhibition of gp91ds-tat (Fig. 8E). Also, gp91ds-tat significantly reversed the plunge in *Et-1* transcript levels caused by H-IOP (Fig. 8F).

To further elucidate the mechanism by which the NOX2/ET-1 axis mediates microglia activation, pure primary microglia cultures were first incubated with ET-1 (100 nM) for 20 min and 24 h. The results showed

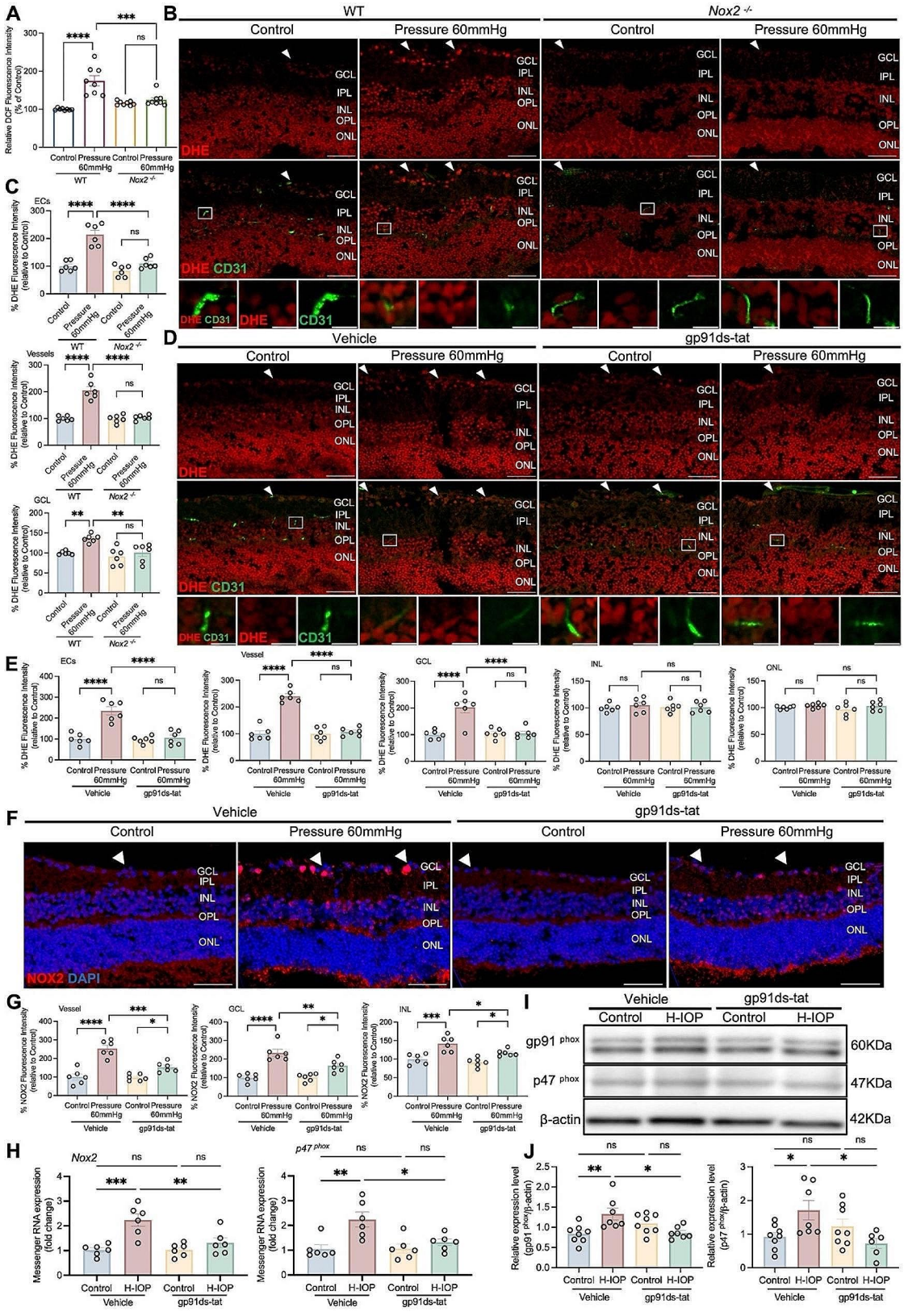

Fig. 5 (See legend on next page.)

(See figure on previous page.)

Fig. 5 gp91ds-tat treatment down-regulates the NOX2 overexpression induced by Pressure 60 mmHg-injured in the retinal vessels and the GCL. (**A**) Retinal ROS production was measured using DCF diacetate probe. Data are presented as the percent fluorescence intensity of the groups versus the WT-Control. (**B**) Representative images of DHE and CD31 co-stained retinal cryosections from WT and Nox2$^{-/-}$retinas after Pressure 60 mmHg 24 h. Scale bar, 50 µm. The white arrows point to cross-sections of retinal blood vessels. Lower panels in (**B**) show the enlarged views of the boxed regions (Scale bars equal 10 µm). (**C**) Analysis of DHE staining intensity in ECs, vessels, and GCL. Data are presented as the percent fluorescence intensity of the groups versus the control. (**D**) Representative images of DHE and CD31 co-stained retinal cryosections from Pressure 60 mmHg 24 h retinas with 300µM gp91ds-tat treatment. Scale bar, 50 µm. The white arrows point to cross-sections of retinal blood vessels. Lower panels in (**D**) show the enlarged views of the boxed regions (Scale bars equal 10 µm). (**E**) Analysis of DHE staining intensity in ECs, vessels, GCL, INL and ONL. Data are presented as the percent fluorescence intensity of the groups versus the control. (**F**) Representative images of retinal cross sections immunostained with NOX2 after Pressure 60 mmHg with 300µM gp91ds-tat treatment. The white arrows point to cross-sections of retinal blood vessels. Scale bar, 50 µm. (**G**) Analysis of NOX2 fluorescence intensity in the retinal vessels and GCL. Data are presented as the percent fluorescence intensity of the groups versus control-Vehicle. (**H**) Messenger RNA expression of Nox2 and p47^{phox}in retinas after H-IOP and with 500µM gp91ds-tat treatment. Data are presented as the fold-change versus control-vehicle. (**I**) After H-IOP and with 500µM gp91ds-tat treatment, retinal extracts were assayed for Western blot analysis of gp91^{phox} and p47^{phox}. Representative Western blots are presented. (**J**) The results obtained from Western blot are expressed as the ratio to β-actin from 6–9 independent experiments. Data are shown as mean ± SEM ($n = 6$ in each group, one-way ANOVA with Tukey's multiple comparisons test, *$p < 0.05$, **$p < 0.01$,***$p < 0.001$, ****$p < 0.0001$)

that ET-1 strongly promoted microglia activation after 24 h, while 20 min was not sufficient to activate microglia (Fig. 8G). Previous studies demonstrated the activation of intracellular pathways by ET-1, including PKC/ERK and p38MAPK [52]. To elucidate the molecular mechanism of ET-1 activation in microglia, we verified whether ET-1 could activate MAPK-dependent signaling pathways, including JNK, ERK1/2, and p38MAPK, in an experimental model. Interestingly, time-course analyses of microglial cultures confirmed that ET-1-induced phosphorylation of pERK1/2 isoforms appeared to drastically increase as early as 20 min after stimulation, while its expression level returned to physiological levels 24 h later (Fig. 8H). In contrast, the same stimulation pattern did not significantly affect the phosphorylation status of pJNK and p38 MAPK isoforms. Further, we treated the primary microglia with MEK1/2 (20µM) (a selective cell permeability inhibitor of the MEK/ERK pathway that blocks upstream kinase activation of MEK1 and MEK2) for 20 min and 24 h. The outcomes reveal that ET-1-induced pERK1/2 phosphorylation was remarkably blocked by MEK1/2 intervention at 20 min, whereas the phosphorylation levels of pJNK and p38 MAPK isoforms were not affected (Fig. 8H). Aiming to verify whether microglia activation is mediated by ERK1/2-dependent signaling, we visualized the co-localization of IB4 and ERK1/2 in microglia. As shown in Fig. 8G, relative to the untreated control group, microglial cell bodies exhibited a minor enlargement 20 min post-ET-1 application, accompanied by a marked increase in ERK1/2 expression, which showed co-localization with IB4. Following 24 h of ET-1 exposure, microglia assumed a characteristic activation phenotype, with ERK1/2 expression levels reverting to baseline. Moreover, we assayed markers of M1 (pro-inflammatory phenotype) to characterize ET-1-induced phenotypic shifts in the response of microglia. Figure 8I shows that ET-1 stimulation significantly increased the protein expression of IL-6, IL-1β, and TNF-α after 24 h of stimulation. Interestingly, with MEK1/2 intervention, the high expression of IL-6 and IL-1ß was significantly suppressed, while TNF-α was the only unaffected cytokine. These data suggest that ET-1 regulates the transition of microglia activation to an M1 pro-inflammatory phenotype through the ERK1/2 pathway.

Discussion

In this study, we determined that NOX2 is the critical key to unlocking the "Pandora's box" of oxidative stress under pathological H-IOP. We found that NOX2-mediated O_2^- overproduction was mainly located in the vasculature and endothelium, which induced reactive glial cell proliferation that mediated neuroinflammation and iBRB injury. Mechanistically, NOX2/ROS induces endothelial-derived ET-1 overexpression, which activates the ERK1/2 signaling pathway to mediate the shift of microglia activation to a pro-inflammatory M1 phenotype that triggers the release of inflammatory mediators. However, NOX2-specific deletion or gp91ds-tat pharmacological inhibition of NOX2 activity effectively impairs ET-1 overexpression, which inhibits ERK1/2 transduction of microglia-mediated neuroinflammation, thereby rescuing glaucomatous RGC loss and ON axonal injury by attenuating iBRB injury and neurovascular unit (NVU) dysfunction (Fig. 9).

Recent evidence suggests that ON damage can continue despite effectively lowering IOP [53–55]. The retina is the most metabolically active tissue in the body [56]. Intraocular oxidative stress leads to direct RGC damage in glaucoma patients [57]. Post-optic nerve crush injury exhibited RGC death and increased mRNA expression of NOX1, NOX2, and NOX4 in the retina [58]. In the mouse retinal ischemia/reperfusion model, NOX2 and p22 ^{phox} gene expression were regulated [22]. NOX2 constitutes a crucial hub associated with oxidative stress in the retina after pathologically H-IOP. Previously, a study verified that NOX2 deficiency prevents apoptosis of RGC [22]. Although it is well-known that NOX2 is distributed throughout the retina [22], interestingly, NOX2 overexpression as a result of increased IOP predominantly takes place in the vasculature and GCL of the retina [19].

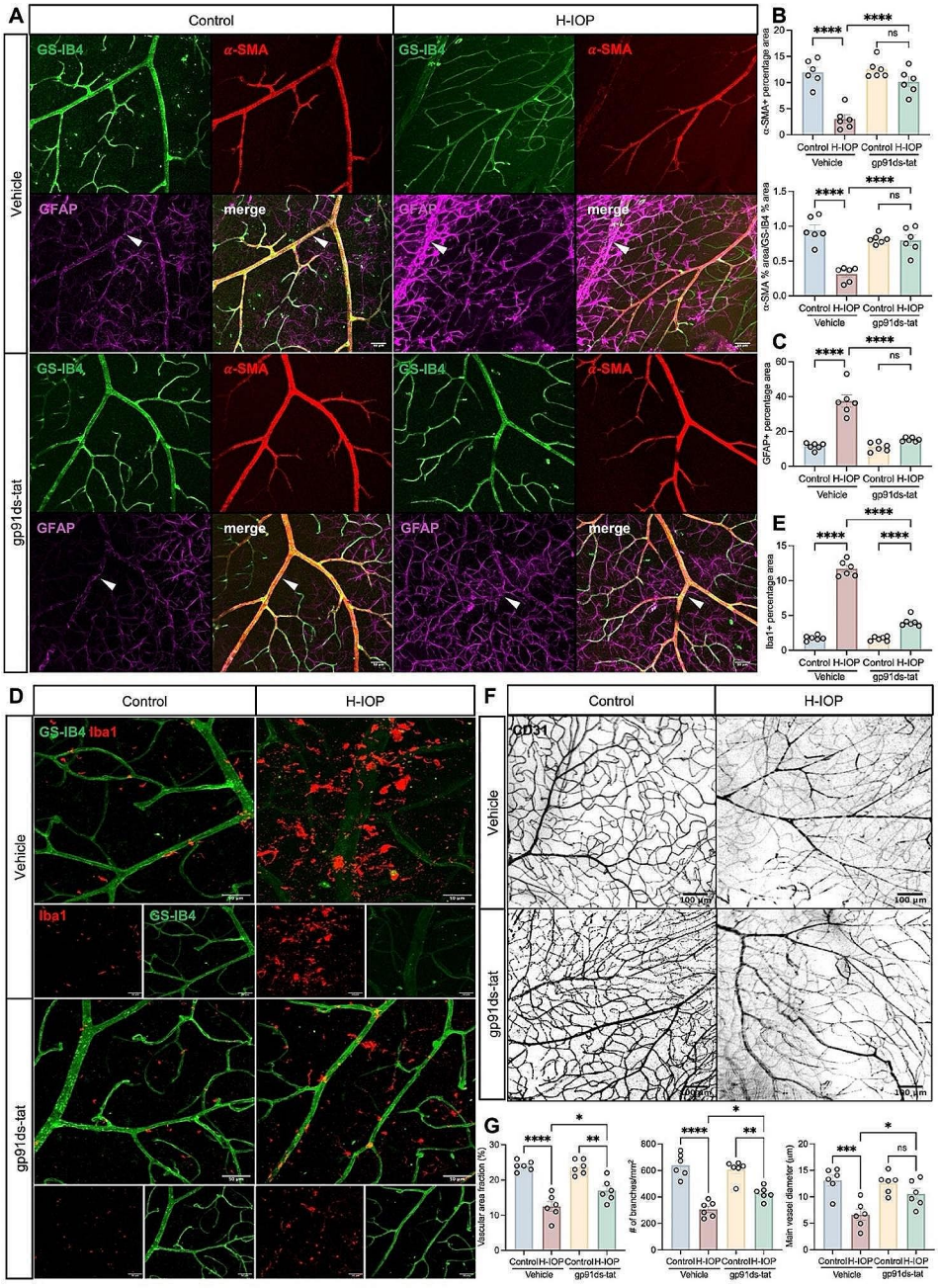

Fig. 6 NOX2/ROS-activated glial cells involved in H-IOP-mediated blood-retinal barrier damage and inflammation. (**A**) Representative images of the iBRB stained by GS-IB4, α-SMA, and GFAP. Scale bar, 50 μm. (**B**) Analysis of the α-SMA positive % area and the α-SMA positive % area/GS-IB4 positive % area in the different groups ($n=6$ in each group). (**C**) GFAP positive percentage area in the different groups ($n=6$ in each group). (**D**) Representative immunostaining of Iba1 and GS-IB4 images of retinas after H-IOP treated by gp91ds-tat. Scale bar, 50 μm. (**E**) Analysis of Iba1 positive percentage area in the different groups ($n=6$ in each group). (**F**) Representative immunostaining of CD31 images of retinas after H-IOP treated by gp91ds-tat. Scale bar, 100 μm. (**G**) Analysis of the vascular area fraction, the number of branches/mm^2, and the main vessel diameter (μm) in the different groups ($n=6$ in each group). Data are shown as mean ± SEM, one-way ANOVA with Tukey's multiple comparisons test, $^{*}p<0.05$,$^{**}p<0.01$,$^{***}p<0.001$, $^{****}p<0.0001$

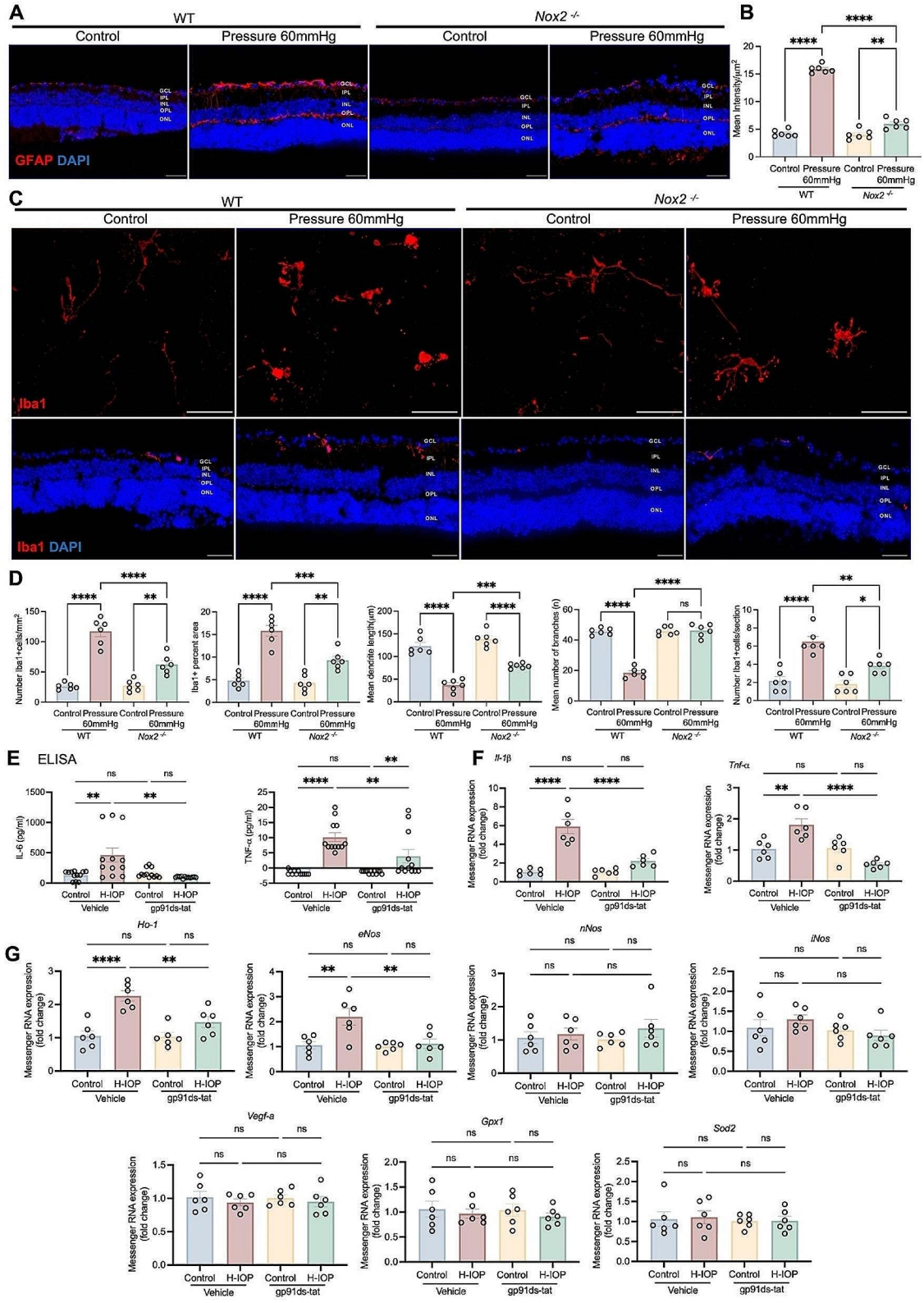

Fig. 7 (See legend on next page.)

(See figure on previous page.)

Fig. 7 NOX2 deletion or pharmacological inhibition dampens pathologically high intraocular pressure injury-mediated reactive glial cell proliferation and neuroinflammation and identifies inflammatory and immune-related protein pathways and functional enrichment in experimental glaucoma. (**A**) Representative images of GFAP stained retinal cryosections from WT and Nox2$^{-/-}$ mice after Pressure 60 mmHg 24 h. Scale bar, 50 µm. (**B**) Analysis of GFAP fluorescence mean intensity/µm^2 ($n=6$ in each group). (**C**) Representative images of Iba1 stained retinal flat-mounts and retinal cryosections from WT and Nox2$^{-/-}$ mice after Pressure 60 mmHg 24 h. Scale bar, 50 µm. (**D**) Analysis of the number of Iba1 + cells/mm^2, Iba1 + percent area, the mean dendrite length (µm), the mean number of branches (n), and the number of Iba1 positive cells per section ($n=6$ in each group). (**E**) ELISA assay was performed to determine the retinal protein of TNF-α and IL-6 with gp91ds-tat treatment ($n=12$ in each group). (**F**) Messenger RNA expression of genes coding for proinflammatory cytokines (Tnf-α and Il-1β) in different groups. Data are presented as the fold-change versus Veh-control ($n=6$ in each group). (**G**) Messenger RNA expression of hypoxia genes (Vegf-a), antioxidant genes (Ho-1, Gpx1, Sod2), and nitric oxide synthases (eNos, iNos, and nNos) in different groups. Data are presented as the fold-change in retinas after H-IOP and with gp91ds-tat treatment versus control-vehicle ($n=6$ in each group). Data are shown as mean ± SEM (one-way ANOVA with Tukey's multiple comparisons test, *$p<0.05$, **$p<0.01$,***$p<0.001$, ****$p<0.0001$)

The vascular endothelium is responsible for regulating the passage of macromolecules and circulating cells from the blood to the tissues, which is a major target of oxidative stress [59]. In retinas with hyper-ophthalmia, mRNA levels of NOX2 are up-regulated, and the subsequent excessive ROS production contributes to reduced vascular endothelium-dependent diastole [19]. These findings address that NOX2 deficiency and gp91ds-tat confer neuroprotection by directly mitigating retinal oxidative stress, especially in ECs, vascular, and GCL, whereas it fails to influence IOP. Treatment with gp91ds-tat effectively reduces NOX2 mRNA expression, indicating decreased gene transcription [60]. Nevertheless, as shown by immunofluorescence, protein levels may not align with mRNA due to various post-transcriptional and post-translational factors. Despite NOX2 inhibitors reducing superoxide production [61, 62], NOX2's complex regulation and other ROS-generating enzymes may result in ongoing or compensatory NOX2 activity, as detected by immunofluorescence. This implies that while NOX2 protein production might drop, active proteins could persist due to stability or post-transcriptional modifications, potentially explaining the increased immunofluorescence observed in Pressure 60 mmHg retinas treated by gp91ds-tat.

NOX2 promotes the development of inflammation, endothelial dysfunction, and ECs senescence in various vessels, including small retinal arteries [63–67]. Beyond ROS homeostasis, a complex cross-talk exists between individual endothelial-derived factors aimed at maintaining proper endothelial function. iBRB consists of retinal ECs, which are covered by astrocytes, pericytes, and end-footed Müller cells and are essential for maintaining the microenvironment of the inner retinal layers. In a rat model of non-arteritic anterior ischemic optic neuropathy with laser injury to the ON, NOX2 induction was again associated with microglia activation in the anterior ON [68]. In a unilateral H-IOP model evoked by cauterization, activation of astrocytes and microglia in the retina is accompanied by induction of NOX2 mRNA [69]. ROS production by NADPH oxidase can activate microglia to impair blood brain barrier (BBB) function [70]. BBB components are preserved and blood-brain barrier disruption is decreased when superoxide produced by NADPH oxidase is blocked with oleuropein [71]. Besides, the loss of pericytes, as well as the decreased pericyte-to-EC ratio, resulted in a localized increase in permeability, and the decreased pericyte coverage implied the central nervous system (CNS) microvascular dysfunction [72]. These data demonstrate that pathologically H-IOP stimulates the NOX2-dependent reactive proliferation of retinal glial cells and iBRB functional impairment. Dysregulation of this cross-talk leads to alterations in normal physiological processes in ECs, including vascular remodeling and impairment of endothelium-dependent vasorelaxation. In neurodegenerative diseases, microglia contract their protrusions and migrate toward the site of injury, where they release pro-inflammatory cytokines such as IL-1β, TNF-α, and IL-6 [73–75]. TNF-α could transmit ROS from neuronal cells to vascular cells [19] and also elicit NOX2-dependent ROS production in microglia [76] and is detected in the atrial fluid of glaucoma patients with TNF-α [77]. In our study, increased NADPH oxidase activity accompanied by upregulation of inflammatory cytokines (TNF-α, IL-6, and IL-1β) provides further support for the role of NADPH oxidase in vascular inflammation, consistent with previous studies [78]. Inhibition of NADPH oxidase activity alleviates H_2O_2-induced endothelial dysfunction via the NO/HO-1 pathway [79]. A previous study demonstrated that endothelial-specific overexpression of NOX2 was accompanied by increased levels of eNOS and SOD2 [80]. SOD2 upregulation is crucial for retinal oxidative balance, with its deficiency resulting in heightened oxidative stress markers and increased oxidative damage [81–83]. The absence of SOD2 upregulation under H-IOP conditions suggests a compromised retinal oxidative equilibrium and potential retinal damage risk.

Blockade of NOS greatly enhanced ET-1-induced endothelial contraction, and both endothelial removal of oleuropein and NADPH oxidase inhibition attenuated the enhanced contraction [84]. ET-1 concentrations were observed to be increased in separate animal models of glaucoma [85–87], and this peptide plays a role in hypertension-related vascular injury [88, 89]. NOX2 activity promotes ET-1 production in ECs [49], and

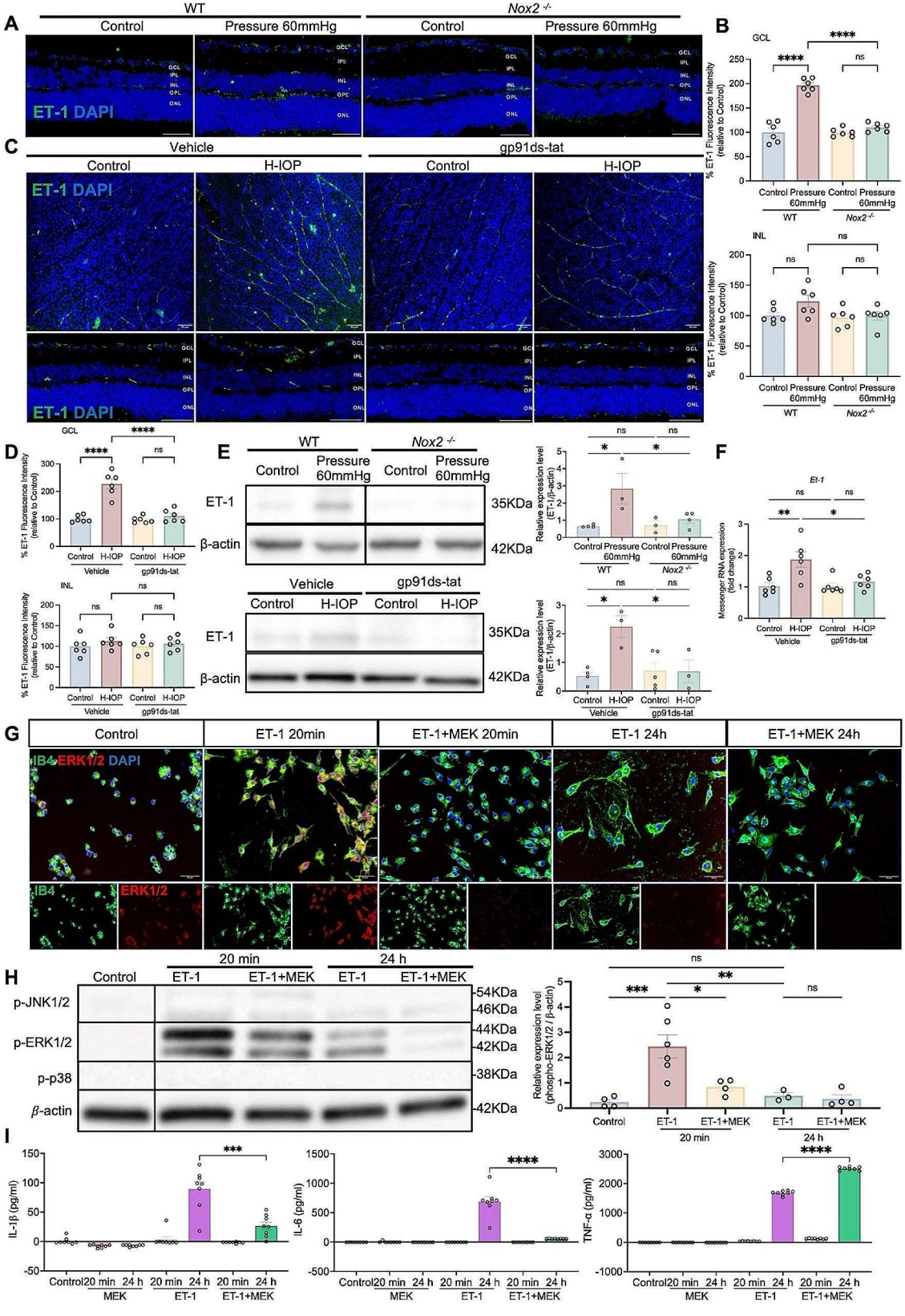

Fig. 8 (See legend on next page.)

(See figure on previous page.)

Fig. 8 NOX2/ET-1 axis mediates microglia activation switching to M1 pro-inflammatory phenotype via ERK1/2 pathway contributing to iBRB inflammatory injury. (**A**) Representative images of ET-1 stained retinal cryosections from WT and Nox2$^{-/-}$ after Pressure 60 mmHg 24 h. Scale bar, 50 μm. (**B**) Analysis of ET-1 fluorescence intensity in the GCL and INL. Data are presented as the percent fluorescence intensity of the groups versus control-WT ($n=6$ in each group). (**C**) Representative images of ET-1 stained retinal flat-mount and cryosections after H-IOP with 500μM gp91ds-tat treatment. Scale bar, 50 μm. (**D**) Analysis of ET-1 fluorescence intensity in the GCL and INL. Data are presented as the percent fluorescence intensity of the groups versus Veh-control ($n=6$ in each group). (**E**) Retinal extracts from WT and Nox2$^{-/-}$ mice under Pressure 60 mmHg and H-IOP retinas with 500μM gp91ds-tat treatment were assayed for Western blot analysis of ET-1. Representative Western blots are presented. The results obtained from Western blot are expressed as the ratio to β-actin from 4–6 independent experiments. (**F**) Messenger RNA expression of Et-1 in retinas after H-IOP and with 500μM gp91ds-tat treatment. $n=6$ in each group. (**G**) Representative images of IB4 and ERK1/2 stained microglia cultured by 100nM ET-1 and 20μM MEK 20–24 h. Scale bar, 50 μm. (**H**) Microglia lysis were assayed for Western blot analysis of p-JNK, p-ERK1/2 and p-p38 MAPK. Representative Western blots are presented. The results obtained from Western blot are expressed as the ratio to β-actin from 3 independent experiments. Data are shown as mean ± SEM, one-way ANOVA with Tukey's multiple comparisons, *$p<0.05$, **$p<0.01$,***$p<0.001$, ****$p<0.0001$). (**I**) ELISA assay was performed to determine the cell protein of IL-6, IL-1β, and TNF-α ($n=8$ in each group). Data are shown as mean ± SEM (unpaired t-test, ***$p<0.001$, ****$p<0.0001$)

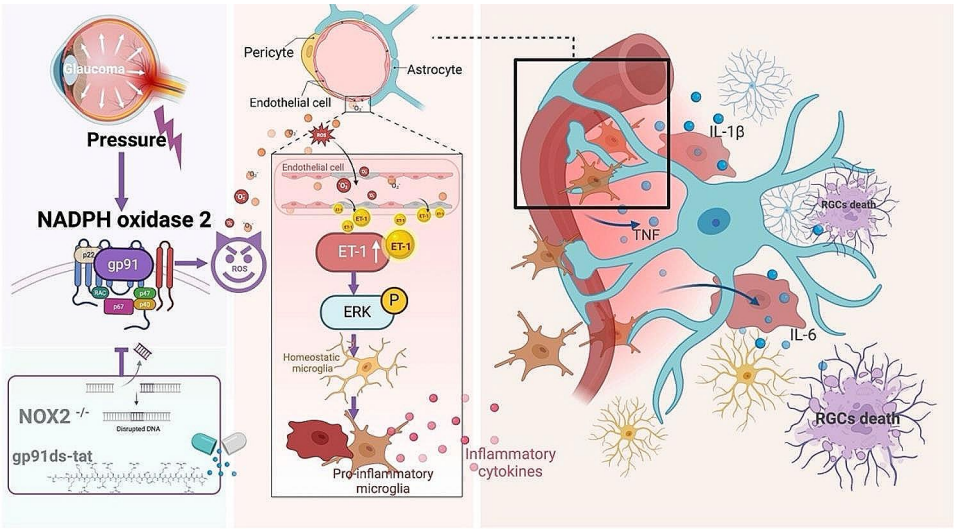

Fig. 9 NADPH oxidase 2 deletion attenuates glaucomatous neurodegeneration induced by pathologically high intraocular pressure

NOX-mediated superoxide production contributes to ET-1-dependent regulation of vascular homeostasis in physiology and disease [90]. In cardiomyocytes, mechanical stretch-released Ang II [91] induces NOX2 activation of the auto-AT1 receptor and induces ET-1 release [92]. We clarified for the first time in retinal vessels, consistent with previous studies, that NOX2 deletion or inhibition of activity is followed by a corresponding alleviation of the H-IOP-induced elevated protein and transcript levels of ET-1, which mediates vascular oxidative stress, inflammation, and remodeling [93, 94]. As the perivascular area is covered by microglia and astrocytes [51], glial cells directly contact and encapsulate the vasculature, which directly affects the structure and function of the EC, rather than passive coexistence [95]. The direct role of ET-1 in reactive gliosis was demonstrated by in vivo infusion of exogenous ET or ET-R agonists, which leads to microglia and astrocyte proliferation [50, 94]. Furthermore, the effect of ET-1 on glial cell proliferation depends on c-Jun signaling through ERK- and JNK-dependent pathways [96]. The primary microglia were morphologically reactive and hypertrophied after the addition of ET-1 dependent on activation of the ERK1/2 pathway. Of particular note, ET-1 induced the activation of microglia toward the M1 pro-inflammatory phenotype, which is consistent with the previous findings [50]. Inhibition of the ERK1/2 pathway with PD98059, a MEK1/2-specific inhibitor, was sufficient to block IL-1β and IL-6 secretion by Listeria monocytogenes-infected macrophages completely and to reduce TNF-α secretion modestly [42]. Although MEK1/2 suppression could completely block IL-1β and IL-6 secreted by ET-1-induced pro-inflammatory phenotype of microglia M1, without affecting TNF-α secretion. The neuroglia that physically encapsulate the blood vessels are considered secondary barriers [97]. Through this close physical interaction between ECs and neuroglia, nutrients required for CNS function are transported from blood vessels to neurons primarily through neuroglia [98], while waste products are passed through neuroglia to microglia or back to the bloodstream [99]. Pro-inflammatory microglia cause damage by releasing inflammatory cytokines, amplifying inflammatory processes, and secondary neuronal death [100, 101]. The NVU glial cells are composed of neurons, vascular

smooth muscle cells (VSMCs), pericytes, microglia, and vasculature [95]. NVU dysfunction is characterized by dysfunctional neurovascular coupling, neuronal death, neuroglial proliferation, microglia activation, mural cell migration, and BBB disruption [102, 103]. Typically, neuroglial dysfunction precedes neuronal and vascular lesions, which work closely with other NVU cells to sustain CNS function and maintenance [95].

Conclusion

In summary, this study identifies NOX2 as a key driver of oxidative stress in the NVU under H-IOP, leading to glial proliferation, neuroinflammation, and iBRB damage. NOX2's interaction with the ROS-ET-1-ERK1/2 axis fosters an inflammatory microglial response, exacerbating RGC and ON axonal injury. Counteracting NOX2 activity via genetic deletion or gp91ds-tat inhibitor not only dampens this inflammatory response but also preserves RGCs and ON integrity, highlighting a promising avenue for glaucoma therapy.

Abbreviations

BBB	Blood brain barrier
BP	Biological processes
Brn3a	Brain-specific homeobox/POU domain protein 3A
CC	Cellular components
CNS	Central nervous system
CT	Comparative threshold
DCF	2,7-dichlorofluorescein derivative 6-carboxy-2,7-dichlorodihydrofluorescein diacetate, di(acetoxymethyl ester)
DEPs	Differentially expressed proteins
DHE	Dye dihydroethidium
ECs	Endothelial cells
ELISA	Enzyme-linked immunosorbent assay
ET-1	Endothelin-1
FDR	False discovery rate
GCL	Ganglion cell layer
GFAP	Glial fibrillary acidic protein
GO	Gene Ontology
Gpx1	Glutathione peroxidases 1
H-IOP	High intra-ocular pressure
Ho-1	Heme oxygenase 1
iBRB	Internal blood-retinal barrier
IL-1β	Interleukin 1beta
IL-6	Interleukin 6
INL	Inner nuclear layer
IOP	Intraocular pressure
IPL	Inner plexiform layer
KEGG	Kyoto Encyclopedia of Genes and Genomes
LFQ	Label-free quantitation
MCE	Mixed Cellulose Ester
MF	Molecular function
NADPH	Nicotinamide adenine dinucleotide phosphate
NOS	Nitric oxide synthase
NOX	NADPH oxidase
NVU	Neurovascular unit
O_2^-	Superoxide
OCT	Optimal cutting temperature
ON	Optic nerve
ONL	Outer nuclear layer
OPL	Outer plexiform layer
PBS	Phosphate-buffered saline
PCA	Principal component analysis
PFA	Paraformaldehyde
PPD	p-phenylenediamine
Pressure 60 mmHg	Elevated hydrostatic pressure
RGC	Retinal ganglion cell
ROS	Reactive oxygen specie
SDS	Sodium dodecyl sulfate
Sod2	Superoxide dismutase type 2
Tbp	TATA-binding protein
TNF-α	Tumor necrosis factor-alpha
Vegf-a	Vascular endothelial growth factor-A
VSMCs	Vascular smooth muscle cells
WT	Wildtype
α-SMA	alpha smooth muscle actin

Supplementary Information

The online version contains supplementary material available at https://doi.org/10.1186/s12974-024-03075-x.

Supplementary Material 1

Acknowledgements

We would like to thank Frau. Rodica-Aurelia Maniu, Dr. Stefan Wagner, and Dr. Haichao Ji for their technical assistance. We are grateful for the financial support scholarships from the China Scholarship Council. The position of M.H was funded by grants from the state of North-Rhine-Westphalia, Germany, (AZ: 323-8.04.10.02-141905), German Center for Infection Research, DZIF (TTU 08.927 and TTU 08.928) and the Deutsche Forschungsgemeinschaft (DFG), SFB 670 procured by Prof. Dr. Martin Krönke. Cartoons in Fig. 1A, C and D, and Fig. 4C, and Fig. 9 were created with BioRender.com.

Author contributions

Conceptualization, X.S., P.L. and V.P.; methodology, X.S., P.L. and V.P.; formal analysis, X.S. and P. L.; investigation, X.S., P.L., M.H., M.W., S.W., Y.F., T.v.B., N.X. and H.L. (Huige Li); resources, M.H., T.v.B., N.X., H.L. (Huige Li) and V.P.; writing—original draft preparation, X.S., P.L. and V.P.; writing—review and editing, X.S., P.L., M.H., H.L. (Hanhan Liu), N.X., H.L. (Huige Li) and V.P.; visualization, X.S. and P.L.; supervision, V.P.; project administration, V.P.; funding acquisition, V.P. All authors have read and agreed to the published version of the manuscript.

Funding

This work was supported by the Deutsche Forschungsgemeinschaft (DFG) with grant PR1569/1–1 and PR 1569/1–3.
Open Access funding enabled and organized by Projekt DEAL.

Data availability

No datasets were generated or analysed during the current study.

Declarations

Ethics approval and consent to participate

Not applicable.

Consent for publication

Not applicable.

Competing interests

The authors declare no competing interests.

Author details

[1]Department of Ophthalmology, Faculty of Medicine, University Hospital of Cologne, University of Cologne, 50937 Cologne, Germany
[2]Institute for Medical Microbiology, Immunology and Hygiene, Faculty of Medicine, University Hospital of Cologne, University of Cologne, Goldenfelsstr. 19-21, 50935 Cologne, Germany
[3]Cologne Cluster of Excellence on Cellular Stress Responses in Aging-Associated Diseases (CECAD), Cologne, Germany
[4]Department of Ophthalmology, Beijing Chaoyang Hospital, Capital Medical University, Beijing 100020, P. R. China
[5]Institut I für Anatomie, Universitätsklinikum Köln (AöR), Cologne, Germany

[6]Department of Pharmacology, University Medical Center, Johannes Gutenberg University Mainz, Langenbeckstr. 1, 55131 Mainz, Germany
[7]German Center for Cardiovascular Research (DZHK), Partner Site Rhine-Main, 55131 Mainz, Germany

Received: 2 January 2024 / Accepted: 26 March 2024
Published online: 22 April 2024

References

1. Tham Y-C, et al. Global prevalence of Glaucoma and projections of Glaucoma Burden through 2040: a systematic review and Meta-analysis. Ophthalmology. 2014;121(11):2081–90.
2. Weinreb RN, Khaw PT. Primary open-angle glaucoma. Lancet. 2004;363(9422):1711–20.
3. Shi X, et al. Oxidative stress, vascular endothelium, and the Pathology of Neurodegeneration in Retina. Antioxidants. 2022;11(3):543.
4. Faraci FM. Reactive oxygen species: influence on cerebral vascular tone J Appl Physiol (1985). 2006;100(2):739 – 43.
5. Himori N, et al. The association between systemic oxidative stress and ocular blood flow in patients with normal-tension glaucoma. Graefe's Archive Clin Experimental Ophthalmol. 2016;254(2):333–41.
6. Ju WK, et al. Elevated hydrostatic pressure triggers mitochondrial fission and decreases cellular ATP in differentiated RGC-5 cells. Invest Ophthalmol Vis Sci. 2007;48(5):2145–51.
7. Hernandez MR, et al. Differential gene expression in astrocytes from human normal and glaucomatous optic nerve head analyzed by cDNA microarray. Glia. 2002;38(1):45–64.
8. Agapova OA, Kaufman PL, Hernandez MR. Androgen receptor and NFkB expression in human normal and glaucomatous optic nerve head astrocytes in vitro and in experimental glaucoma. Exp Eye Res. 2006;82(6):1053–9.
9. Ruan Y, et al. Oxidative stress and vascular dysfunction in the retina: therapeutic strategies. Antioxidants (Basel); 2020;9:8.
10. Göllner M, et al. NOX2ko mice show largely increased expression of a mutated NOX2 mRNA encoding an inactive NOX2 protein. Antioxidants. 2020;9(11):1043.
11. Lambeth JD. NOX enzymes and the biology of reactive oxygen. Nat Rev Immunol. 2004;4(3):181–9.
12. Lassegue B, Clempus RE. Vascular NAD (P) H oxidases: specific features, expression, and regulation. Am J Physiology-Regulatory Integr Comp Physiol. 2003;285(2):R277–97.
13. Fan Gaskin JC, Shah MH, Chan EC. Oxidative stress and the role of NADPH oxidase in Glaucoma. Antioxidants. 2021;10(2):238.
14. Henry E, et al. Peripheral endothelial dysfunction in normal pressure Glaucoma. Investig Ophthalmol Vis Sci. 1999;40(8):1710–4.
15. Sugiyama T, et al. Association of endothelin-1 with normal tension glaucoma: clinical and fundamental studies. Surv Ophthalmol. 1995;39:S49–56.
16. Kaiser HJ, et al. Endothelin-1 plasma levels in normal-tension glaucoma: abnormal response to postural changes. Graefe's Archive Clin Experimental Ophthalmol. 1995;233(8):484–8.
17. Noske W, Hensen J, Wiederholt M. Endothelin-like immunoreactivity in aqueous humor of patients with primary open-angle glaucoma and cataract. Graefe's Archive Clin Experimental Ophthalmol. 1997;235(9):551–2.
18. Wilkinson-Berka JL, et al. Identification of a retinal aldosterone system and the protective effects of mineralocorticoid receptor antagonism on retinal vascular pathology. Circul Res. 2009;104(1):124–33.
19. Gericke A et al. Elevated intraocular pressure causes abnormal reactivity of mouse retinal arterioles Oxidative medicine and cellular longevity, 2019. 2019.
20. Bode K, et al. Unlocking the power of NOX2: a comprehensive review on its role in immune regulation. Redox Biol. 2023;64:102795.
21. Urner S, et al. NADPH oxidase inhibition: preclinical and clinical studies in diabetic complications. Antioxid Redox Signal. 2020;33(6):415–34.
22. Yokota H, et al. Neuroprotection from retinal ischemia/reperfusion injury by NOX2 NADPH oxidase deletion. Investig Ophthalmol Vis Sci. 2011;52(11):8123–31.
23. Ruiz-Ederra J, Verkman AS. Mouse model of sustained elevation in intraocular pressure produced by episcleral vein occlusion. Exp Eye Res. 2006;82(5):879–84.
24. Chen H, et al. Progressive Degeneration of Retinal and Superior Collicular Functions in mice with sustained ocular hypertension. Investig Ophthalmol Vis Sci. 2015;56(3):1971–84.
25. Thomson BR, et al. Angiopoietin-1 knockout mice as a genetic model of Open-Angle Glaucoma. Translational Vision Science & Technology; 2020;9(4):16–16.
26. Cai H, Griendling KK, Harrison DG. The vascular NAD (P) H oxidases as therapeutic targets in cardiovascular diseases. Trends Pharmacol Sci. 2003;24(9):471–8.
27. Rey F, et al. Novel competitive inhibitor of NAD (P) H oxidase assembly attenuates vascular O2 – and systolic blood pressure in mice. Circul Res. 2001;89(5):408–14.
28. Fawell S, et al. Tat-mediated delivery of heterologous proteins into cells. Proc Natl Acad Sci. 1994;91(2):p664–668.
29. Lian H, Roy E, Zheng H. Protocol for primary Microglial Culture Preparation. Bio Protoc, 2016. 6(21).
30. Miller WP, et al. Deletion of the Akt/mTORC1 Repressor REDD1 prevents visual dysfunction in a Rodent Model of type 1 diabetes. Diabetes. 2018;67(1):110–9.
31. Zadeh JK et al. Apolipoprotein e deficiency causes endothelial dysfunction in the mouse retina Oxidative medicine and cellular longevity, 2019. 2019.
32. Wang M, et al. Intraocular pressure-Induced endothelial dysfunction of retinal blood vessels is persistent, but does not trigger retinal ganglion cell loss. Antioxidants. 2022;11(10):1864.
33. Oelze M, et al. NADPH oxidase accounts for enhanced superoxide production and impaired endothelium-dependent smooth muscle relaxation in BKβ1−/− mice. Arterioscler Thromb Vasc Biol. 2006;26(8):p1753–1759.
34. Stein JD, Khawaja AP, Weizer JS. Glaucoma in Adults-Screening, diagnosis, and management: a review. JAMA. 2021;325(2):164–74.
35. Tonner H, et al. A monoclonal Anti-HMGB1 antibody attenuates neurodegeneration in an experimental animal model of Glaucoma. Int J Mol Sci. 2022;23(8):4107.
36. Chidlow G, et al. Spatiotemporal characterization of optic nerve degeneration after chronic hypoperfusion in the rat. Investig Ophthalmol Vis Sci. 2010;51(3):1483–97.
37. Wisniewski J, et al. Universal sample preparation method for proteome analysis. Nat Meth. 2009;6(5):359–62.
38. Karpievitch YV, Dabney AR, Smith RD. Normalization and missing value imputation for label-free LC-MS analysis. BMC Bioinformatics. 2012;13(16):S5.
39. Laspas P, et al. The M1 muscarinic acetylcholine receptor subtype is important for retinal neuron survival in aging mice. Sci Rep. 2019;9(1):1–12.
40. Ruan Y, et al. Oxidative stress and vascular dysfunction in the retina: therapeutic strategies. Antioxidants. 2020;9(8):761.
41. Chan EC, et al. Regulation of cell proliferation by NADPH oxidase-mediated signaling: potential roles in tissue repair, regenerative medicine and tissue engineering. Pharmacol Ther. 2009;122(2):97–108.
42. Herb M, et al. Mitochondrial reactive oxygen species enable proinflammatory signaling through disulfide linkage of NEMO. Sci Signal. 2019;12(568):eaar5926.
43. Fan Gaskin JC, Shah MH, Chan EC. Oxidative stress and the role of NADPH oxidase in Glaucoma. Antioxid (Basel), 2021. 10(2).
44. O'Leary F, Campbell M. The blood-retina barrier in health and disease. Febs j. 2023;290(4):878–91.
45. Bringmann A, et al. Müller cells in the healthy and diseased retina. Prog Retin Eye Res. 2006;25(4):397–424.
46. Ravelli KG, et al. Nox2-dependent neuroinflammation in an EAE Model of multiple sclerosis. Transl Neurosci. 2019;10:1–9.
47. Surace MJ, Block ML. Targeting microglia-mediated neurotoxicity: the potential of NOX2 inhibitors. Cell Mol Life Sci. 2012;69(14):2409–27.
48. Jha MK, Jeon S, Suk K. Glia as a link between Neuroinflammation and Neuropathic Pain. Immune Netw. 2012;12(2):41–7.
49. Kamhieh-Milz J, et al. Ang II promotes ET-1 production by regulating NOX2 activity through transcription factor Oct-1. Arterioscler Thromb Vasc Biol. 2023;43(8):1429–40.
50. Abdul Y, et al. Endothelin-1 (ET-1) promotes a proinflammatory microglia phenotype in diabetic conditions. Can J Physiol Pharmacol. 2020;98(9):596–603.
51. Zlokovic BV. The blood-brain barrier in health and chronic neurodegenerative disorders. Neuron. 2008;57(2):178–201.
52. Schinelli S, et al. Stimulation of endothelin B receptors in astrocytes induces cAMP response element-binding protein phosphorylation and c-fos

expression via multiple mitogen-activated protein kinase signaling pathways. J Neurosci. 2001;21(22):8842–53.
53. Group CN-TGS. Comparison of glaucomatous progression between untreated patients with normal-tension glaucoma and patients with therapeutically reduced intraocular pressures. Am J Ophthalmol. 1998;126(4):487–97.
54. Lichter PR, et al. Interim clinical outcomes in the collaborative initial Glaucoma treatment study comparing initial treatment randomized to medications or surgery. Ophthalmology. 2001;108(11):1943–53.
55. Heijl A, et al. Reduction of intraocular pressure and glaucoma progression: results from the early manifest Glaucoma trial. Arch Ophthalmol. 2002;120(10):1268–79.
56. Tokarz P, Kaarniranta K, Blasiak J. Role of antioxidant enzymes and small molecular weight antioxidants in the pathogenesis of age-related macular degeneration (AMD). Biogerontology. 2013;14:461–82.
57. Tezel G. Oxidative stress in glaucomatous neurodegeneration: mechanisms and consequences. Prog Retin Eye Res. 2006;25(5):490–513.
58. Yamamoto K, et al. The novel rho kinase (ROCK) inhibitor K-115: a new candidate drug for neuroprotective treatment in glaucoma. Investig Ophthalmol Vis Sci. 2014;55(11):7126–36.
59. Hadi HA, Carr CS, Al J, Suwaidi. Endothelial dysfunction: cardiovascular risk factors, therapy, and outcome. Vasc Health Risk Manag. 2005;1(3):183–98.
60. Singh PK, et al. Specific inhibition of NADPH oxidase 2 modifies chronic epilepsy. Redox Biol. 2022;58:102549.
61. Maqbool A, et al. Divergent effects of genetic and pharmacological inhibition of Nox2 NADPH oxidase on insulin resistance-related vascular damage. Am J Physiol Cell Physiol. 2020;319(1):C64–74.
62. Sukumar P, et al. Nox2 NADPH oxidase has a critical role in insulin resistance-related endothelial cell dysfunction. Diabetes. 2013;62(6):2130–4.
63. Zadeh JK, et al. Responses of retinal arterioles and ciliary arteries in pigs with acute respiratory distress syndrome (ARDS). Exp Eye Res. 2019;184:152–61.
64. Rojas M, et al. NOX2-induced activation of arginase and diabetes-induced retinal endothelial cell senescence. Antioxidants. 2017;6(2):43.
65. Fan LM, et al. Aging-associated metabolic disorder induces Nox2 activation and oxidative damage of endothelial function. Free Radic Biol Med. 2017;108:940–51.
66. Cahill-Smith S, Li JM. Oxidative stress, redox signalling and endothelial dysfunction in ageing-related neurodegenerative diseases: a role of NADPH oxidase 2. Br J Clin Pharmacol. 2014;78(3):441–53.
67. Konior A, et al. NADPH oxidases in vascular pathology. Antioxid Redox Signal. 2014;20(17):2794–814.
68. Mehrabian Z, et al. Oligodendrocyte death, neuroinflammation, and the effects of minocycline in a rodent model of nonarteritic anterior ischemic optic neuropathy (rNAION). Mol Vis. 2017;23:963.
69. Sapienza A, et al. Bilateral neuroinflammatory processes in visual pathways induced by unilateral ocular hypertension in the rat. J Neuroinflamm. 2016;13(1):1–16.
70. Sumi N, et al. Lipopolysaccharide-activated microglia induce dysfunction of the blood–brain barrier in rat microvascular endothelial cells co-cultured with microglia. Cell Mol Neurobiol. 2010;30:247–53.
71. Yenari MA, et al. Microglia potentiate damage to blood–brain barrier constituents: improvement by minocycline in vivo and in vitro. Stroke. 2006;37(4):1087–93.
72. Bonkowski D, et al. The CNS microvascular pericyte: pericyte-astrocyte crosstalk in the regulation of tissue survival. Fluids Barriers CNS. 2011;8(1):8.
73. Kreutzberg GW. Microglia: a sensor for pathological events in the CNS. Trends Neurosci. 1996;19(8):312–8.
74. Clayton DF, George JM. Synucleins in synaptic plasticity and neurodegenerative disorders. J Neurosci Res. 1999;58(1):120–9.
75. Becher B, Prat A, Antel JP. Brain-immune connection: immuno-regulatory properties of CNS-resident cells. Glia. 2000;29(4):293–304.
76. Geng L, et al. Nox2 dependent redox-regulation of microglial response to amyloid-β stimulation and microgliosis in aging. Sci Rep. 2020;10(1):1582.
77. Soto I, Howell GR. The complex role of neuroinflammation in glaucoma. Cold Spring Harb Perspect Med, 2014. 4(8).
78. Zhang L, et al. Diabetes-induced oxidative stress and low-grade inflammation in porcine coronary arteries. Circulation. 2003;108(4):472–8.
79. Luo M, Tian R, Lu N. Nitric oxide protected against NADPH oxidase-derived superoxide generation in vascular endothelium: critical role for heme oxygenase-1. Int J Biol Macromol. 2019;126:549–54.
80. Bendall JK, et al. Endothelial Nox2 overexpression potentiates vascular oxidative stress and hemodynamic response to angiotensin II: studies in endothelial-targeted Nox2 transgenic mice. Circul Res. 2007;100(7):1016–25.
81. Sandbach JM, et al. Ocular pathology in mitochondrial superoxide dismutase (Sod2)-deficient mice. Invest Ophthalmol Vis Sci. 2001;42(10):2173–8.
82. Usui S, et al. Overexpression of SOD in retina: need for increase in H2O2-detoxifying enzyme in same cellular compartment. Free Radic Biol Med. 2011;51(7):1347–54.
83. Justilien V, et al. SOD2 knockdown mouse model of early AMD. Invest Ophthalmol Vis Sci. 2007;48(10):4407–20.
84. Sánchez A, et al. Endothelin-1 contributes to endothelial dysfunction and enhanced vasoconstriction through augmented superoxide production in penile arteries from insulin-resistant obese rats: role of ET(A) and ET(B) receptors. Br J Pharmacol. 2014;171(24):5682–95.
85. Källberg ME, et al. Endothelin 1 levels in the aqueous humor of dogs with glaucoma. J Glaucoma. 2002;11(2):105–9.
86. Thanos S, Naskar R. Correlation between retinal ganglion cell death and chronically developing inherited glaucoma in a new rat mutant. Exp Eye Res. 2004;79(1):119–29.
87. Prasanna G, et al. Effect of elevated intraocular pressure on endothelin-1 in a rat model of glaucoma. Pharmacol Res. 2005;51(1):41–50.
88. Maki S, et al. The endothelin receptor antagonist ameliorates the hypertensive phenotypes of transgenic hypertensive mice with renin-angiotensin genes and discloses roles of organ specific activation of endothelin system in transgenic mice. Life Sci. 2004;74(9):1105–18.
89. Rautureau Y, et al. Inducible human endothelin-1 overexpression in endothelium raises blood pressure via endothelin type A receptors. Hypertension. 2015;66(2):347–55.
90. Meyer MR, Barton M, Prossnitz ER. Functional heterogeneity of NADPH oxidase-mediated contractions to endothelin with vascular aging. Life Sci. 2014;118(2):226–31.
91. Sadoshima J-i, et al. Autocrine release of angiotensin II mediates stretch-induced hypertrophy of cardiac myocytes in vitro. Cell. 1993;75(5):977–84.
92. Ito H, et al. Endothelin-1 is an autocrine/paracrine factor in the mechanism of angiotensin II-induced hypertrophy in cultured rat cardiomyocytes. J Clin Investig. 1993;92(1):398–403.
93. Amiri F, et al. Endothelium-restricted overexpression of human endothelin-1 causes vascular remodeling and endothelial dysfunction. Circulation. 2004;110(15):2233–40.
94. Amiri F, et al. Vascular inflammation in absence of blood pressure elevation in transgenic murine model overexpressing endothelin-1 in endothelial cells. J Hypertens. 2008;26(6):1102–9.
95. Kugler EC, Greenwood J, MacDonald RB. The Neuro-glial-vascular unit: the role of Glia in neurovascular unit formation and dysfunction. Front Cell Dev Biology, 2021. 9.
96. Gadea A, Schinelli S, Gallo V. Endothelin-1 regulates astrocyte proliferation and reactive gliosis via a JNK/c-Jun signaling pathway. J Neurosci. 2008;28(10):2394–408.
97. Kutuzov N, Flyvbjerg H, Lauritzen M. Contributions of the glycocalyx, endothelium, and extravascular compartment to the blood–brain barrier. Proc Natl Acad Sci. 2018;115(40):E9429–38.
98. Hurley JB, Lindsay KJ, Du J. Glucose, lactate, and shuttling of metabolites in vertebrate retinas. J Neurosci Res. 2015;93(7):1079–92.
99. Marina N, et al. Brain metabolic sensing and metabolic signaling at the level of an astrocyte. Glia. 2018;66(6):1185–99.
100. Brown GC, Neher JJ. Microglial phagocytosis of live neurons. Nat Rev Neurosci. 2014;15(4):209–16.
101. Hu X, et al. Microglial and macrophage polarization—new prospects for brain repair. Nat Reviews Neurol. 2015;11(1):56–64.
102. Zlokovic BV. Neurovascular mechanisms of Alzheimer's neurodegeneration. Trends Neurosci. 2005;28(4):202–8.
103. Willis CL. Glia-induced reversible disruption of blood–brain barrier integrity and neuropathological response of the neurovascular unit. Toxicol Pathol. 2011;39(1):172–85.

Publisher's Note

6. DISCUSSION

Glaucoma, characterized by the progressive degeneration of RGCs, involves complex, interrelated pathologies, including oxidative stress, neuroinflammation, and the compromise of iBRB and neurovascular unit integrity. Emerging evidence underscores the pivotal role of NOX2-derived ROS in exacerbating these pathological processes. Our study tries to gain insights into NOX2's impacts on neuroinflammation, neuronal death, iBRB integrity, and neurovascular unit health, highlighting therapeutic potentials.

6.1. Neuronal damage and neuroinflammation is induced by NOX2-derived ROS.

Low levels of ROS generation are essential for maintaining physiological functions, including proliferation, host defense, signal transduction, and gene expression [123]. However, when the intracellular production of ROS exceeds the intrinsic antioxidant capacity, oxidative stress occurs, which can lead to damage to biomolecules in normal cells and tissues [123]. The rate of ROS generation increases under normal aging as well as acute or chronic pathophysiological conditions [124-126]. Several rodent models have been developed to elevate IOP, most of which have been shown to induce oxidative stress. For example, IOP elevation following the intravitreal injection of hyaluronic acid in rats results in a significant reduction in retinal antioxidants and an increase in retinal lipid peroxidation [127]. Similarly, IOP elevation following episcleral vein cauterization in rats leads to a significant increase in ROS and nitrite levels, accompanied by lipid peroxidation [128,129]. In another study where hypertonic saline was injected into the episcleral vein to elevate IOP, protein oxidation was found to be confined to the inner retinal layers containing RGCs [130]. Short-term IOP elevation in aged mice induces reversible dysfunction of the inner retina [131] and significantly increases oxidative stress [132] . In our study, following IOP elevation induced by episcleral vein cauterization in mice, we observed the accumulation of O_2- radicals in the retinal ganglion cell layer (GCL). Regardless of the mechanism or duration of the injury, elevated IOP appears capable of inducing oxidative stress in the retina. The typical pathogenesis of glaucoma involves oxidative stress, which subsequently leads to mitochondrial dysfunction and the production of excessive ROS. These ROS then activate a cascade of death signaling pathways within RGCs, leading to direct damage to RGCs in glaucoma patients [133].

The sole function of the NOX enzyme family is to generate ROS in a controlled manner [134]. A deficiency in NOX2 has been shown to prevent RGC apoptosis [115]. NOX2 serves as a critical hub in the oxidative stress response of the retina following pathological H-IOP. ROS are considered key physiological mediators in various cell types, most notably in innate immune

cells such as neutrophils and eosinophils, where they act as effectors of antimicrobial activity during oxidative bursts [135]. Under oxidative conditions, the neuroprotective capacity of glial cells may diminish or even become neurotoxic. Retinal and optic nerve glial cells exhibit strong responses to ROS stimuli. An activated autoimmune response may promote primary and/or secondary RGC degeneration by stimulating aberrant immune reactions [133]. The activation of Nox2 and the translocation of the Nox2 p47phox subunit to the plasma membrane are crucial steps in initiating α-synuclein-induced microglial chemotaxis [136]. Dysregulated microglial Nox2 activity is a key mechanism in various neurodegenerative diseases, such as Parkinson's disease [137] and Alzheimer's disease [138]. Microglia retract their processes and migrate toward the site of injury, releasing pro-inflammatory cytokines such as IL-1β, TNF-α, and IL-6 [139-141]. In the study by Tezel et al., glial cells exposed to ROS more effectively induced T cell activation in a cell density- and time-dependent manner, evidenced by a roughly threefold increase in T cell proliferation and a sixfold increase in TNF-α secretion ($p < 0.01$) [142]. . TNF-α can transmit ROS from neuronal cells to vascular cells [143] and also trigger NOX2-dependent ROS production in microglia [144]. NOX2's contribution to retinal oxidative stress and neuroinflammation disrupts cellular function and leads to RGC apoptosis, furthering the progression of glaucoma. ROS derived from NOX2 directly damage neuronal cells by inducing oxidative stress and triggering apoptotic pathways.

6.2. The influence of NOX2-derived ROS on the dysfunction of the iBRB and the neurovascular unit accelerates neurodegenerative processes.

NOX/ROS can activate microglia, leading to the impairment of BBB function [145]. The iBRB is generally composed of the NVU, which shares structural and functional similarities with the BBB [146]. The retinal NVU is made up of retinal vascular endothelial cells encased within a dual-layered basement membrane, surrounded by pericytes and glial cells, including astrocytes, Müller cells, and microglia [146,147]. The NVU plays a crucial role in maintaining the overall integrity of the iBRB. Retinal pericytes contribute significantly to the integrity of the iBRB; they are contractile phagocytic cells embedded in the capillary basement membrane [148]. These cells stabilize microvessels, regulate blood flow, and control endothelial cell proliferation [147]. Additionally, they can further regulate the retinal microenvironment by secreting extracellular matrix components such as fibronectin [147,149]. Microglia, which are resident glial macrophages primarily located near retinal blood vessels, play a role in clearing cellular debris [146]. Although the eye is relatively immune-privileged, microglia can be activated in an inflammatory environment, releasing pro-inflammatory molecules and engaging in phagocytosis [146]. Beyond their pro-inflammatory immune functions, microglia interact with and secrete biochemical

factors that influence neuronal transmission, synaptic plasticity, and other cells within the NVU [150,151].

In the eye, the nature of hemodynamic disturbances involves alterations in the regulation of perfusion in terminal or pre-terminal arteries, rather than being an obstructive vascular disease like arteriosclerosis [152]. ROS and oxidative stress contribute to ocular hemodynamic dysregulation, which can also lead to RGC apoptosis. HIF-1α has been observed in the inner retina of patients with primary open-angle glaucoma [153], and both endothelin-1 and erythropoietin-1, two targets activated by HIF-1α, are significantly upregulated in glaucoma patients [154,155]. Under conditions of elevated intraocular pressure, NOX2 overexpression predominantly occurs in the retinal vasculature and the GCL, leading to excessive ROS production, which subsequently results in decreased endothelium-dependent vasodilation [143]. The disruption of tight junction complexes between endothelial cells causes iBRB breakdown and subsequent retinal edema [147,156,157]. Although the osmotic pressure within the retina is normally close to zero, increased iBRB permeability allows proteins to accumulate in the retina behind the external limiting membrane (ELM), thereby increasing osmotic pressure and leading to the formation of edema [158].

Elevated IOP can lead to dysfunction in retinal arterioles [159] . Clinical studies have shown that plasma levels of ET-1 are higher in glaucoma patients compared to healthy controls [160] , and patients with deteriorating visual fields have higher plasma ET-1 levels than those with stable visual fields [161,162] . Chronic administration of low doses of ET-1 in primates and rabbits can induce glaucomatous changes[163]. ET-1 blockers have been shown to increase retinal blood flow [164]. NOX2 activity promotes the production of ET-1 in EC [165,166]. ET-1 mediates vascular oxidative stress, inflammation, and remodeling [167]. Upon the addition of ET-1, primary microglia exhibit a reactive and hypertrophic morphology, which depends on the activation of the ERK1/2 pathway. Notably, ET-1 induces microglial activation to an M1 pro-inflammatory phenotype, consistent with previous findings [168]. Inhibition of the ERK1/2 pathway with the MEK1/2-specific inhibitor PD98059 is sufficient to completely block IL-1β and IL-6 secretion by macrophages infected with *Listeria monocytogenes* while slightly reducing TNF-α secretion [169]. Although MEK1/2 inhibition can fully block the secretion of IL-1β and IL-6 by ET-1-induced pro-inflammatory M1 microglia, it does not affect TNF-α secretion. NOX2-induced oxidative stress and inflammation can impair the function of the neurovascular unit, contributing to neurodegenerative diseases, including glaucoma.

6.3. Neuroprotection through NOX2 targeting: therapeutic potentials and hurdles.

The deletion or inhibition of NOX2 leads to reduced ROS production, decreased neuroinflammation, and improved neuronal survival in models of glaucoma and other neurodegenerative conditions, pointing toward NOX2 as a potential therapeutic target [170]. For instance, the use of apocynin, a NOX2 inhibitor, in experimental models has been associated with decreased oxidative stress and improved neuronal survival, highlighting the potential of NOX2 inhibitors as therapeutic agents in neurodegenerative diseases [171].

Glial cells, integral to maintaining the iBRB's integrity, express NOX2. Modulating NOX2 expression in glial and endothelial cells offers a targeted approach to protect the iBRB and neurovascular unit, reducing the progression of glaucomatous damage. Implicated in the activation of several neuroinflammatory pathways are ROS derived from NOX2, including those pathways involving NF-κB and MAPKs that contribute to the upregulation of proinflammatory cytokines, exacerbating neuronal death. Targeting NOX2, therefore, not only reduces oxidative stress but modulates these neuroinflammatory signaling pathways, providing a dual mechanism of neuroprotection [172]. Inhibition or modulation of NOX2 reduces ROS production, decreases neuroinflammation, and improves neuronal and neurovascular health, positioning NOX2 as a viable therapeutic target in glaucoma.

While targeting NOX2 presents a promising therapeutic strategy, it's crucial to consider the specificity of inhibition and the potential for off-target effects. NOX2 is also involved in host defense mechanisms, and its complete inhibition could impair immune responses. Developing selective NOX2 inhibitors or modulators targeting pathological ROS production without affecting physiological functions is a significant challenge. Furthermore, ongoing research is focusing on the role of NOX2 in glial cells and its contributions to neuroinflammation and oxidative stress, which will clarify the therapeutic potential of NOX2 inhibition in glaucoma and other neurodegenerative diseases.

6.4. Conclusion

In summary, NOX2-ROS plays a crucial role in promoting neuroinflammation, neuronal death, iBRB breakdown, and dysfunction in the neurovascular unit in glaucoma, highlighting the potential of targeting the NOX2-ROS pathway as a therapeutic strategy to mitigate neurodegenerative changes in glaucoma. Future research should focus on developing selective inhibitors or modulators of NOX2 that can alleviate its pathological effects without impairing physiological functions.

6.5. Limitations of the project

This research project has made significant progress in exploring the role of the NOX2/ET-1/ERK1/2 pathway in the pathophysiology of glaucoma. However, several limitations remain. RGC axons transmit visual information from the eye to the brain, and irreversible progressive vision loss occurs when RGCs and their axons degenerate [173,174]. In clinical practice, RGC loss is estimated by quantifying the thickness of the neuroretinal rim at the ONH, the retinal nerve fiber layer (RNFL), and the GCL using optical coherence tomography (OCT) [175]. This technique has also been applied in experimental animals, including monkeys, to study changes in retinal thickness and to assess RGC loss in vivo [176,177]. In post-mortem tissue, all RGC quantifications must be performed at the same time point. However, it is well known that there is significant inter-animal variability in RGC numbers, even among laboratory animals [176,178]. This study did not evaluate visual function in vivo in mice, such as visual field testing, OCT scanning, and visual evoked potentials, which would have provided a more comprehensive understanding of glaucoma progression and treatment efficacy. Furthermore, gender differences present another limitation of this study. There is evidence suggesting a higher age-adjusted incidence of primary open-angle glaucoma in males [179]. Female rats with chronic glaucoma exhibit lower IOP and structural loss than male rats, and their neuroretinal function is superior to that of male rats [180]. However, this study exclusively used male mice, failing to explore potential gender differences in the neuroprotective role of NOX2. Additionally, age is an important risk factor for glaucoma [181]. At the same IOP, older mice suffer more damage than adult mice [181]. However, this study did not examine the responses of mice of different ages under the same IOP conditions, potentially overlooking the impact of age on glaucoma pathology and treatment response. Moreover, although animal models provide valuable experimental data, they cannot fully capture the complexity and heterogeneity of human glaucoma, which may limit the generalizability of the study's findings to clinical applications. Overall, these limitations highlight the need for broader research to further validate the effectiveness of NOX2 as a therapeutic target for glaucoma and to facilitate its clinical application.

7. REFERENCES

1. Quigley HA, Broman AT. The number of people with glaucoma worldwide in 2010 and 2020. *Br J Ophthalmol* 2006; **90**(3): 262-7.
2. You M, Rong R, Zeng Z, Xia X, Ji D. Transneuronal Degeneration in the Brain During Glaucoma. *Front Aging Neurosci* 2021; **13**: 643685.
3. Kingman S. Glaucoma is second leading cause of blindness globally. *Bull World Health Organ* 2004; **82**(11): 887-8.
4. Basavarajappa D, Galindo-Romero C, Gupta V, et al. Signalling pathways and cell death mechanisms in glaucoma: Insights into the molecular pathophysiology. *Molecular Aspects of Medicine* 2023; **94**: 101216.
5. Jonas JB, Aung T, Bourne RR, Bron AM, Ritch R, Panda-Jonas S. Glaucoma. *The Lancet* 2017; **390**(10108): 2183-93.
6. Weinreb RN, Aung T, Medeiros FA. The pathophysiology and treatment of glaucoma: a review. *Jama* 2014; **311**(18): 1901-11.
7. Marcic TS, Belyea DA, Katz B. Neuroprotection in glaucoma: a model for neuroprotection in optic neuropathies. *Curr Opin Ophthalmol* 2003; **14**(6): 353-6.
8. Kuehn MH, Fingert JH, Kwon YH. Retinal ganglion cell death in glaucoma: mechanisms and neuroprotective strategies. *Ophthalmol Clin North Am* 2005; **18**(3): 383-95, vi.
9. Vernazza S, Oddone F, Tirendi S, Bassi AM. Risk Factors for Retinal Ganglion Cell Distress in Glaucoma and Neuroprotective Potential Intervention. *Int J Mol Sci* 2021; **22**(15).
10. Jammal AA, Berchuck SI, Thompson AC, Costa VP, Medeiros FA. The effect of age on increasing susceptibility to retinal nerve fiber layer loss in glaucoma. *Investigative ophthalmology & visual science* 2020; **61**(13): 8-.
11. Hurley DJ, Normile C, Irnaten M, O'Brien C. The intertwined roles of oxidative stress and endoplasmic reticulum stress in glaucoma. *Antioxidants* 2022; **11**(5): 886.
12. Chan KK, Tang F, Tham CC, Young AL, Cheung CY. Retinal vasculature in glaucoma: a review. *BMJ open ophthalmology* 2017; **1**(1).
13. Chitranshi N, Dheer Y, Abbasi M, You Y, Graham SL, Gupta V. Glaucoma pathogenesis and neurotrophins: focus on the molecular and genetic basis for therapeutic prospects. *Current neuropharmacology* 2018; **16**(7): 1018-35.
14. Chitranshi N, Dheer Y, Kumar S, Graham SL, Gupta V. Molecular docking, dynamics, and pharmacology studies on bexarotene as an agonist of ligand‐activated transcription factors, retinoid X receptors. *Journal of Cellular Biochemistry* 2019; **120**(7): 11745-60.
15. Baudouin C, Kolko M, Melik-Parsadaniantz S, Messmer EM. Inflammation in Glaucoma: From the back to the front of the eye, and beyond. *Progress in retinal and eye research* 2021; **83**: 100916.

16. Tezel G. Molecular regulation of neuroinflammation in glaucoma: Current knowledge and the ongoing search for new treatment targets. *Progress in Retinal and eye Research* 2022; **87**: 100998.
17. Naik S, Pandey A, Lewis SA, Rao BSS, Mutalik S. Neuroprotection: A versatile approach to combat glaucoma. *Eur J Pharmacol* 2020; **881**: 173208.
18. Pardue MT, Allen RS. Neuroprotective strategies for retinal disease. *Prog Retin Eye Res* 2018; **65**: 50-76.
19. Kimura A, Namekata K, Guo X, Noro T, Harada C, Harada T. Targeting Oxidative Stress for Treatment of Glaucoma and Optic Neuritis. *Oxid Med Cell Longev* 2017; **2017**: 2817252.
20. Qi Y, Zhao M, Bai Y, et al. Retinal ischemia/reperfusion injury is mediated by Toll-like receptor 4 activation of NLRP3 inflammasomes. *Invest Ophthalmol Vis Sci* 2014; **55**(9): 5466-75.
21. Yoneda S, Tanihara H, Kido N, et al. Interleukin-1beta mediates ischemic injury in the rat retina. *Exp Eye Res* 2001; **73**(5): 661-7.
22. Abramov AY, Scorziello A, Duchen MR. Three distinct mechanisms generate oxygen free radicals in neurons and contribute to cell death during anoxia and reoxygenation. *J Neurosci* 2007; **27**(5): 1129-38.
23. Tezel G. Oxidative stress in glaucomatous neurodegeneration: mechanisms and consequences. *Progress in retinal and eye research* 2006; **25**(5): 490-513.
24. Vecino E, Rodriguez FD, Ruzafa N, Pereiro X, Sharma SC. Glia–neuron interactions in the mammalian retina. *Progress in Retinal and Eye Research* 2016; **51**: 1-40.
25. Chen L, Yang P, Kijlstra A. Distribution, markers, and functions of retinal microglia. *Ocular immunology and inflammation* 2002; **10**(1): 27-39.
26. Wei X, Cho KS, Thee EF, Jager MJ, Chen DF. Neuroinflammation and microglia in glaucoma: time for a paradigm shift. *Journal of neuroscience research* 2019; **97**(1): 70-6.
27. Rashid K, Akhtar-Schaefer I, Langmann T. Microglia in retinal degeneration. *Frontiers in immunology* 2019; **10**: 1975.
28. Kaur C, Foulds WS, Ling EA. Hypoxia-ischemia and retinal ganglion cell damage. *Clin Ophthalmol* 2008; **2**(4): 879-89.
29. Vohra R, Tsai JC, Kolko M. The role of inflammation in the pathogenesis of glaucoma. *Surv Ophthalmol* 2013; **58**(4): 311-20.
30. Vernazza S, Tirendi S, Bassi AM, Traverso CE, Saccà SC. Neuroinflammation in primary open-angle glaucoma. *Journal of clinical medicine* 2020; **9**(10): 3172.
31. Yan X, Tezel G, Wax MB, Edward DP. Matrix metalloproteinases and tumor necrosis factor α in glaucomatous optic nerve head. *Archives of ophthalmology* 2000; **118**(5): 666-73.
32. Tezel G, Li LY, Patil RV, Wax MB. TNF-alpha and TNF-alpha receptor-1 in the retina of normal and glaucomatous eyes. *Invest Ophthalmol Vis*

Sci 2001; **42**(8): 1787-94.
33. Tezel G. TNF-alpha signaling in glaucomatous neurodegeneration. *Prog Brain Res* 2008; **173**: 409-21.
34. Yang X, Luo C, Cai J, et al. Neurodegenerative and inflammatory pathway components linked to TNF-α/TNFR1 signaling in the glaucomatous human retina. *Investigative ophthalmology & visual science* 2011; **52**(11): 8442-54.
35. Sharif NA. Chapter 14 - Inflammatory and immunological aspects of glaucoma, optic neuritis, and neuromyelitis optica impacting eyesight. In: Rezaei N, Yazdanpanah N, eds. Translational Neuroimmunology, Volume 7: Academic Press; 2023: 287-329.
36. Tezel G, Wax MB. Glial modulation of retinal ganglion cell death in glaucoma. *Journal of glaucoma* 2003; **12**(1): 63-8.
37. Bambrick L, Kristian T, Fiskum G. Astrocyte mitochondrial mechanisms of ischemic brain injury and neuroprotection. *Neurochemical research* 2004; **29**: 601-8.
38. Tezel G, Wax MB. Increased production of tumor necrosis factor-alpha by glial cells exposed to simulated ischemia or elevated hydrostatic pressure induces apoptosis in cocultured retinal ganglion cells. *J Neurosci* 2000; **20**(23): 8693-700.
39. Tezel G, Yang X. Caspase-independent component of retinal ganglion cell death, in vitro. *Invest Ophthalmol Vis Sci* 2004; **45**(11): 4049-59.
40. Tezel G, Yang X, Cai J. Proteomic identification of oxidatively modified retinal proteins in a chronic pressure-induced rat model of glaucoma. *Invest Ophthalmol Vis Sci* 2005; **46**(9): 3177-87.
41. Tezel G, Chauhan BC, LeBlanc RP, Wax MB. Immunohistochemical assessment of the glial mitogen-activated protein kinase activation in glaucoma. *Invest Ophthalmol Vis Sci* 2003; **44**(7): 3025-33.
42. Tezel G, Wax MB. The immune system and glaucoma. *Curr Opin Ophthalmol* 2004; **15**(2): 80-4.
43. Liu B, Neufeld AH. Activation of epidermal growth factor receptor signals induction of nitric oxide synthase-2 in human optic nerve head astrocytes in glaucomatous optic neuropathy. *Neurobiology of disease* 2003; **13**(2): 109-23.
44. Hernandez MR, Miao H, Lukas T. Astrocytes in glaucomatous optic neuropathy. *Progress in brain research* 2008; **173**: 353-73.
45. Williams PA, Marsh-Armstrong N, Howell GR, et al. Neuroinflammation in glaucoma: A new opportunity. *Experimental eye research* 2017; **157**: 20-7.
46. Casson RJ, Chidlow G, Crowston JG, Williams PA, Wood JPM. Retinal energy metabolism in health and glaucoma. *Prog Retin Eye Res* 2021; **81**: 100881.
47. Yang X, Yu XW, Zhang DD, Fan ZG. Blood-retinal barrier as a converging pivot in understanding the initiation and development of retinal

diseases. *Chin Med J (Engl)* 2020; **133**(21): 2586-94.
48. Jiang S, Kametani M, Chen DF. Adaptive Immunity: New Aspects of Pathogenesis Underlying Neurodegeneration in Glaucoma and Optic Neuropathy. *Front Immunol* 2020; **11**: 65.
49. Luna JD, Chan CC, Derevjanik NL, et al. Blood-retinal barrier (BRB) breakdown in experimental autoimmune uveoretinitis: comparison with vascular endothelial growth factor, tumor necrosis factor alpha, and interleukin-1beta-mediated breakdown. *J Neurosci Res* 1997; **49**(3): 268-80.
50. Chen H, Cho KS, Vu THK, et al. Commensal microflora-induced T cell responses mediate progressive neurodegeneration in glaucoma. *Nat Commun* 2018; **9**(1): 3209.
51. Santiago AR, Bernardino L, Agudo-Barriuso M, Gonçalves J. Microglia in health and disease: a double-edged sword. Hindawi; 2017.
52. Fernandez-Albarral JA, Ramírez AI, de Hoz R, Salazar JJ. Retinal microglial activation in glaucoma: evolution over time in a unilateral ocular hypertension model. *Neural Regen Res* 2022; **17**(4): 797-9.
53. Fernández-Albarral JA, Salazar JJ, de Hoz R, et al. Retinal Molecular Changes Are Associated with Neuroinflammation and Loss of RGCs in an Experimental Model of Glaucoma. *Int J Mol Sci* 2021; **22**(4).
54. Tan Z, Guo Y, Shrestha M, Sun D, Gregory-Ksander M, Jakobs TC. Microglia depletion exacerbates retinal ganglion cell loss in a mouse model of glaucoma. *Experimental Eye Research* 2022; **225**: 109273.
55. Ruan Y, Jiang S, Musayeva A, Gericke A. Oxidative Stress and Vascular Dysfunction in the Retina: Therapeutic Strategies. *Antioxidants (Basel)* 2020; **9**(8).
56. Fan Gaskin JC, Shah MH, Chan EC. Oxidative Stress and the Role of NADPH Oxidase in Glaucoma. *Antioxidants* 2021; **10**(2): 238.
57. C Chan E, Liu G-S, J Dusting G. Redox mechanisms in pathological angiogenesis in the retina: roles for NADPH oxidase. *Current Pharmaceutical Design* 2015; **21**(41): 5988-98.
58. Griendling KK, Sorescu D, Ushio-Fukai M. NAD (P) H oxidase: role in cardiovascular biology and disease. *Circulation research* 2000; **86**(5): 494-501.
59. Panday A, Sahoo MK, Osorio D, Batra S. NADPH oxidases: an overview from structure to innate immunity-associated pathologies. *Cellular & Molecular Immunology* 2015; **12**(1): 5-23.
60. Babior BM. NADPH oxidase: an update. *Blood* 1999; **93**(5): 1464-76.
61. Borregaard N, Heiple JM, Simons ER, Clark RA. Subcellular localization of the b-cytochrome component of the human neutrophil microbicidal oxidase: translocation during activation. *J Cell Biol* 1983; **97**(1): 52-61.
62. Groemping Y, Rittinger K. Activation and assembly of the NADPH oxidase: a structural perspective. *Biochem J* 2005; **386**(Pt 3): 401-16.

63. Nauseef WM. Assembly of the phagocyte NADPH oxidase. *Histochem Cell Biol* 2004; **122**(4): 277-91.
64. Sumimoto H, Miyano K, Takeya R. Molecular composition and regulation of the Nox family NAD(P)H oxidases. *Biochem Biophys Res Commun* 2005; **338**(1): 677-86.
65. Diebold BA, Bokoch GM. Molecular basis for Rac2 regulation of phagocyte NADPH oxidase. *Nat Immunol* 2001; **2**(3): 211-5.
66. Koga H, Terasawa H, Nunoi H, Takeshige K, Inagaki F, Sumimoto H. Tetratricopeptide repeat (TPR) motifs of p67(phox) participate in interaction with the small GTPase Rac and activation of the phagocyte NADPH oxidase. *J Biol Chem* 1999; **274**(35): 25051-60.
67. Suh YA, Arnold RS, Lassegue B, et al. Cell transformation by the superoxide-generating oxidase Mox1. *Nature* 1999; **401**(6748): 79-82.
68. Bánfi B, Maturana A, Jaconi S, et al. A mammalian H+ channel generated through alternative splicing of the NADPH oxidase homolog NOH-1. *Science* 2000; **287**(5450): 138-42.
69. Hilenski LL, Clempus RE, Quinn MT, Lambeth JD, Griendling KK. Distinct subcellular localizations of Nox1 and Nox4 in vascular smooth muscle cells. *Arterioscler Thromb Vasc Biol* 2004; **24**(4): 677-83.
70. Szanto I, Rubbia-Brandt L, Kiss P, et al. Expression of NOX1, a superoxide-generating NADPH oxidase, in colon cancer and inflammatory bowel disease. *J Pathol* 2005; **207**(2): 164-76.
71. Cheng G, Lambeth JD. NOXO1, regulation of lipid binding, localization, and activation of Nox1 by the Phox homology (PX) domain. *J Biol Chem* 2004; **279**(6): 4737-42.
72. Geiszt M, Lekstrom K, Witta J, Leto TL. Proteins homologous to p47phox and p67phox support superoxide production by NAD(P)H oxidase 1 in colon epithelial cells. *J Biol Chem* 2003; **278**(22): 20006-12.
73. Ueyama T, Geiszt M, Leto TL. Involvement of Rac1 in activation of multicomponent Nox1- and Nox3-based NADPH oxidases. *Mol Cell Biol* 2006; **26**(6): 2160-74.
74. Ueno N, Takeya R, Miyano K, Kikuchi H, Sumimoto H. The NADPH oxidase Nox3 constitutively produces superoxide in a p22phox-dependent manner: its regulation by oxidase organizers and activators. *J Biol Chem* 2005; **280**(24): 23328-39.
75. Kawahara T, Ritsick D, Cheng G, Lambeth JD. Point mutations in the proline-rich region of p22phox are dominant inhibitors of Nox1- and Nox2-dependent reactive oxygen generation. *J Biol Chem* 2005; **280**(36): 31859-69.
76. Cheng G, Ritsick D, Lambeth JD. Nox3 regulation by NOXO1, p47phox, and p67phox. *J Biol Chem* 2004; **279**(33): 34250-5.
77. Geiszt M, Kopp JB, Várnai P, Leto TL. Identification of renox, an NAD(P)H oxidase in kidney. *Proc Natl Acad Sci U S A* 2000; **97**(14): 8010-4.

78. Abate C, Patel L, Rauscher FJ, 3rd, Curran T. Redox regulation of fos and jun DNA-binding activity in vitro. *Science* 1990; **249**(4973): 1157-61.
79. Ambasta RK, Kumar P, Griendling KK, Schmidt HH, Busse R, Brandes RP. Direct interaction of the novel Nox proteins with p22phox is required for the formation of a functionally active NADPH oxidase. *J Biol Chem* 2004; **279**(44): 45935-41.
80. Martyn KD, Frederick LM, Von Loehneysen K, Dinauer MC, Knaus UG. Functional analysis of Nox4 reveals unique characteristics compared to other NADPH oxidases. *Cellular signalling* 2006; **18**(1): 69-82.
81. Gorin Y, Ricono JM, Kim NH, Bhandari B, Choudhury GG, Abboud HE. Nox4 mediates angiotensin II-induced activation of Akt/protein kinase B in mesangial cells. *Am J Physiol Renal Physiol* 2003; **285**(2): F219-29.
82. Bánfi B, Molnár G, Maturana A, et al. A Ca(2+)-activated NADPH oxidase in testis, spleen, and lymph nodes. *J Biol Chem* 2001; **276**(40): 37594-601.
83. Cheng G, Cao Z, Xu X, van Meir EG, Lambeth JD. Homologs of gp91phox: cloning and tissue expression of Nox3, Nox4, and Nox5. *Gene* 2001; **269**(1-2): 131-40.
84. Bánfi B, Tirone F, Durussel I, et al. Mechanism of Ca2+ activation of the NADPH oxidase 5 (NOX5). *J Biol Chem* 2004; **279**(18): 18583-91.
85. Fu X, Beer DG, Behar J, Wands J, Lambeth D, Cao W. cAMP-response element-binding protein mediates acid-induced NADPH oxidase NOX5-S expression in Barrett esophageal adenocarcinoma cells. *J Biol Chem* 2006; **281**(29): 20368-82.
86. Colas C, Ortiz de Montellano PR. Autocatalytic radical reactions in physiological prosthetic heme modification. *Chem Rev* 2003; **103**(6): 2305-32.
87. De Deken X, Wang D, Dumont JE, Miot F. Characterization of ThOX proteins as components of the thyroid H(2)O(2)-generating system. *Exp Cell Res* 2002; **273**(2): 187-96.
88. Dupuy C, Ohayon R, Valent A, Noël-Hudson MS, Dème D, Virion A. Purification of a novel flavoprotein involved in the thyroid NADPH oxidase. Cloning of the porcine and human cdnas. *J Biol Chem* 1999; **274**(52): 37265-9.
89. De Deken X, Wang D, Many MC, et al. Cloning of two human thyroid cDNAs encoding new members of the NADPH oxidase family. *J Biol Chem* 2000; **275**(30): 23227-33.
90. Grasberger H, Refetoff S. Identification of the maturation factor for dual oxidase. Evolution of an eukaryotic operon equivalent. *J Biol Chem* 2006; **281**(27): 18269-72.
91. Ameziane-El-Hassani R, Morand S, Boucher JL, et al. Dual oxidase-2 has an intrinsic Ca2+-dependent H2O2-generating activity. *J Biol Chem* 2005; **280**(34): 30046-54.
92. Wang D, De Deken X, Milenkovic M, et al. Identification of a novel

partner of duox: EFP1, a thioredoxin-related protein. *J Biol Chem* 2005; **280**(4): 3096-103.
93. Magnani F, Mattevi A. Structure and mechanisms of ROS generation by NADPH oxidases. *Current opinion in structural biology* 2019; **59**: 91-7.
94. Evangelho K, Mastronardi CA, De-La-Torre A. Experimental models of glaucoma: A powerful translational tool for the future development of new therapies for glaucoma in humans—A review of the literature. *Medicina* 2019; **55**(6): 280.
95. Chidlow G, Wood JP, Casson RJ. Investigations into hypoxia and oxidative stress at the optic nerve head in a rat model of glaucoma. *Frontiers in neuroscience* 2017; **11**: 478.
96. Sapienza A, Raveu A-L, Reboussin E, et al. Bilateral neuroinflammatory processes in visual pathways induced by unilateral ocular hypertension in the rat. *Journal of neuroinflammation* 2016; **13**: 1-16.
97. Cherry JD, Olschowka JA, O'Banion MK. Neuroinflammation and M2 microglia: the good, the bad, and the inflamed. *Journal of neuroinflammation* 2014; **11**(1): 1-15.
98. Kumar A, Barrett JP, Alvarez-Croda DM, Stoica BA, Faden AI, Loane DJ. NOX2 drives M1-like microglial/macrophage activation and neurodegeneration following experimental traumatic brain injury. *Brain Behav Immun* 2016; **58**: 291-309.
99. Gericke A, Mann C, Zadeh JK, et al. Elevated intraocular pressure causes abnormal reactivity of mouse retinal arterioles. *Oxidative medicine and cellular longevity* 2019; **2019**.
100. Li Y, Pagano PJ. Microvascular NADPH oxidase in health and disease. *Free Radical Biology and Medicine* 2017; **109**: 33-47.
101. Van Buul JD, Hordijk PL. Signaling in leukocyte transendothelial migration. *Arteriosclerosis, thrombosis, and vascular biology* 2004; **24**(5): 824-33.
102. Soto I, Howell GR. The complex role of neuroinflammation in glaucoma. *Cold Spring Harbor perspectives in medicine* 2014; **4**(8).
103. Chang EE, Goldberg JL. Glaucoma 2.0: neuroprotection, neuroregeneration, neuroenhancement. *Ophthalmology* 2012; **119**(5): 979-86.
104. CHEN S-d, Lu W, ZHANG X-l. Neuroprotection in glaucoma: present and future. *Chinese medical journal* 2013; **126**(8): 1567-77.
105. Naik S, Pandey A, Lewis SA, Rao BSS, Mutalik S. Neuroprotection: A versatile approach to combat glaucoma. *European Journal of Pharmacology* 2020; **881**: 173208.
106. Ju W-K, Kim K-Y, Lindsey JD, et al. Elevated hydrostatic pressure triggers release of OPA1 and cytochrome C, and induces apoptotic cell death in differentiated RGC-5 cells. *Molecular vision* 2009; **15**: 120.
107. Wang YX, Jonas JB, Wang N, et al. Intraocular pressure and

estimated cerebrospinal fluid pressure. The Beijing Eye Study 2011. *PloS one* 2014; **9**(8): e104267.
108. Jonas J, Yang D, Wang N. Einfluss des Liquordrucks auf die glaukomatöse Schädigung des Nervus opticus. *Der Ophthalmologe* 2014; **2**(111): 181-90.
109. Izzotti A, Bagnis A, Saccà SC. The role of oxidative stress in glaucoma. *Mutation Research/Reviews in Mutation Research* 2006; **612**(2): 105-14.
110. Osborne NN, Núñez-Álvarez C, Joglar B, del Olmo-Aguado S. Glaucoma: focus on mitochondria in relation to pathogenesis and neuroprotection. *European journal of pharmacology* 2016; **787**: 127-33.
111. Drummond GR, Selemidis S, Griendling KK, Sobey CG. Combating oxidative stress in vascular disease: NADPH oxidases as therapeutic targets. *Nature reviews Drug discovery* 2011; **10**(6): 453-71.
112. Urner S, Ho F, Jha JC, Ziegler D, Jandeleit-Dahm K. NADPH oxidase inhibition: preclinical and clinical studies in diabetic complications. *Antioxidants & redox signaling* 2020; **33**(6): 415-34.
113. Deliyanti D, Wilkinson-Berka JL. Inhibition of NOX1/4 with GKT137831: a potential novel treatment to attenuate neuroglial cell inflammation in the retina. *Journal of neuroinflammation* 2015; **12**(1): 1-13.
114. Wilkinson-Berka JL, Deliyanti D, Rana I, et al. NADPH oxidase, NOX1, mediates vascular injury in ischemic retinopathy. *Antioxidants & redox signaling* 2014; **20**(17): 2726-40.
115. Yokota H, Narayanan SP, Zhang W, et al. Neuroprotection from retinal ischemia/reperfusion injury by NOX2 NADPH oxidase deletion. *Investigative ophthalmology & visual science* 2011; **52**(11): 8123-31.
116. Teixeira G, Szyndralewiez C, Molango S, et al. Therapeutic potential of NADPH oxidase 1/4 inhibitors. *British journal of pharmacology* 2017; **174**(12): 1647-69.
117. Augsburger F, Filippova A, Rasti D, et al. Pharmacological characterization of the seven human NOX isoforms and their inhibitors. *Redox Biology* 2019; **26**: 101272.
118. Elbatreek MH, Mucke H, Schmidt HH. NOX inhibitors: From bench to naxibs to bedside: Springer; 2021.
119. Hirano K, Chen WS, Chueng AL, et al. Discovery of GSK2795039, a novel small molecule NADPH oxidase 2 inhibitor. *Antioxidants & redox signaling* 2015; **23**(5): 358-74.
120. Buck A, Sanchez Klose FP, Venkatakrishnan V, et al. DPI selectively inhibits intracellular NADPH oxidase activity in human neutrophils. *Immunohorizons* 2019; **3**(10): 488-97.
121. Chai Y, Cao Z, Yu R, Liu Y, Yuan D, Lei L. Dexmedetomidine attenuates LPS-induced monocyte-endothelial adherence via inhibiting Cx43/PKC-α/NOX2/ROS signaling pathway in monocytes. *Oxidative Medicine and Cellular Longevity* 2020; **2020**.

122. Wang M, Luo L. An effective NADPH oxidase 2 inhibitor provides neuroprotection and improves functional outcomes in animal model of traumatic brain injury. *Neurochemical Research* 2020; **45**(5): 1097-106.
123. Dröge W. Free radicals in the physiological control of cell function. *Physiol Rev* 2002; **82**(1): 47-95.
124. Cui H, Kong Y, Zhang H. Oxidative stress, mitochondrial dysfunction, and aging. *J Signal Transduct* 2012; **2012**: 646354.
125. Finkel T. Signal transduction by reactive oxygen species. *J Cell Biol* 2011; **194**(1): 7-15.
126. Evans MD, Dizdaroglu M, Cooke MS. Oxidative DNA damage and disease: induction, repair and significance. *Mutat Res* 2004; **567**(1): 1-61.
127. Moreno MC, Campanelli J, Sande P, Sáenz DA, Keller Sarmiento MI, Rosenstein RE. Retinal Oxidative Stress Induced by High Intraocular Pressure. *Free Radical Biology and Medicine* 2004; **37**(6): 803-12.
128. Ferreira SM, Lerner SF, Brunzini R, Reides CG, Evelson PA, Llesuy SF. Time course changes of oxidative stress markers in a rat experimental glaucoma model. *Investigative Ophthalmology & Visual Science* 2010; **51**(9): 4635-40.
129. Ko M-L, Peng P-H, Ma M-C, Ritch R, Chen C-F. Dynamic changes in reactive oxygen species and antioxidant levels in retinas in experimental glaucoma. *Free Radical Biology and Medicine* 2005; **39**(3): 365-73.
130. Tezel Gln, Yang X, Cai J. Proteomic identification of oxidatively modified retinal proteins in a chronic pressure-induced rat model of glaucoma. *Investigative ophthalmology & visual science* 2005; **46**(9): 3177-87.
131. Kong YX, Crowston JG, Vingrys AJ, Trounce IA, Bui BV. Functional changes in the retina during and after acute intraocular pressure elevation in mice. *Investigative ophthalmology & visual science* 2009; **50**(12): 5732-40.
132. Kong YXG, van Bergen N, Bui BV, et al. Impact of aging and diet restriction on retinal function during and after acute intraocular pressure injury. *Neurobiology of aging* 2012; **33**(6): 1126. e15-. e25.
133. Tezel G. Oxidative stress in glaucomatous neurodegeneration: mechanisms and consequences. *Prog Retin Eye Res* 2006; **25**(5): 490-513.
134. Sies H, Jones DP. Reactive oxygen species (ROS) as pleiotropic physiological signalling agents. *Nat Rev Mol Cell Biol* 2020; **21**(7): 363-83.
135. Maghzal GJ, Krause KH, Stocker R, Jaquet V. Detection of reactive oxygen species derived from the family of NOX NADPH oxidases. *Free Radic Biol Med* 2012; **53**(10): 1903-18.
136. Wang S, Chu CH, Stewart T, et al. α-Synuclein, a chemoattractant, directs microglial migration via H2O2-dependent Lyn phosphorylation. *Proc Natl Acad Sci U S A* 2015; **112**(15): E1926-35.
137. Hou L, Zhou X, Zhang C, et al. NADPH oxidase-derived H(2)O(2)

mediates the regulatory effects of microglia on astrogliosis in experimental models of Parkinson's disease. *Redox Biol* 2017; **12**: 162-70.
138. Ma MW, Wang J, Zhang Q, et al. NADPH oxidase in brain injury and neurodegenerative disorders. *Mol Neurodegener* 2017; **12**(1): 7.
139. Kreutzberg GW. Microglia: a sensor for pathological events in the CNS. *Trends Neurosci* 1996; **19**(8): 312-8.
140. Clayton DF, George JM. Synucleins in synaptic plasticity and neurodegenerative disorders. *J Neurosci Res* 1999; **58**(1): 120-9.
141. Becher B, Prat A, Antel JP. Brain-immune connection: immuno-regulatory properties of CNS-resident cells. *Glia* 2000; **29**(4): 293-304.
142. Tezel G, Yang X, Luo C, Peng Y, Sun SL, Sun D. Mechanisms of immune system activation in glaucoma: oxidative stress-stimulated antigen presentation by the retina and optic nerve head glia. *Invest Ophthalmol Vis Sci* 2007; **48**(2): 705-14.
143. Gericke A, Mann C, Zadeh JK, et al. Elevated Intraocular Pressure Causes Abnormal Reactivity of Mouse Retinal Arterioles. *Oxid Med Cell Longev* 2019; **2019**: 9736047.
144. Geng L, Fan LM, Liu F, Smith C, Li J. Nox2 dependent redox-regulation of microglial response to amyloid-β stimulation and microgliosis in aging. *Sci Rep* 2020; **10**(1): 1582.
145. Sumi N, Nishioku T, Takata F, et al. Lipopolysaccharide-activated microglia induce dysfunction of the blood-brain barrier in rat microvascular endothelial cells co-cultured with microglia. *Cell Mol Neurobiol* 2010; **30**(2): 247-53.
146. Nian S, Lo ACY, Mi Y, Ren K, Yang D. Neurovascular unit in diabetic retinopathy: pathophysiological roles and potential therapeutical targets. *Eye Vis (Lond)* 2021; **8**(1): 15.
147. Gardner TW, Davila JR. The neurovascular unit and the pathophysiologic basis of diabetic retinopathy. *Graefes Arch Clin Exp Ophthalmol* 2017; **255**(1): 1-6.
148. Frank RN, Turczyn TJ, Das A. Pericyte coverage of retinal and cerebral capillaries. *Invest Ophthalmol Vis Sci* 1990; **31**(6): 999-1007.
149. Trost A, Lange S, Schroedl F, et al. Brain and Retinal Pericytes: Origin, Function and Role. *Front Cell Neurosci* 2016; **10**: 20.
150. Newman EA. Glial cell regulation of neuronal activity and blood flow in the retina by release of gliotransmitters. *Philos Trans R Soc Lond B Biol Sci* 2015; **370**(1672).
151. Vecino E, Rodriguez FD, Ruzafa N, Pereiro X, Sharma SC. Glia-neuron interactions in the mammalian retina. *Prog Retin Eye Res* 2016; **51**: 1-40.
152. Flammer J, Pache M, Resink T. Vasospasm, its role in the pathogenesis of diseases with particular reference to the eye. *Prog Retin Eye Res* 2001; **20**(3): 319-49.
153. Tezel G, Wax MB. Hypoxia-inducible factor 1alpha in the

glaucomatous retina and optic nerve head. *Arch Ophthalmol* 2004; **122**(9): 1348-56.
154. Mokbel TH, Ghanem AA, Kishk H, Arafa LF, El-Baiomy AA. Erythropoietin and soluble CD44 levels in patients with primary open-angle glaucoma. *Clin Exp Ophthalmol* 2010; **38**(6): 560-5.
155. Choritz L, Machert M, Thieme H. Correlation of endothelin-1 concentration in aqueous humor with intraocular pressure in primary open angle and pseudoexfoliation glaucoma. *Invest Ophthalmol Vis Sci* 2012; **53**(11): 7336-42.
156. Klaassen I, Van Noorden CJ, Schlingemann RO. Molecular basis of the inner blood-retinal barrier and its breakdown in diabetic macular edema and other pathological conditions. *Prog Retin Eye Res* 2013; **34**: 19-48.
157. Rizzolo LJ, Peng S, Luo Y, Xiao W. Integration of tight junctions and claudins with the barrier functions of the retinal pigment epithelium. *Prog Retin Eye Res* 2011; **30**(5): 296-323.
158. Daruich A, Matet A, Moulin A, et al. Mechanisms of macular edema: Beyond the surface. *Prog Retin Eye Res* 2018; **63**: 20-68.
159. Gericke A, Mann C, Zadeh JK, et al. Elevated intraocular pressure causes abnormal reactivity of mouse retinal arterioles. *Oxidative medicine and cellular longevity* 2019; **2019**(1): 9736047.
160. Lommatzsch C, Rothaus K, Schopmeyer L, et al. Elevated endothelin-1 levels as risk factor for an impaired ocular blood flow measured by OCT-A in glaucoma. *Scientific Reports* 2022; **12**(1): 11801.
161. Krupin T, Orgül S, Cioffi GA, Bacon DR, Van Buskirk EM. An endothelin-1-induced model of chronic optic nerve ischemia in rhesus monkeys. *Journal of glaucoma* 1996; **5**(2): 135-8.
162. Orgül S, Cioffi GA, Wilson DJ, Bacon DR, Van Buskirk EM. An endothelin-1 induced model of optic nerve ischemia in the rabbit. *Investigative ophthalmology & visual science* 1996; **37**(9): 1860-9.
163. van der Graaff D, Chotkoe S, De Winter B, et al. Vasoconstrictor antagonism improves functional and structural vascular alterations and liver damage in rats with early NAFLD. *JHEP Reports* 2022; **4**(2): 100412.
164. Kamhieh-Milz J, Chen L, Goettsch C, et al. Ang II Promotes ET-1 Production by Regulating NOX2 Activity Through Transcription Factor Oct-1. *Arterioscler Thromb Vasc Biol* 2023; **43**(8): 1429-40.
165. Amiri F, Virdis A, Neves MF, et al. Endothelium-restricted overexpression of human endothelin-1 causes vascular remodeling and endothelial dysfunction. *Circulation* 2004; **110**(15): 2233-40.
166. Amiri F, Paradis P, Reudelhuber TL, Schiffrin EL. Vascular inflammation in absence of blood pressure elevation in transgenic murine model overexpressing endothelin-1 in endothelial cells. *J Hypertens* 2008; **26**(6): 1102-9.
167. Gadea A, Schinelli S, Gallo V. Endothelin-1 regulates astrocyte

proliferation and reactive gliosis via a JNK/c-Jun signaling pathway. *J Neurosci* 2008; **28**(10): 2394-408.
168. Abdul Y, Jamil S, He L, Li W, Ergul A. Endothelin-1 (ET-1) promotes a proinflammatory microglia phenotype in diabetic conditions. *Can J Physiol Pharmacol* 2020; **98**(9): 596-603.
169. Herb M, Gluschko A, Wiegmann K, et al. Mitochondrial reactive oxygen species enable proinflammatory signaling through disulfide linkage of NEMO. *Sci Signal* 2019; **12**(568).
170. Olguín-Albuerne M, Morán J. ROS produced by NOX2 control in vitro development of cerebellar granule neurons development. *ASN Neuro* 2015; **7**(2).
171. Ahmad A, Nawaz MI, Siddiquei MM, Abu El-Asrar AM. Apocynin ameliorates NADPH oxidase 4 (NOX4) induced oxidative damage in the hypoxic human retinal Müller cells and diabetic rat retina. *Mol Cell Biochem* 2021; **476**(5): 2099-109.
172. Yokota H, Narayanan SP, Zhang W, et al. Neuroprotection from retinal ischemia/reperfusion injury by NOX2 NADPH oxidase deletion. *Invest Ophthalmol Vis Sci* 2011; **52**(11): 8123-31.
173. Goldberg JL, Espinosa JS, Xu Y, Davidson N, Kovacs GT, Barres BA. Retinal ganglion cells do not extend axons by default: promotion by neurotrophic signaling and electrical activity. *Neuron* 2002; **33**(5): 689-702.
174. Carelli V, La Morgia C, Ross-Cisneros FN, Sadun AA. Optic neuropathies: the tip of the neurodegeneration iceberg. *Hum Mol Genet* 2017; **26**(R2): R139-r50.
175. Bussel II, Wollstein G, Schuman JS. OCT for glaucoma diagnosis, screening and detection of glaucoma progression. *British Journal of Ophthalmology* 2014; **98**(Suppl 2): ii15-ii9.
176. Fortune B, Cull G, Reynaud J, Wang L, Burgoyne CF. Relating retinal ganglion cell function and retinal nerve fiber layer (RNFL) retardance to progressive loss of RNFL thickness and optic nerve axons in experimental glaucoma. *Investigative ophthalmology & visual science* 2015; **56**(6): 3936-44.
177. Yang H, Reynaud J, Lockwood H, et al. The connective tissue phenotype of glaucomatous cupping in the monkey eye-Clinical and research implications. *Progress in retinal and eye research* 2017; **59**: 1-52.
178. Williams RW, Strom RC, Rice DS, Goldowitz D. Genetic and environmental control of variation in retinal ganglion cell number in mice. *Journal of Neuroscience* 1996; **16**(22): 7193-205.
179. Tham YC, Li X, Wong TY, Quigley HA, Aung T, Cheng CY. Global prevalence of glaucoma and projections of glaucoma burden through 2040: a systematic review and meta-analysis. *Ophthalmology* 2014; **121**(11): 2081-90.
180. Rodrigo MJ, Martinez-Rincon T, Subias M, et al. Influence of Sex on

Neuroretinal Degeneration: Six-Month Follow-Up in Rats With Chronic Glaucoma. *Invest Ophthalmol Vis Sci* 2021; **62**(13): 9.
181. Di Pierdomenico J, Henderson DCM, Giammaria S, et al. Age and intraocular pressure in murine experimental glaucoma. *Progress in Retinal and Eye Research* 2022; **88**: 101021.

8. APPENDIX

8.1. List of figures

8.2. PRE-PUBLICATION OF RESULTS

1. **Shi X**, Li P, Liu H, Prokosch V. Oxidative Stress, Vascular Endothelium, and the Pathology of Neurodegeneration in Retina. Antioxidants (Basel). 2022 Mar 12;11(3):543. doi: 10.3390/antiox11030543. PMID: 35326193; PMCID: PMC8944517.
2. **Shi X**, Li P, Herb M, Liu H, Wang M, Wang X, Feng Y, van Beers T, Xia N, Li H, Prokosch V. Pathological high intraocular pressure induces glial cell reactive proliferation contributing to neuroinflammation of the blood-retinal barrier via the NOX2/ET-1 axis-controlled ERK1/2 pathway. J Neuroinflammation. 2024 Apr 22;21(1):105. doi: 10.1186/s12974-024-03075-x. PMID: 38649885; PMCID: PMC11034147.

This Cumulative thesis includes the papers of No. 1 and No. 2.